

Lattice and phenomenology of the Quark-Gluon plasma

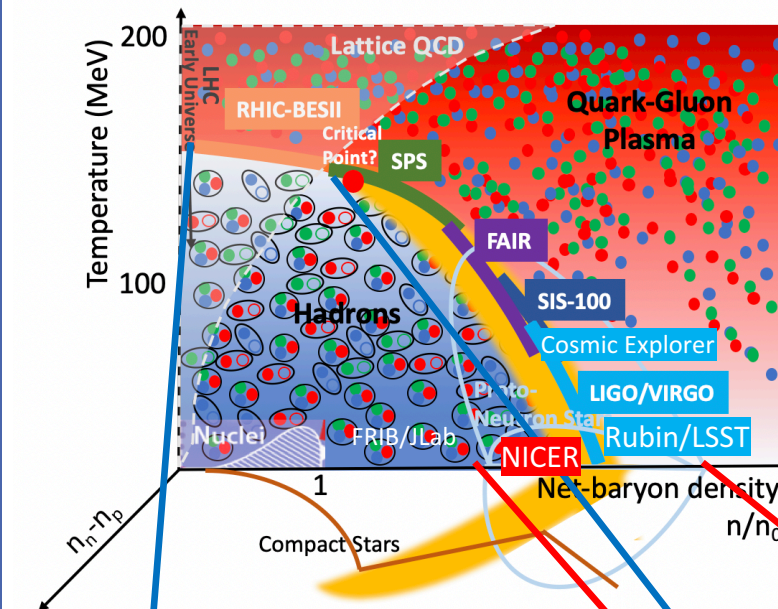
CLAUDIA RATTI

UNIVERSITY of
HOUSTON

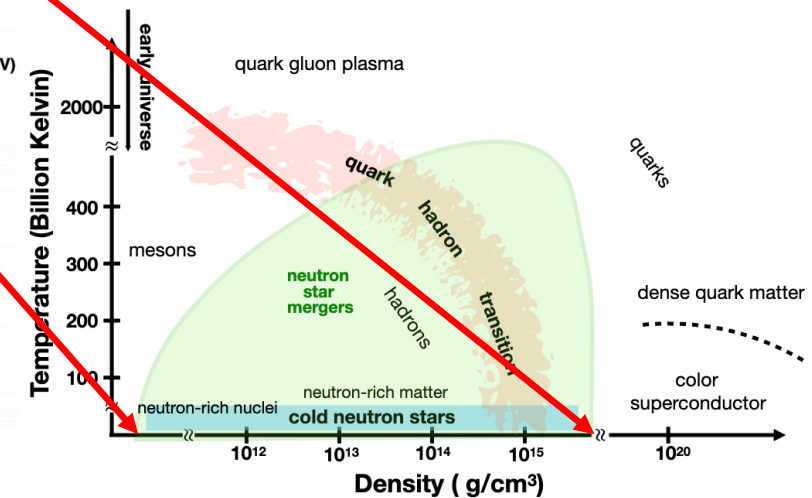
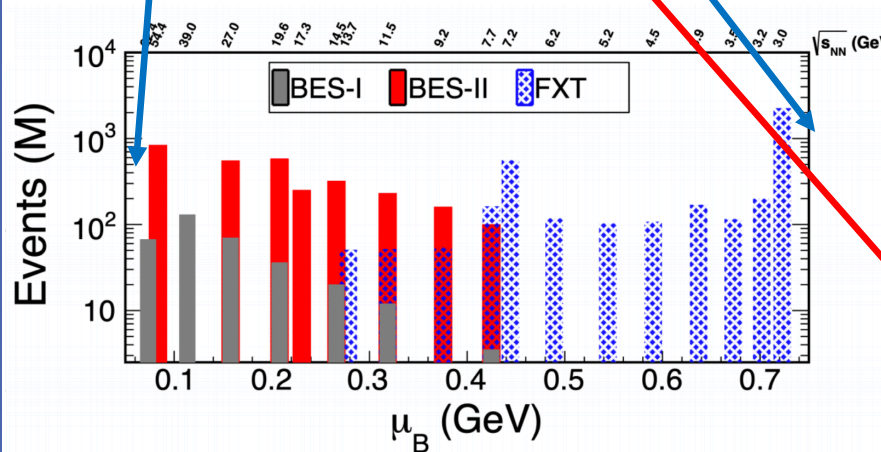


Motivating science goals

- Is there a critical point in the QCD phase diagram?
- What are the degrees of freedom in the vicinity of the phase transition?
- Where is the transition line at high density?
- What are the phases of QCD at high density?
- What is the nature of matter in the core of neutron stars?



- Run 2019:
 - Collider: $v_{NN}=14.6, 19.6, 200$ GeV
 - Fixed target: $v_{NN}=3.2$ GeV
- Run 2020:
 - Collider: $v_{NN}=9.2, 11.5$ GeV
 - Fixed target: $v_{NN}=3.5, 3.9, 4.5, 5.2, 6.2, 7.2, 7.7$ GeV
- Run 2021:
 - Collider: $v_{NN}=7.7, 17.3$ GeV
 - Fixed target: $v_{NN}=3.0, 9.2, 11.5, 13.7$ GeV



What can we obtain from lattice QCD?

Equation of state

- Needed for **hydrodynamic** description of the QGP
- Needed for simulations of Neutron Stars and their mergers

QCD phase diagram

- Transition line at finite density
- Constraints on the location of the critical point

Fluctuations of conserved charges

- Can be **simulated** on the lattice and **measured** in experiments
- Can give information on the **evolution** of heavy-ion collisions
- Can give information on the **critical point**

What can we obtain from lattice QCD?

Equation of state

- Needed for **hydrodynamic** description of the QGP
- Needed for simulations of Neutron Stars and their mergers

QCD phase diagram

- Transition line at finite density
- Constraints on the location of the critical point

Fluctuations of conserved charges

- Can be **simulated** on the lattice and **measured** in experiments
- Can give information on the **evolution** of heavy-ion collisions
- Can give information on the **critical point**

Talk by R. Bellwied on Wednesday

QCD Equation of State from the lattice

STATUS

Taylor expansion of EoS

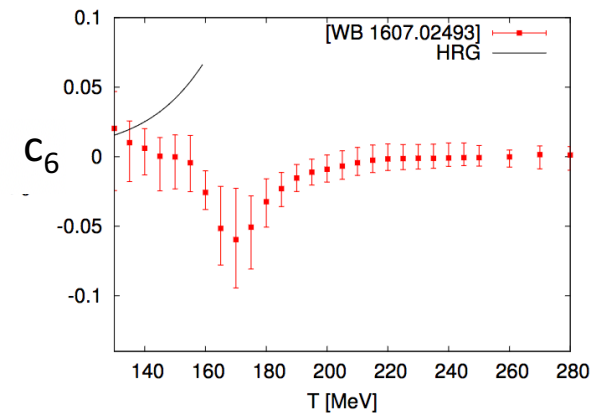
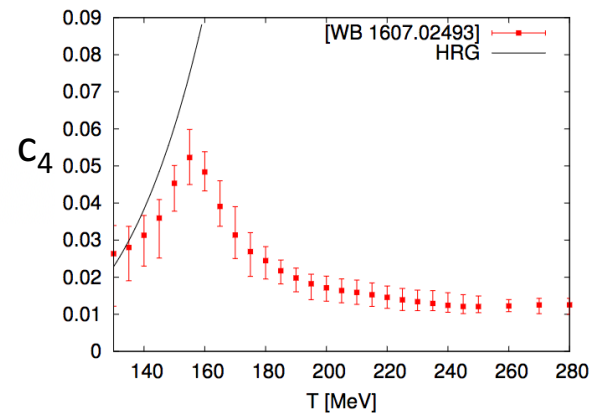
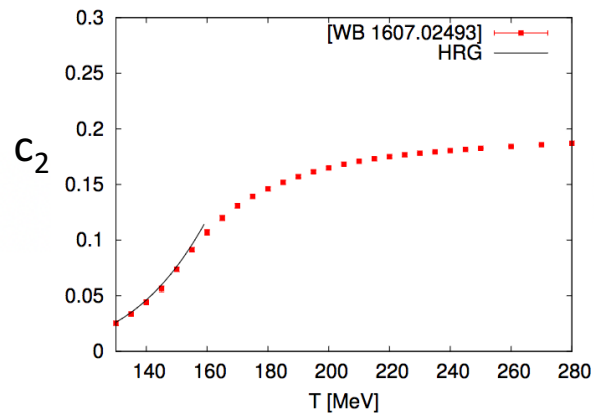
- Taylor expansion of the pressure:

$$\frac{p(T, \mu_B)}{T^4} = \frac{p(T, 0)}{T^4} + \sum_{n=1}^{\infty} \frac{1}{(2n)!} \chi_{2n}^B \left(\frac{\mu_B}{T} \right)^{2n} = \sum_{n=0}^{\infty} c_{2n}(T) \left(\frac{\mu_B}{T} \right)^{2n}$$

Simulations at imaginary μ_B :

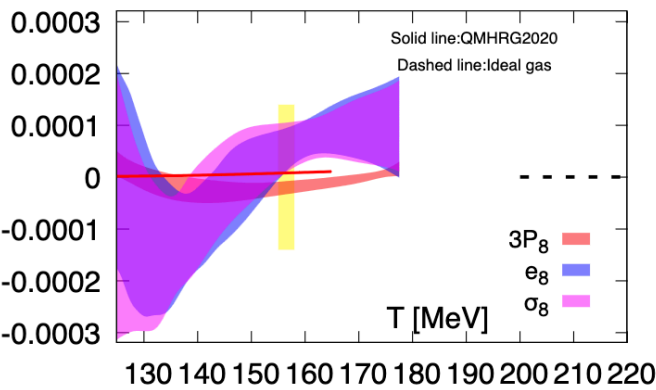
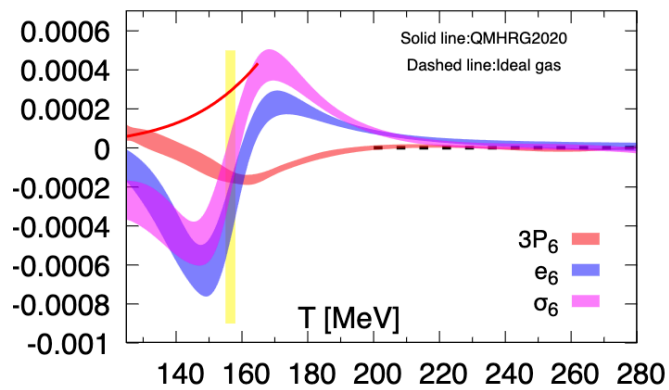
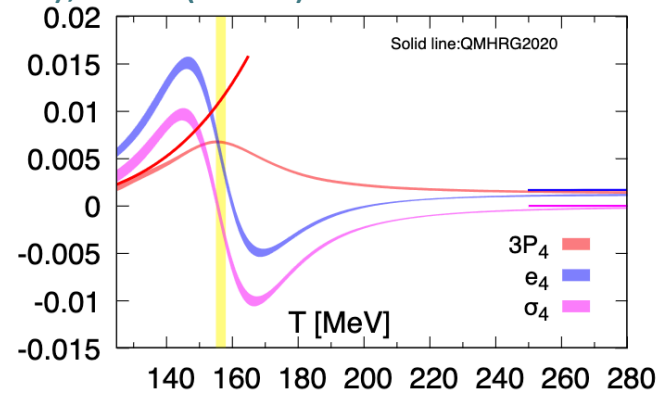
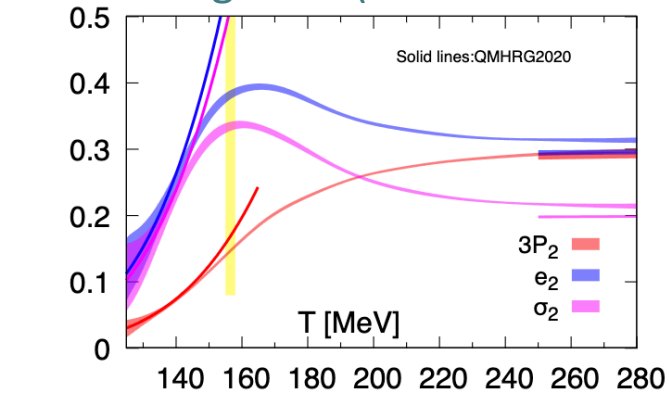
Continuum, $O(10^4)$ configurations, errors include systematics

WB: S. Borsanyi, C. R. et al, NPA (2017)



New results for expansion coefficients

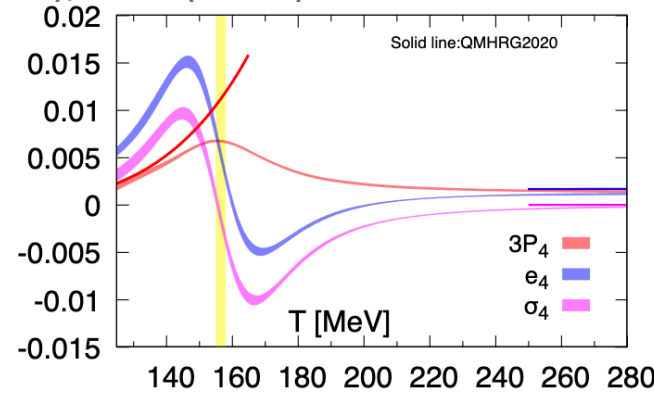
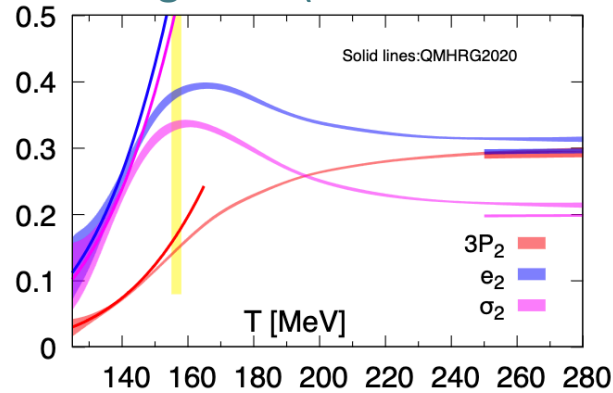
D. Bollweg et al. (HotQCD collaboration), PRD (2023)



- Continuum extrapolation for 2nd and 4th order
- 6th and 8th order are $N_t=8$ splines
- Taylor-expanded equation of state covers the range $\mu_B/T \leq 3$

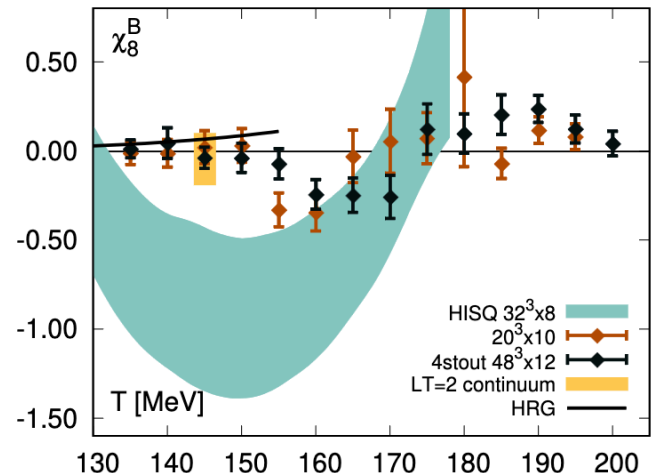
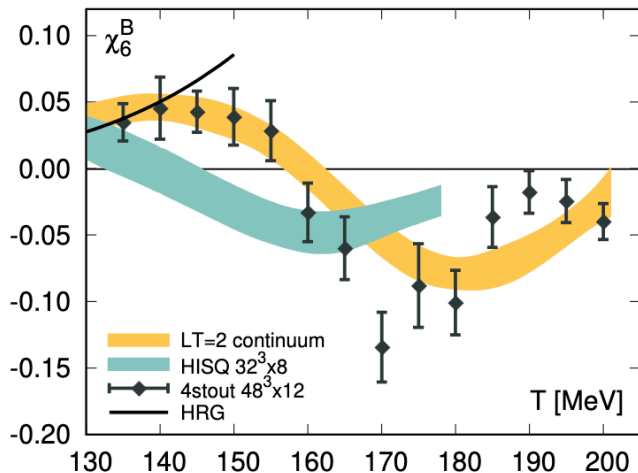
New results for expansion coefficients

D. Bollweg et al. (HotQCD collaboration), PRD (2023)



- Continuum extrapolation for 2nd and 4th order

- 6th and 8th order are $N_t=8$ splines



- Taylor-expanded equation of state covers the range $\mu_B/T \leq 3$

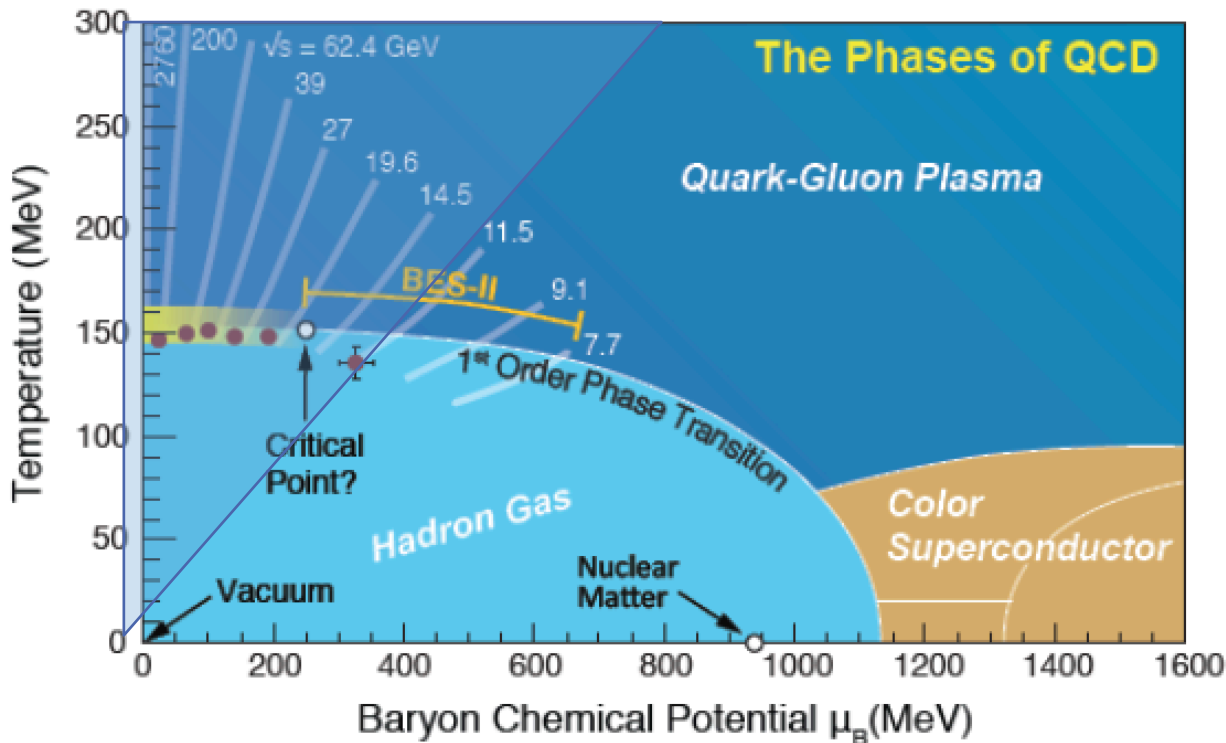
- New, continuum extrapolated results for 6th and 8th order in a small volume look quite different

S. Borsanyi et al. (WB collab.), PRD (2024)

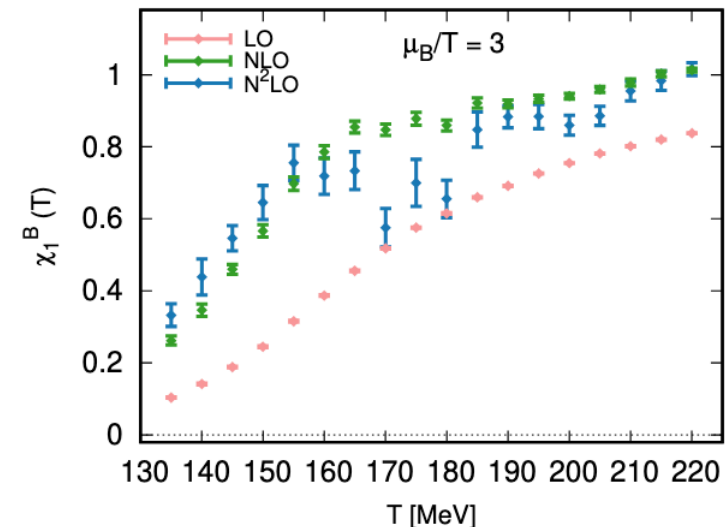
Range of validity of equation of state

- From Taylor expansion we have the equation of state for $\mu_B/T \leq 3$:

$$\sqrt{s} = 200, 62.4, 39, 27, 19.6, 14.5, 11.5 \text{ GeV}$$

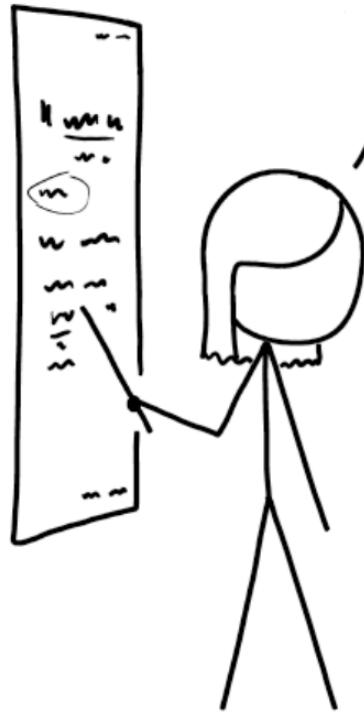


- Problems with Taylor:
 - Large errors on higher order terms
 - Wiggles on Taylor coefficients reflected on observables



AT THIS POINT, YOU'RE PROBABLY
THINKING, "I LOVE THIS EQUATION
AND WISH IT WOULD NEVER END!"

WELL, GOOD NEWS!



TAYLOR SERIES EXPANSION IS THE WORST.

Novel expansion method

WB: S. Borsanyi, C. R. et al, PRL (2021), PRD (2022)

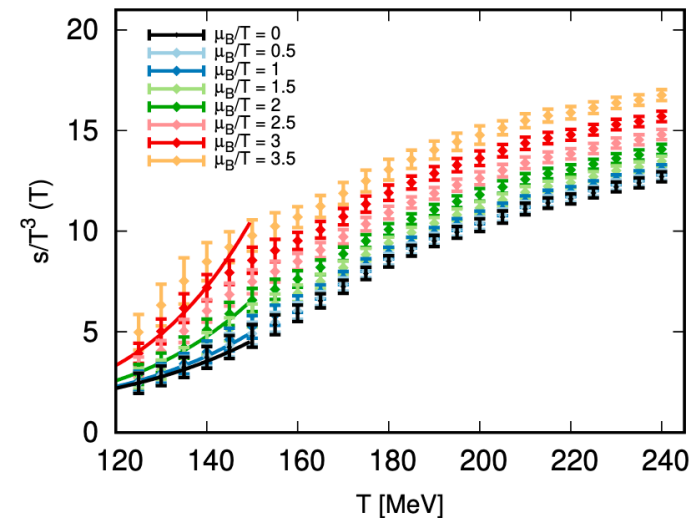
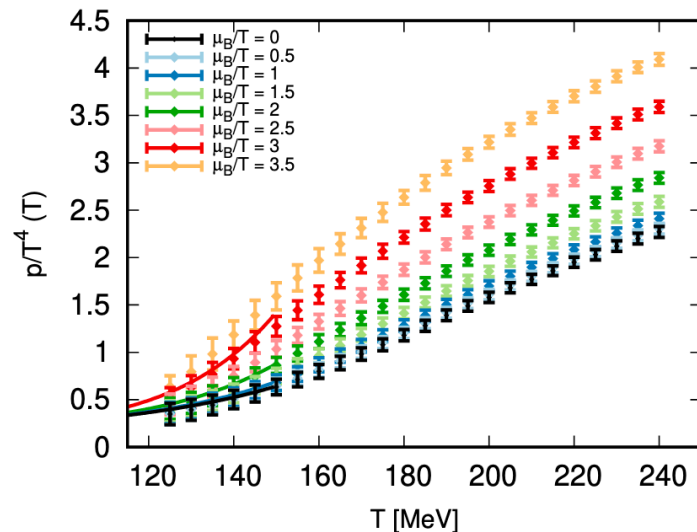
Observation: the temperature-dependence of baryonic density

$$n_B(T)/\bar{\hat{\mu}}_B = \chi_1^B(T, \hat{\mu}_B)/\bar{\hat{\mu}}_B$$

at finite imaginary chemical potential is just a shift in temperature from the $\mu_B = 0$ results for χ_2^B :

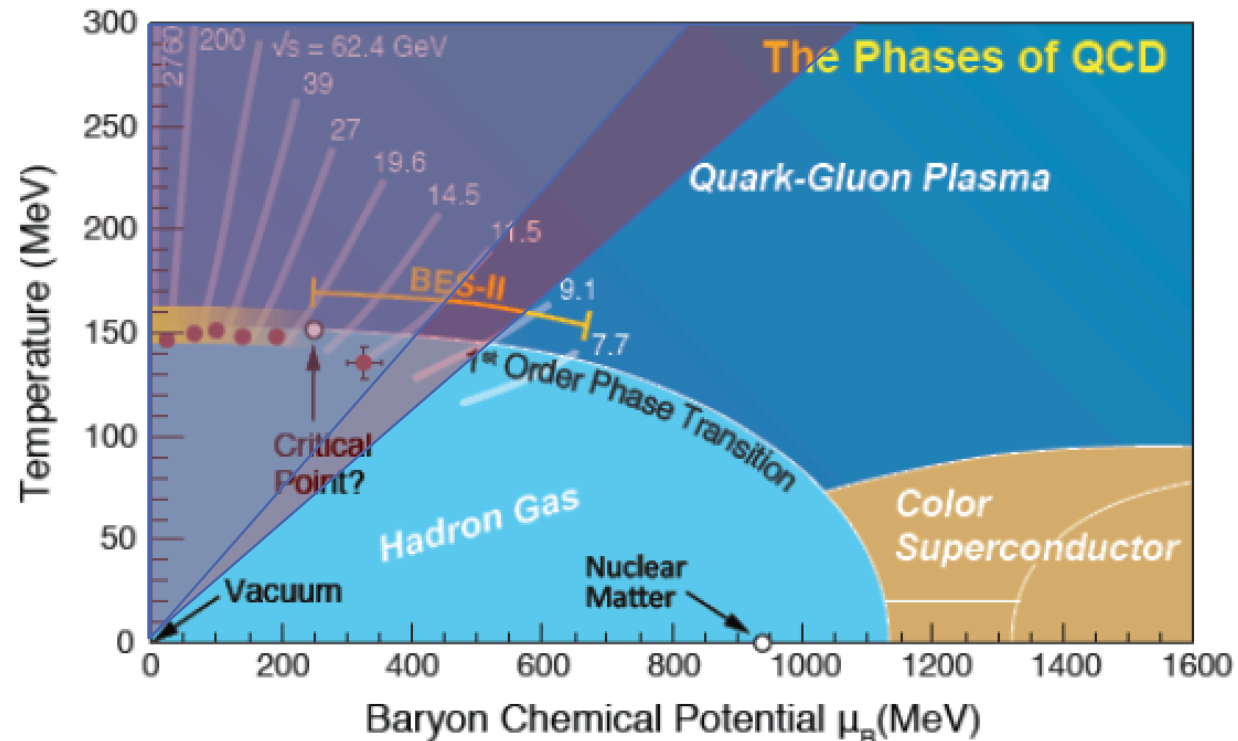
$$\frac{\chi_1^B(T, \hat{\mu}_B)}{\hat{\mu}_B} = \chi_2^B(T', 0),$$

$$T'(T, \hat{\mu}_B) = T \left(1 + \kappa_2^{BB}(T)\hat{\mu}_B^2 + \kappa_4^{BB}(T)\hat{\mu}_B^4 + \mathcal{O}(\hat{\mu}_B^6) \right)$$



New range of validity of equation of state

- New expansion scheme provides the equation of state for $\mu_B/T \leq 3.5$



- For comparison between the Taylor and new expansion scheme performance, see e.g. [M. Kahangirwe et al., 2408.04588](#)

→ Finding: the new scheme performs better with models that exhibit chiral critical scaling

Equation of state in 4D

- QCD has three conserved charges: Baryon Number B , Strangeness S and Electric Charge Q (or Isospin I)

- Heavy-ion collisions

- Global $S=0$
- Global $Q=0.4B$
- Local (large) fluctuations in the fluid cells with finite S and $Q \neq 0.4B$ possible

- Neutron Stars

- Global $Q=0$ for stability
- Strangeness is most likely not in equilibrium
- Finite isospin density

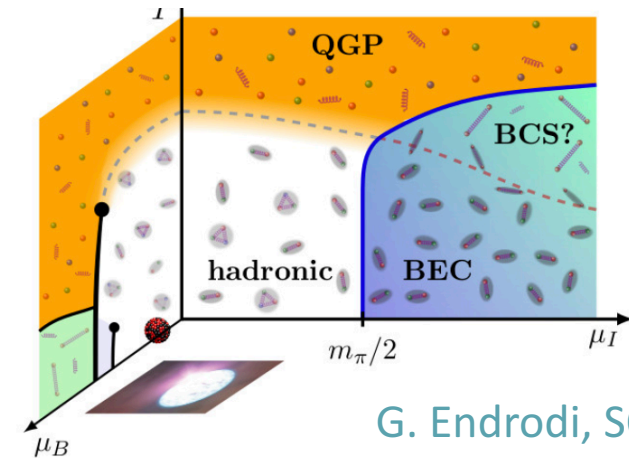
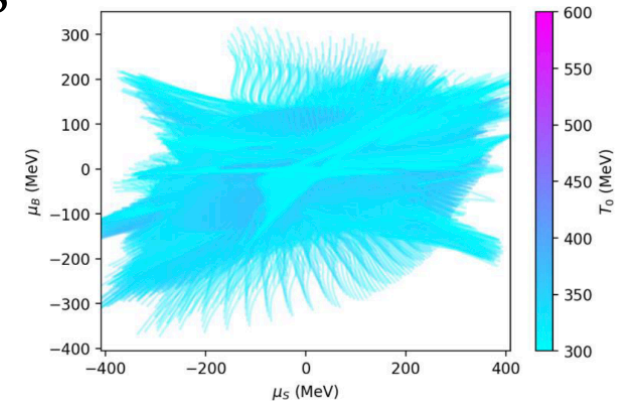
B. Brandt et al., JHEP (2023)

- Cosmological trajectories

- Large lepton flavor asymmetries possible \rightarrow large asymmetries between quark flavors (lead to finite B , Q , S values)
- How would the critical point move in the 4D phase diagram?
- First-order cosmological phase transition could lead to stable strange quark matter droplets + gravitational waves similar to those observed recently by NANOGrav

A. Bodmer, PRD (1971); E. Witten, PRD (1984); F. Di Clemente, C. R. et al, 2404.12094

C. Plumberg et al., 2405.09648



G. Endrodi, SQM2024

Gao & Oldengott, PRL (2022)

Lattice QCD EoS in 4D from Taylor expansion

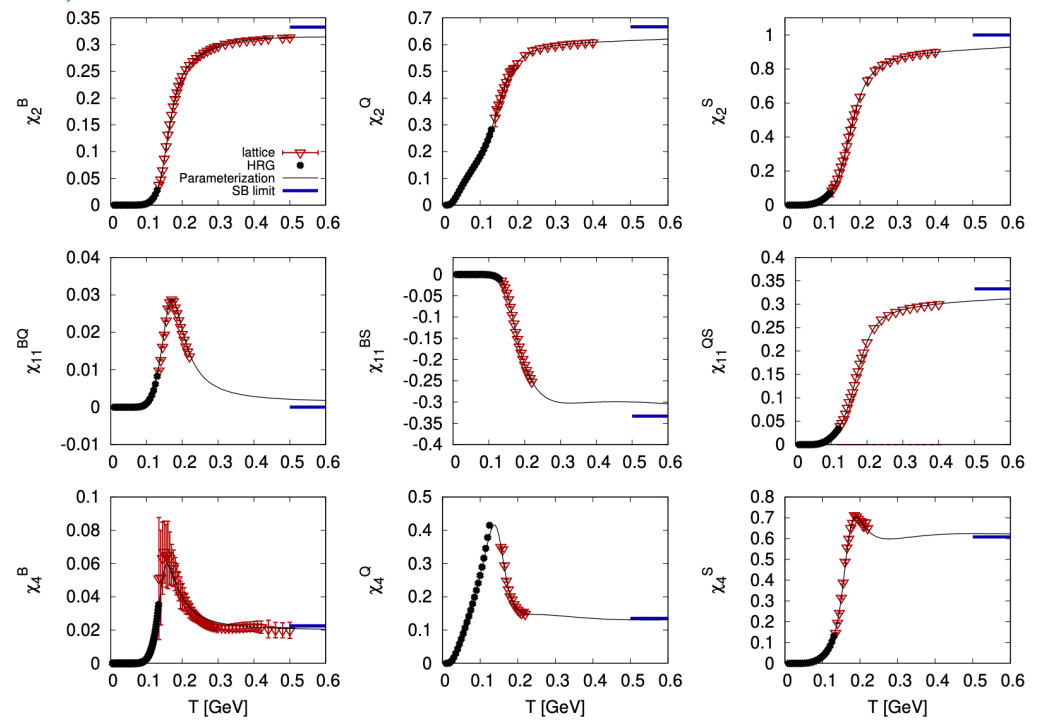
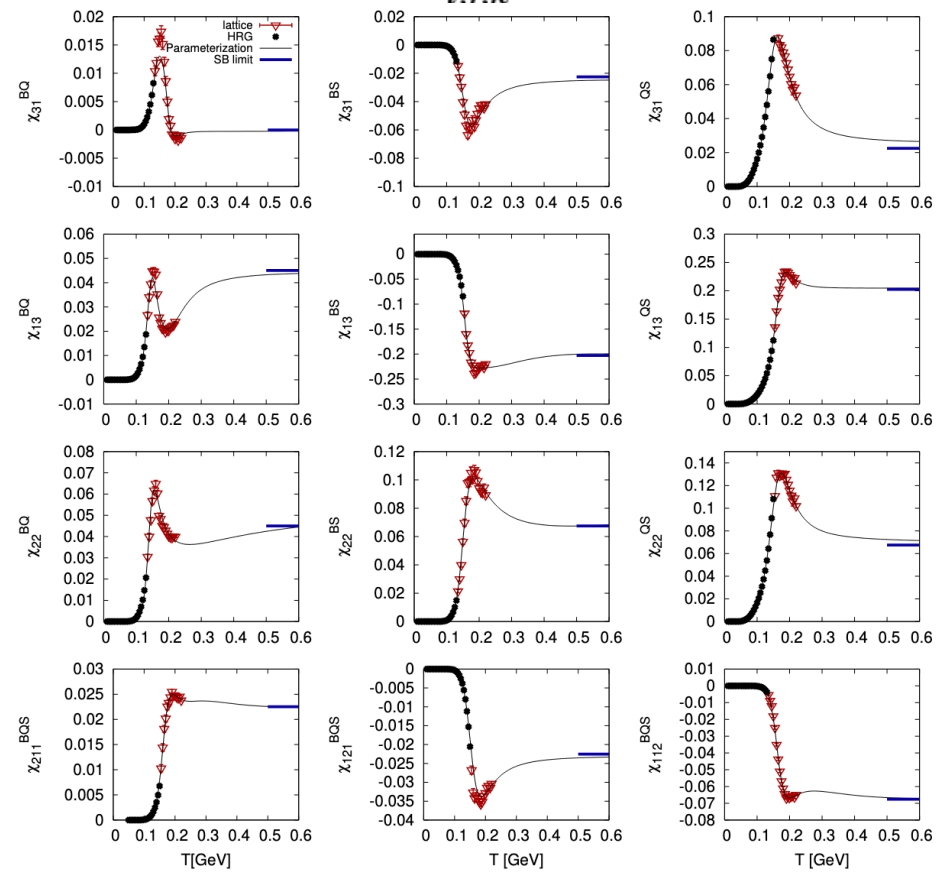


- One can generalize the Taylor expansion to 3 conserved charges

Talk by A. Monnai on Wednesday

$$\frac{P(T, \hat{\mu}_B, \hat{\mu}_S, \hat{\mu}_Q)}{T^4} = \sum_{i,j,k} \frac{1}{i!j!k!} \chi_{ijk}^{BSQ}(T) \hat{\mu}_B^i \hat{\mu}_S^j \hat{\mu}_Q^k \quad \left(\text{with } \hat{\mu}_i = \frac{\mu_i}{T}\right) \quad \text{where} \quad \chi_{ijk}^{BQS}(T) = \left. \frac{\partial^{i+j+k}(P/T^4)}{\partial \hat{\mu}_B^i \hat{\mu}_S^j \hat{\mu}_Q^k} \right|_{\hat{\mu}_B, \hat{\mu}_S, \hat{\mu}_Q = 0}$$

J. Noronha-Hostler, C. R. et al., PRC (2019); A. Monnai et al., PRC (2019), A. Monnai et al., 2406.11610



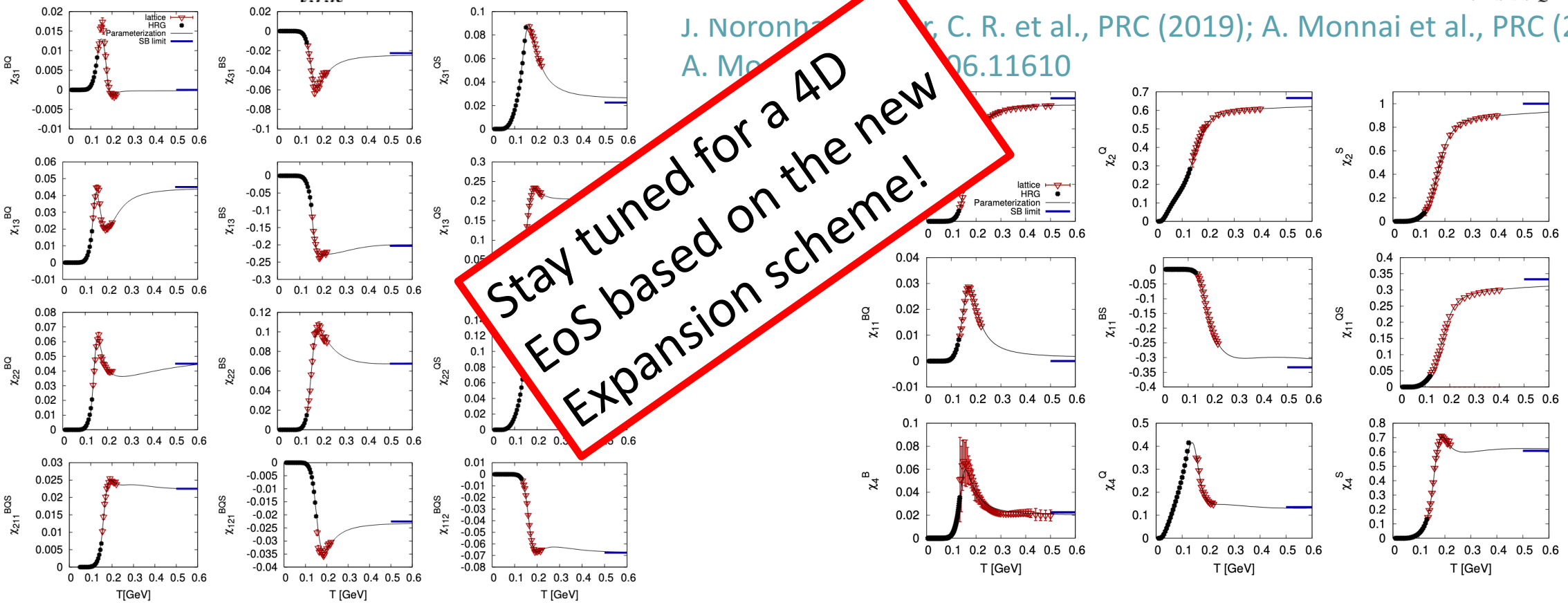
Lattice QCD EoS in 4D from Taylor expansion

- One can generalize the Taylor expansion to 3 conserved charges

Talk by A. Monnai on Wednesday

$$\frac{P(T, \hat{\mu}_B, \hat{\mu}_S, \hat{\mu}_Q)}{T^4} = \sum_{i,j,k} \frac{1}{i!j!k!} \chi_{ijk}^{BSQ}(T) \hat{\mu}_B^i \hat{\mu}_S^j \hat{\mu}_Q^k \quad \left(\text{with } \hat{\mu}_i = \frac{\mu_i}{T}\right) \quad \text{where} \quad \chi_{ijk}^{BQS}(T) = \left. \frac{\partial^{i+j+k}(P/T^4)}{\partial \hat{\mu}_B^i \hat{\mu}_S^j \hat{\mu}_Q^k} \right|_{\hat{\mu}_B, \hat{\mu}_S, \hat{\mu}_Q=0}$$

J. Noronha-Neto, C. R. et al., PRC (2019); A. Monnai et al., PRC (2019), A. Monnai et al., PRD (2019) 100.11610



QCD transition line from the lattice

$$\frac{T_c(\mu_B)}{T_c(\mu_B = 0)} = 1 - \kappa_2 \left(\frac{\mu_B}{T_c(\mu_B)} \right)^2 - \kappa_4 \left(\frac{\mu_B}{T_c(\mu_B)} \right)^4$$

Observables and results

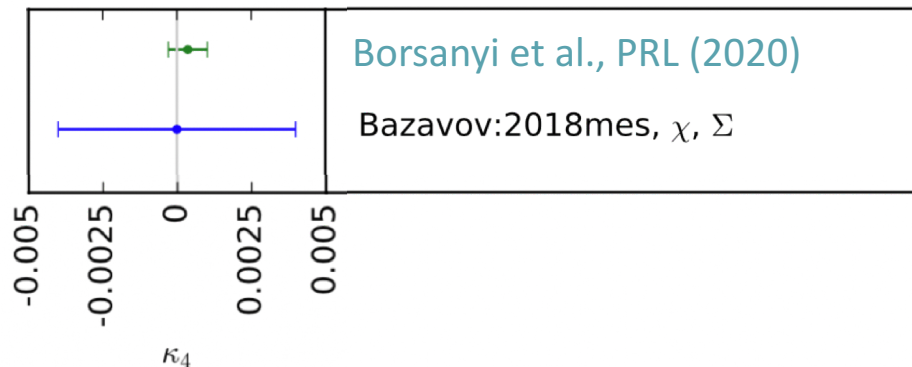
- We consider the following chiral observables:

$$\langle \bar{\psi}\psi \rangle = - [\langle \bar{\psi}\psi \rangle_T - \langle \bar{\psi}\psi \rangle_0] \frac{m_{ud}}{f_\pi^4},$$

$$\chi = [\chi_T - \chi_0] \frac{m_{ud}^2}{f_\pi^4}, \quad \text{with}$$

$$\langle \bar{\psi}\psi \rangle_{T,0} = \frac{T}{V} \frac{\partial \log Z}{\partial m_{ud}} \quad \chi_{T,0} = \frac{T}{V} \frac{\partial^2 \log Z}{\partial m_{ud}^2}$$

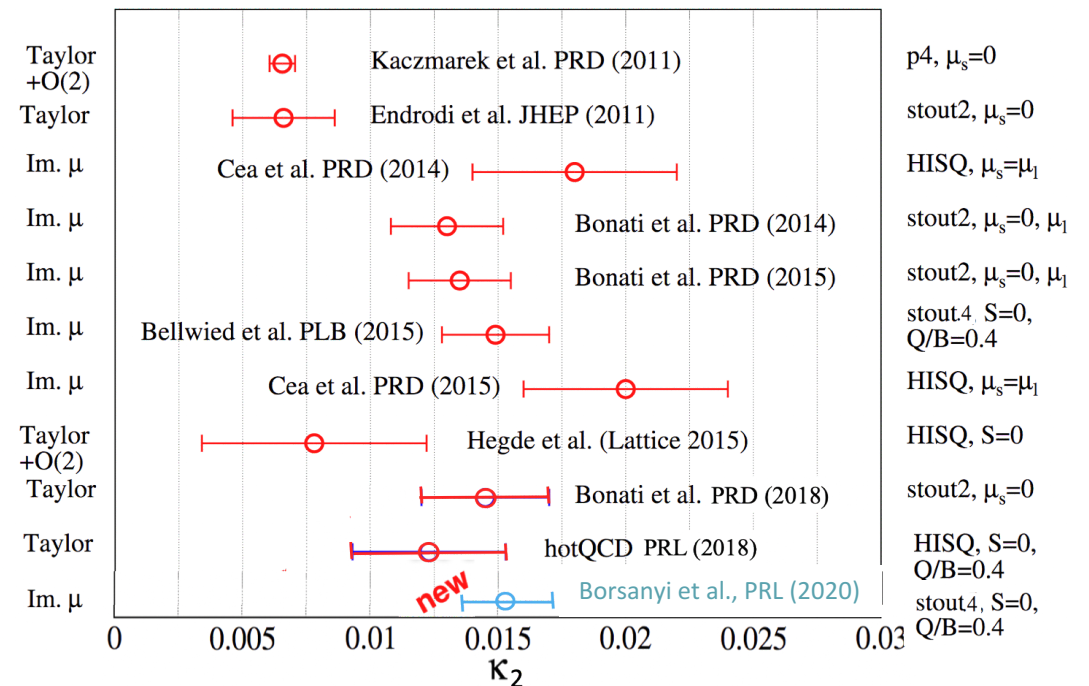
- The peak position of the susceptibility serves as a definition for the chiral cross-over temperature



$$T_c(LT = 4, \mu_B = 0) = 158.0 \pm 0.6 \text{ MeV}$$

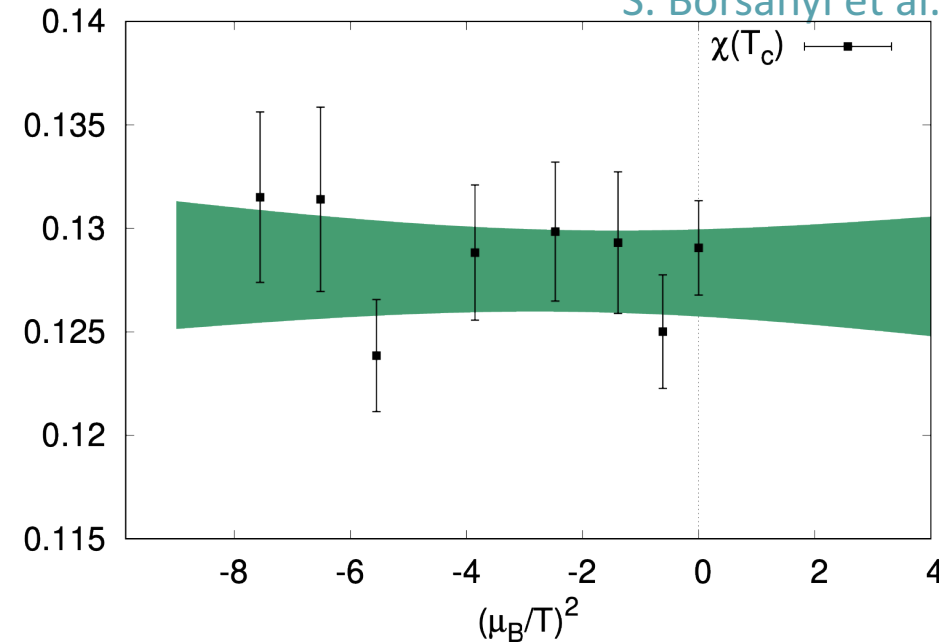
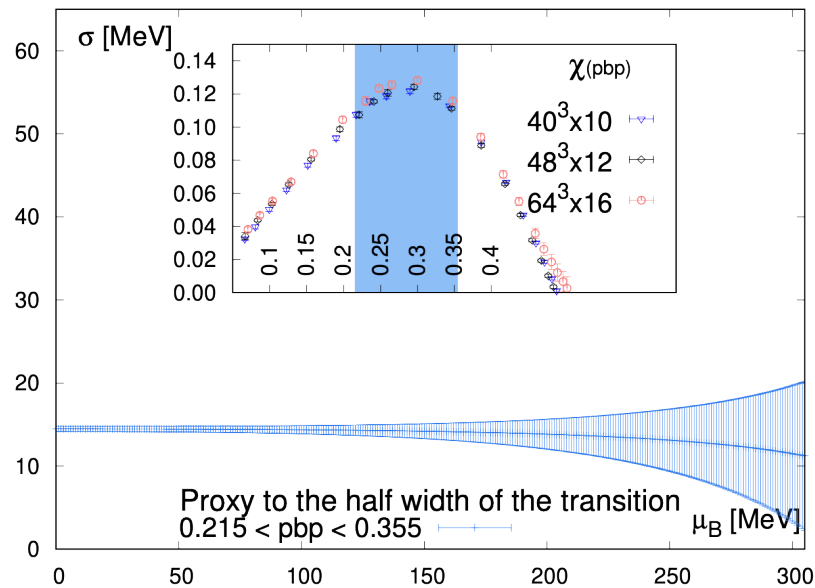
$$\kappa_2 = 0.0153 \pm 0.0018,$$

$$\kappa_4 = 0.00032 \pm 0.00067$$



Width and strength of the transition

S. Borsanyi et al., PRL 2020

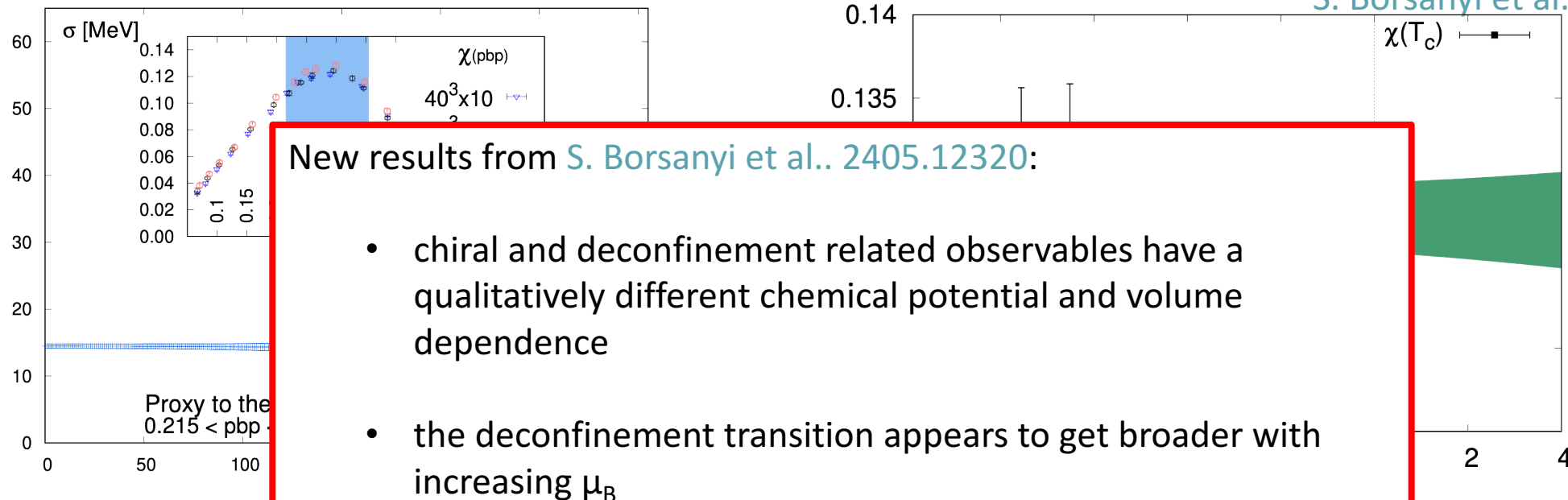


- The width of the transition is constant up to $\mu_B \sim 300$ MeV
- Height of the peak of the chiral susceptibility at the crossover temperature: proxy for the strength of the crossover \rightarrow Also constant up to $\mu_B \sim 300$ MeV
 - \rightarrow Critical point strongly disfavored for $\mu_B < 300$ MeV

Talk by F. Rennecke on Monday for lattice estimates of CP location based on Lee-Yang singularities

Width and strength of the transition

S. Borsanyi et al., PRL 2020



New results from S. Borsanyi et al.. 2405.12320:

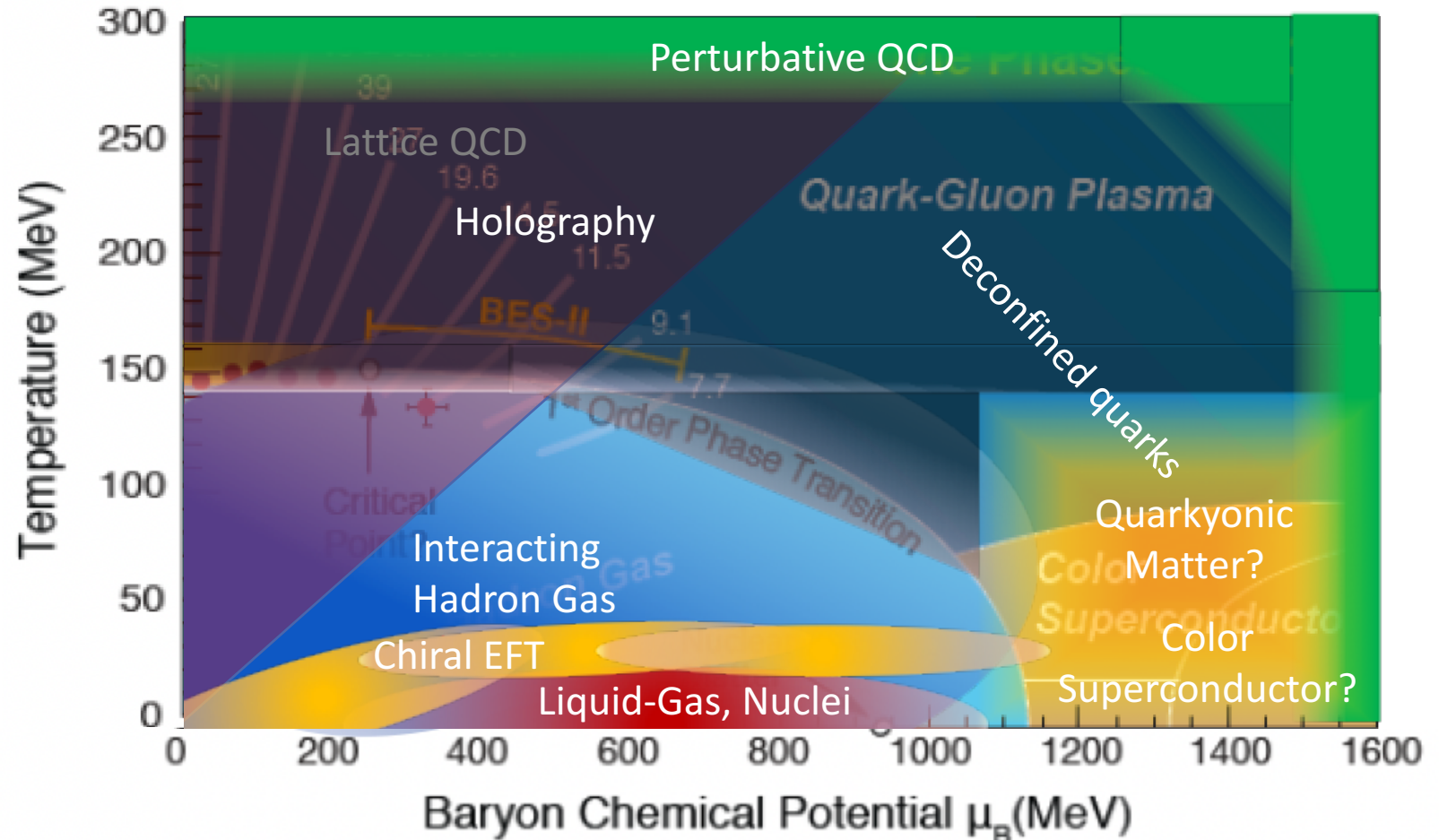
- chiral and deconfinement related observables have a qualitatively different chemical potential and volume dependence
- the deconfinement transition appears to get broader with increasing μ_B

- The width of the transition is constant up to $\mu_B \sim 300$ MeV
- Height of the peak of the chiral susceptibility at the crossover temperature: proxy for the strength of the crossover \rightarrow Also constant up to $\mu_B \sim 300$ MeV
 - \rightarrow Critical point strongly disfavored for $\mu_B < 300$ MeV

Talk by F. Rennecke on Monday for lattice estimates of CP location based on Lee-Yang singularities

Different approaches to the QCD Equation of State

- Lattice QCD is limited
- We need to merge the lattice QCD equation of state with other effective theories
- Careful study of their respective range of validity
- Constrain the parameters to reproduce known limits
- Test different possibilities and validate/exclude them



Lattice QCD: WB: PLB (2014)
 Interacting HRG: V. Vovchenko et al., PRL (2017)
 Liquid-gas, Nuclei: see e.g. Du et al. PRC (2019)
 Chiral EFT: see e.g. Holt, Kaiser, PRD (2017)
 Holography: see e.g. R. Critelli et al., PRD (2017)

pQCD: Andersen et al., PRD (2002); Annala et al., Nat. Ph. (2020)
 quarks: Dexheimer et al., PRC (2009); Baym et al., Astr. J. (2019)
 quarkyonic: McLerran, Pisarski NPA (2007)
 CSC: Alford et al., PLB (1998); Rapp et al., PRL (1998).

Examples of phenomenological approaches

Holographic model

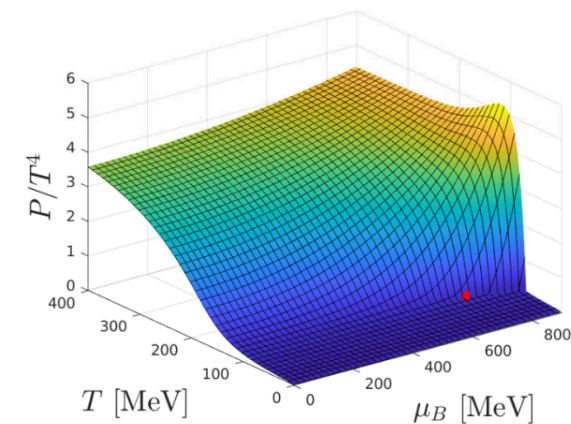
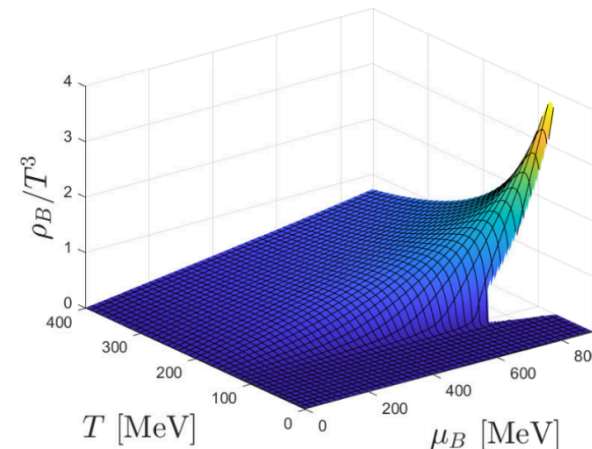
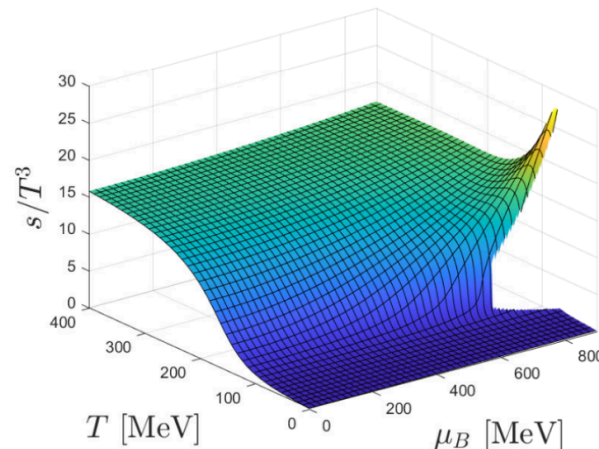
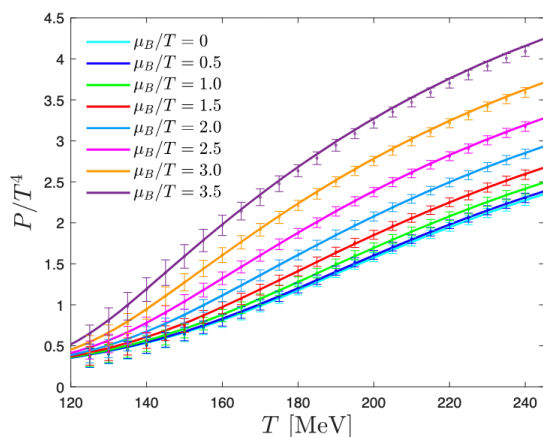
- “Black hole engineering”: tweak holographic model to reproduce lattice QCD results

S. S. Gubser and A. Nellore, PRD (2008)
 O. DeWolfe, S. S. Gubser and C. Rosen, PRD (2011)
 R. Critelli, C. R., et al., PRD (2017)
 J. Grefa, C. R. et al. PRD (2021)

- Action:

$$S = \frac{1}{2\kappa_5^2} \int_{\mathcal{M}_5} d^5x \sqrt{-g} \left[R - \frac{(\partial_\mu \phi)^2}{2} - V(\phi) - \frac{f(\phi) F_{\mu\nu}^2}{4} \right]$$

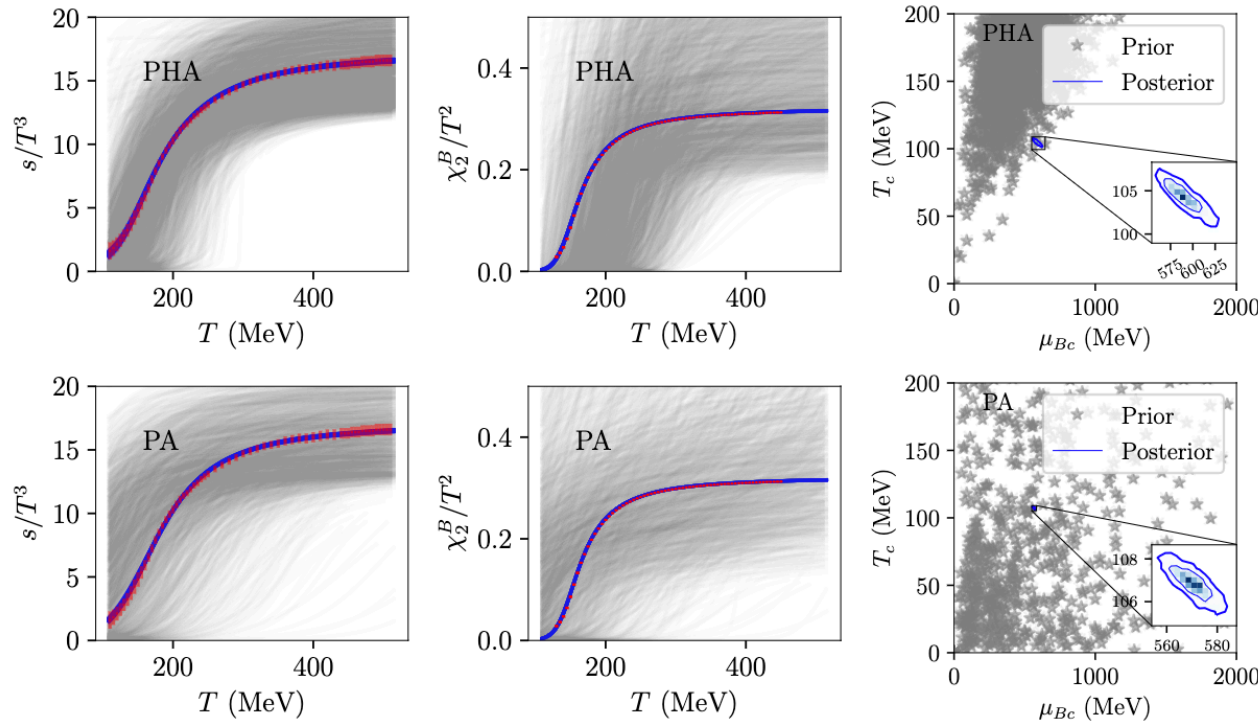
- Two potentials: $V(\phi)$ and $f(\phi)$, tweaked to fit lattice QCD results
- Reproduces lattice EoS where available, but extends it to $\mu_B \sim 900$ MeV.



Bayesian location of QCD critical point from holographic model

M. Hippert, C. R. et al, arXiv:2309.00579.

- Flat prior for parameters
- 20% of prior samples give no critical point



Polynomial-Hyperbolic Ansatz (PHA)

$$V(\phi) = -12 \cosh(\gamma \phi) + b_2 \phi^2 + b_4 \phi^4 + b_6 \phi^6$$

$$f(\phi) = \frac{\text{sech}(c_1 \phi + c_2 \phi^2 + c_3 \phi^3)}{1 + d_1} + \frac{d_1}{1 + d_1} \text{sech}(d_2 \phi)$$

Parametric Ansatz (PA)

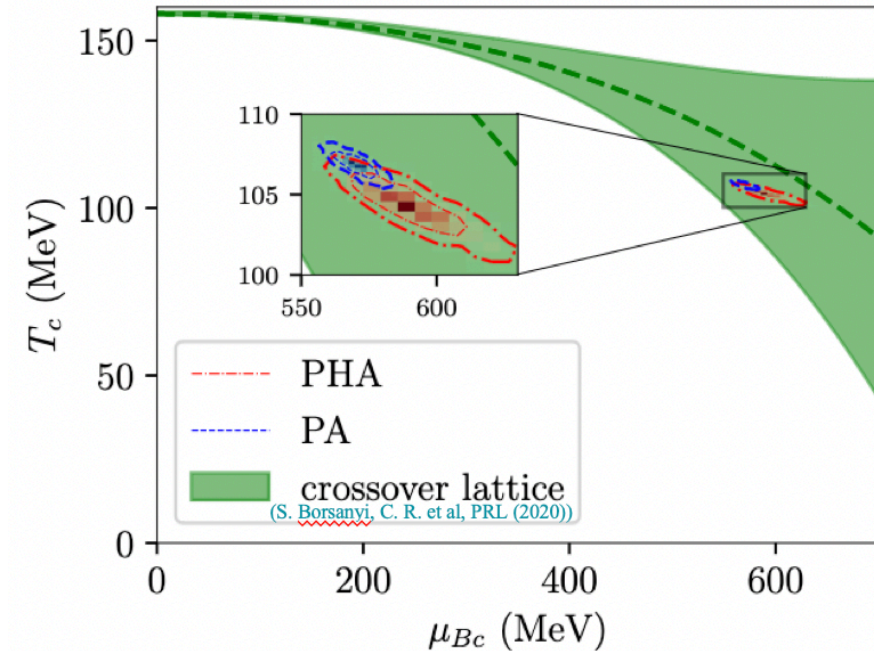
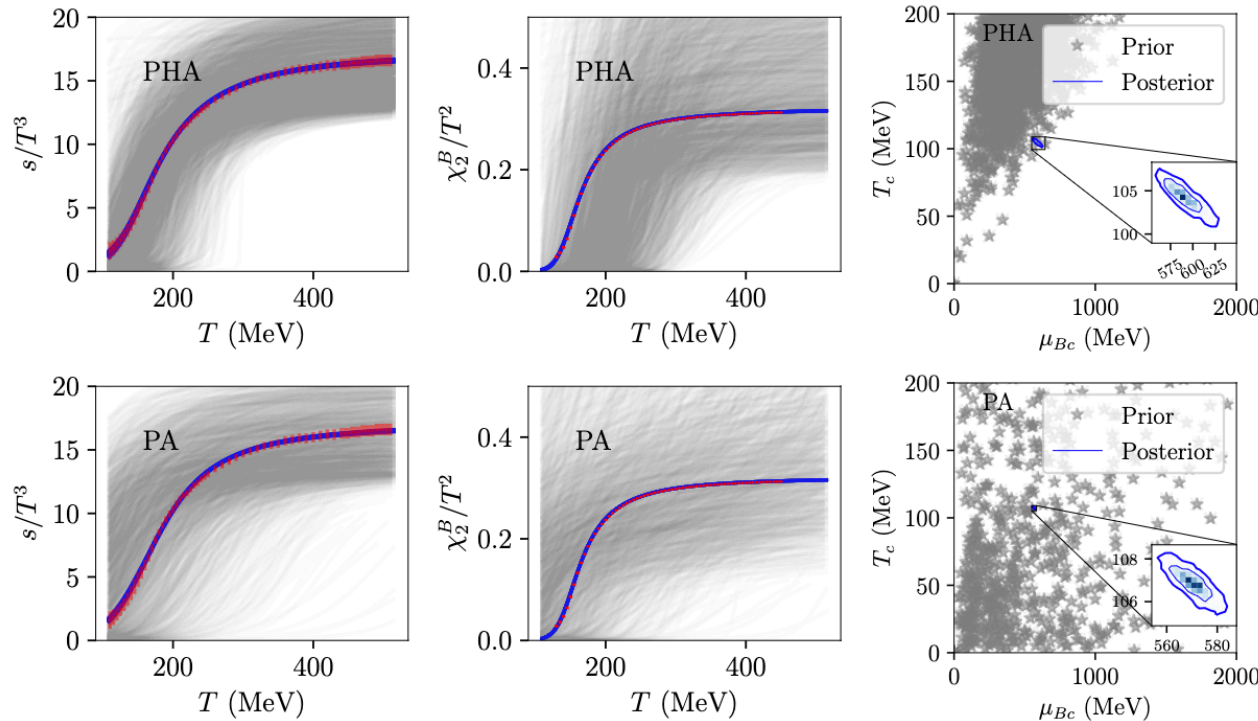
$$V(\phi) = -12 \cosh \left[\left(\frac{\gamma_1 \Delta \phi_V^2 + \gamma_2 \phi^2}{\Delta \phi_V^2 + \phi^2} \right) \phi \right]$$

$$f(\phi) = 1 - (1 - A_1) \left[\frac{1}{2} + \frac{1}{2} \tanh \left(\frac{\phi - \phi_1}{\delta \phi_1} \right) \right] - A_1 \left[\frac{1}{2} + \frac{1}{2} \tanh \left(\frac{\phi - \phi_2}{\delta \phi_2} \right) \right]$$

Bayesian location of QCD critical point from holographic model

M. Hippert, C. R. et al, arXiv:2309.00579.

- Flat prior for parameters
- 20% of prior samples give no critical point



Both Ansätze overlap at 1σ . **Robust results!**
 Similar locations are found in FRG, DSE and lattice estimates

Talk by F. Rennecke on Monday

$$(T_c, \mu_{Bc})_{PHA} = (104 \pm 3, 589^{+36}_{-26}) \text{ MeV}, \quad (T_c, \mu_{Bc})_{PA} = (107 \pm 1, 571 \pm 11) \text{ MeV}$$

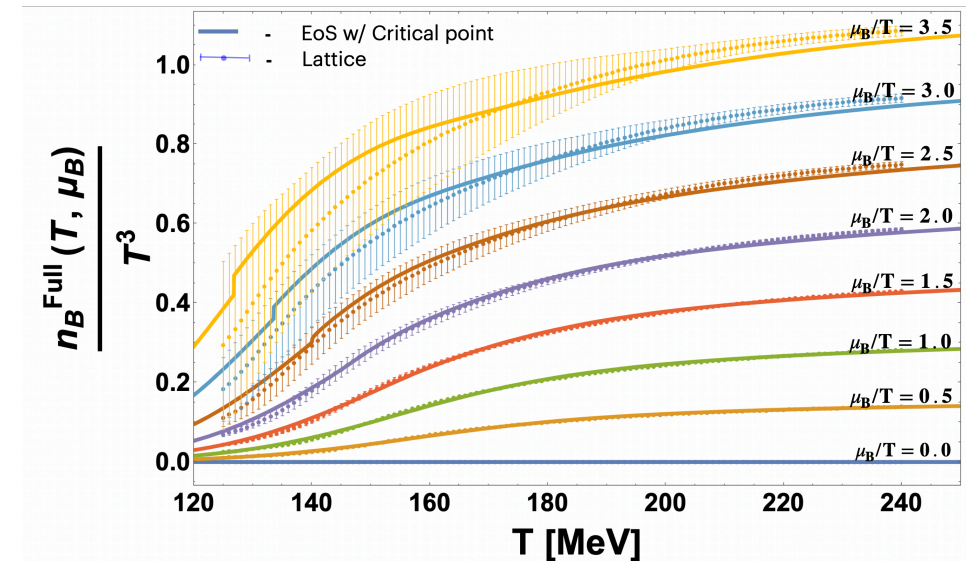
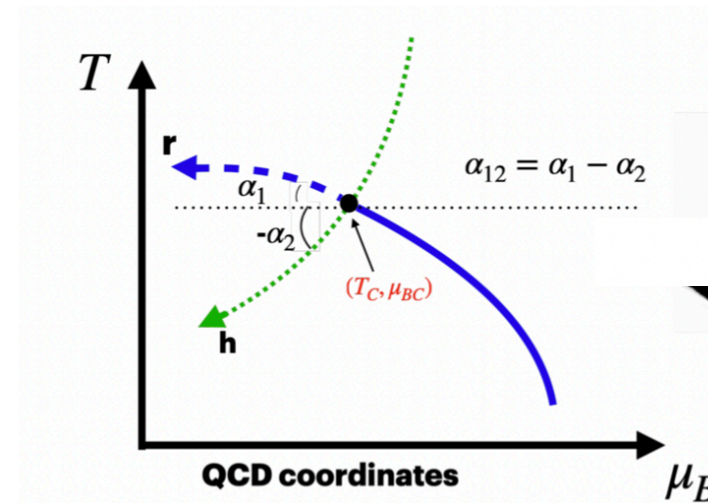
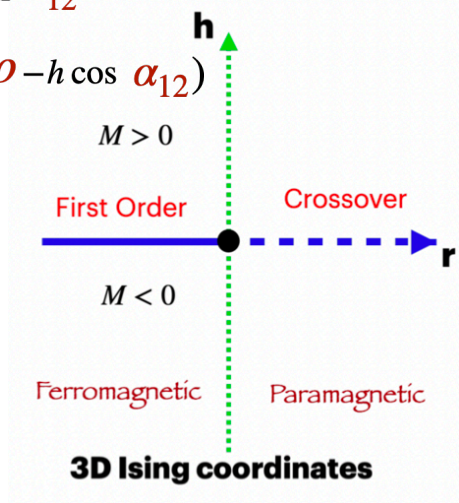
New expansion scheme + 3D-Ising critical point

- Build a family of Equations of State that:
 - Match the lattice QCD one where available
 - Contain a critical point in the 3D-Ising model universality class
 - Have a set of tunable parameters that can be fixed in Bayesian analyses of heavy-ion data

P. Parotto, C. R. et al., PRC (2020)
J. Karthein, C. R. et al., EPJ Plus (2021)

$$\frac{T - T_0}{T_0} = w h \sin \alpha_{12}$$

$$\frac{\mu_B^2 - \mu_{BC}^2}{T_0^2} = w(-r\rho - h \cos \alpha_{12})$$



M. Kahangirwe, C. R. et al., PRD (2024)

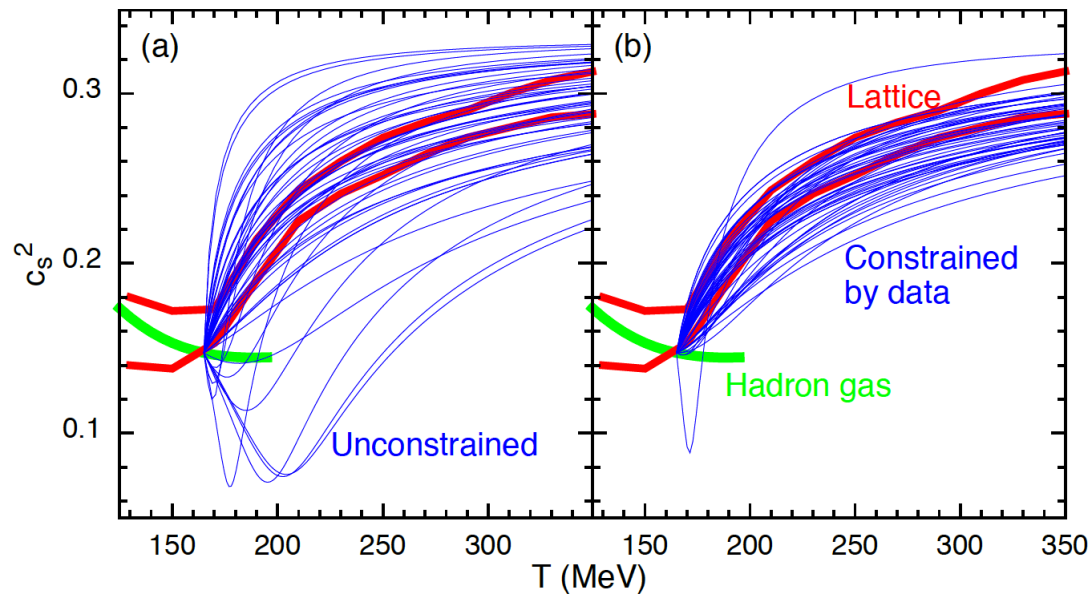
User Input $\mu_{BC}, w, \rho, \alpha_{12}$

Lessons from heavy-ion collisions

See also speed of sound results from CMS collaboration

- Extract EoS from data through Bayesian analyses

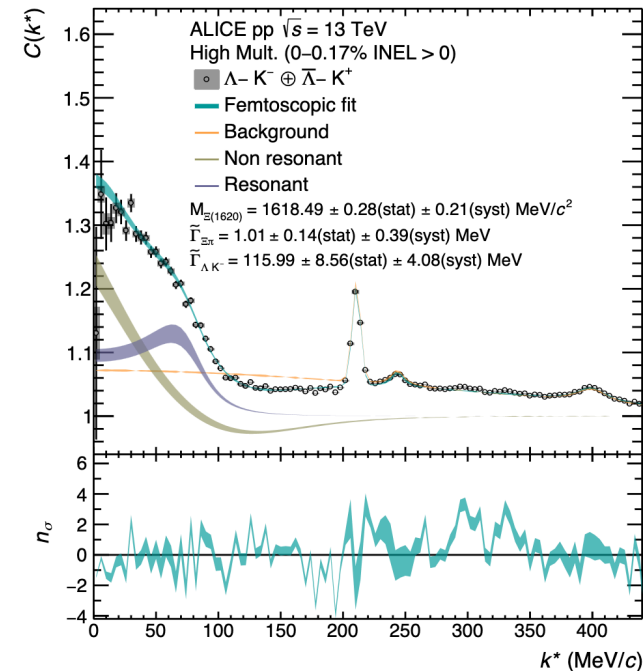
S. Pratt et al., PRL (2015)



- Comparison of data from HICs to theoretical models through Bayesian analysis
- The posterior distribution of EoS is consistent with the lattice QCD one

- Extract hadronic interactions from data

ALICE, PLB (2023)

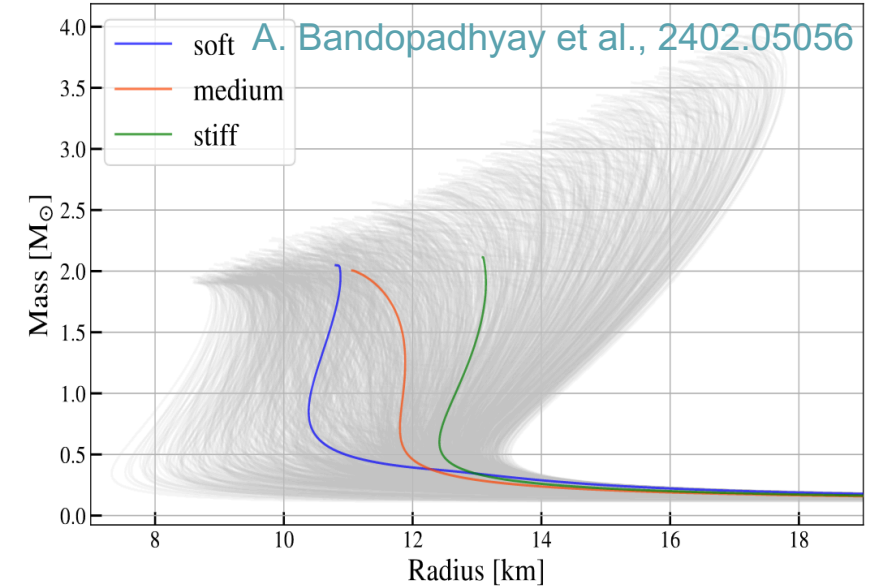
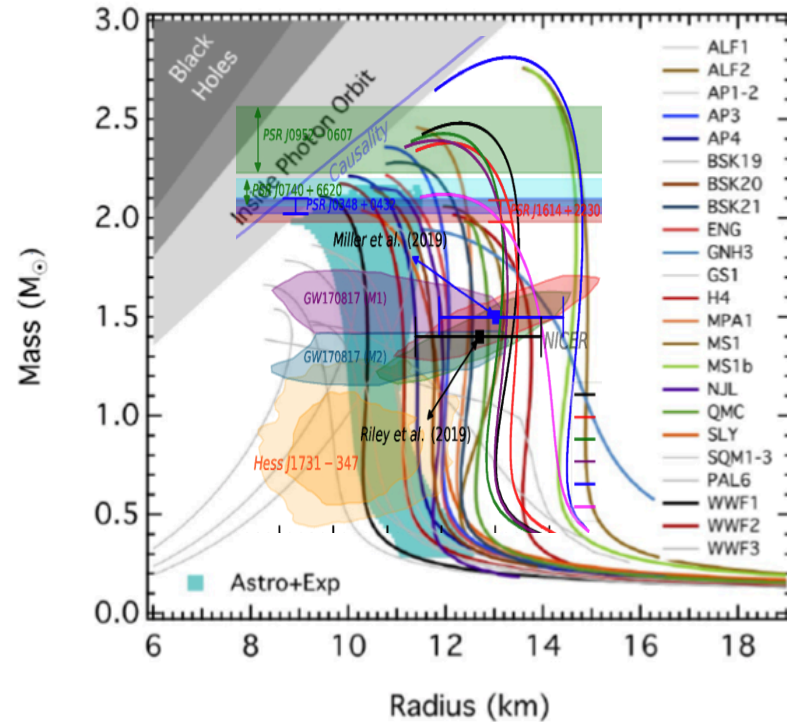
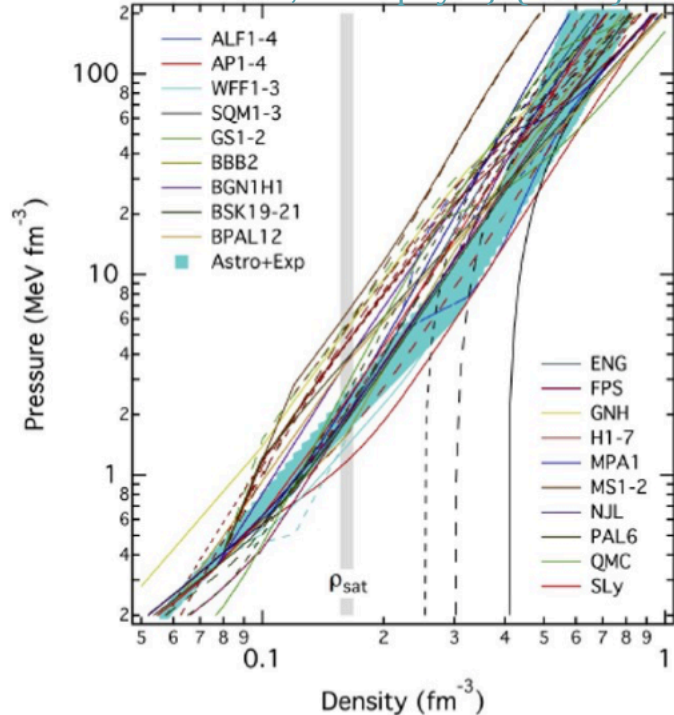


- Access interaction e.g. between Λ and kaons with femtoscopy at the LHC

Talk by T. Hatsuda on Monday and by T. Hyodo on Tuesday

Lessons from Neutron Stars

F. Ozel et al., *Astrophys. J.* (2016)



Detector network	Soft EoS	Medium EoS	Stiff EoS
LIGO-Virgo	$2e5^{+4e4}_{-4e4}$	$5e4^{+1e4}_{-1e4}$	7000^{+900}_{-900}
3 A [#]	300^{+50}_{-50}	100^{+40}_{-40}	20^{+4}_{-4}
CE20	21^{+10}_{-10}	15^{+7}_{-7}	3^{+1}_{-1}
CE40	12^{+3}_{-3}	8^{+1}_{-1}	$1^{+0.6}_{-0.6}$
CE40+2 A [#]	9^{+4}_{-4}	6^{+2}_{-2}	$0.4^{+0.2}_{-0.2}$
CE40+CE20+A [#]	5^{+2}_{-2}	3^{+1}_{-1}	$0.2^{+0.07}_{-0.07}$

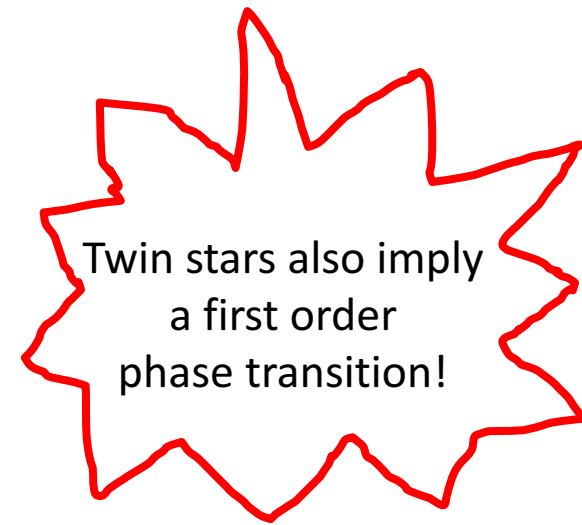
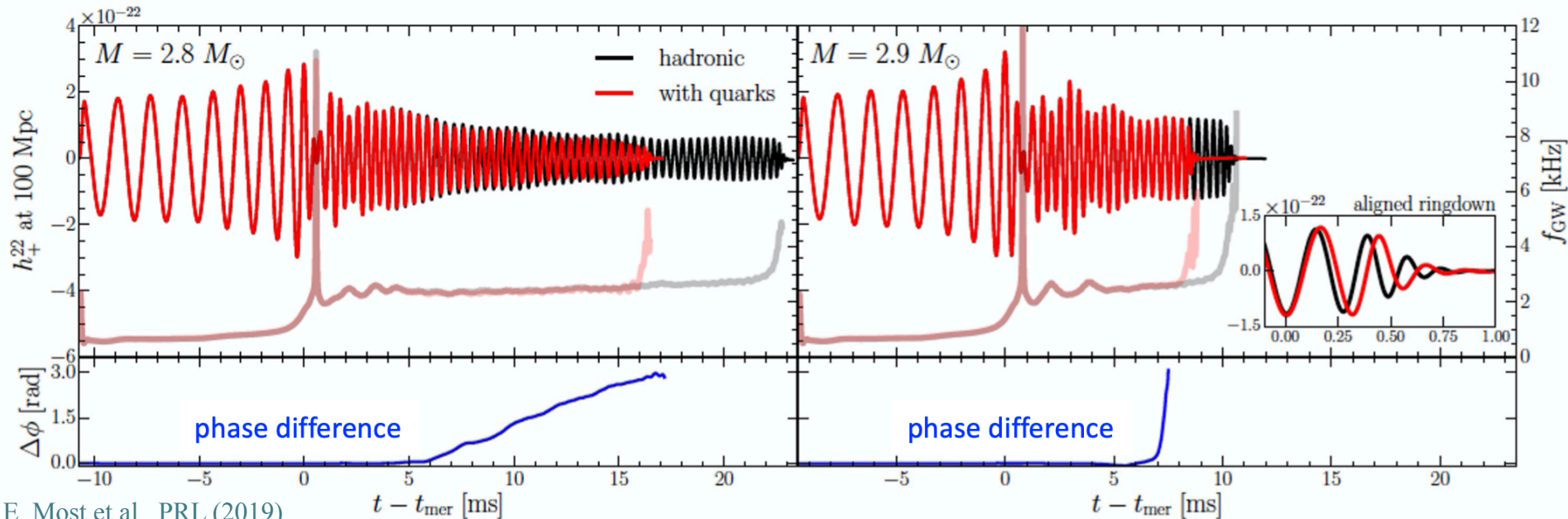
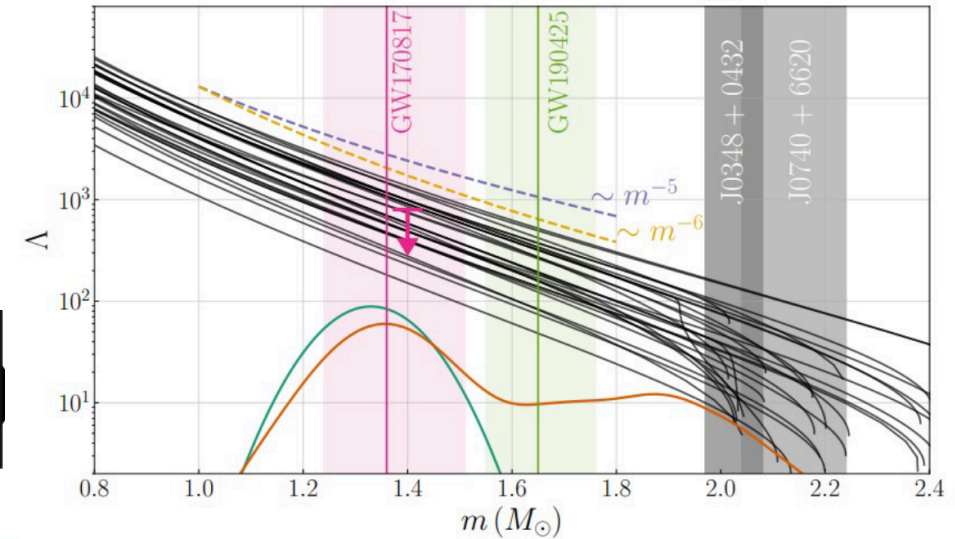
- Current uncertainty on NS radius measurements are large
- CE network will achieve an uncertainty of 10 m very quickly
- Narrowing down the equation of state still requires understanding the underlying nuclear physics

Lessons from mergers

- Tidal deformability sensitive to EoS
- Post-merger signal sensitive to order of the phase transition
- Next generation observatories will be able to detect it!



Talk by P. Lasky on Tuesday

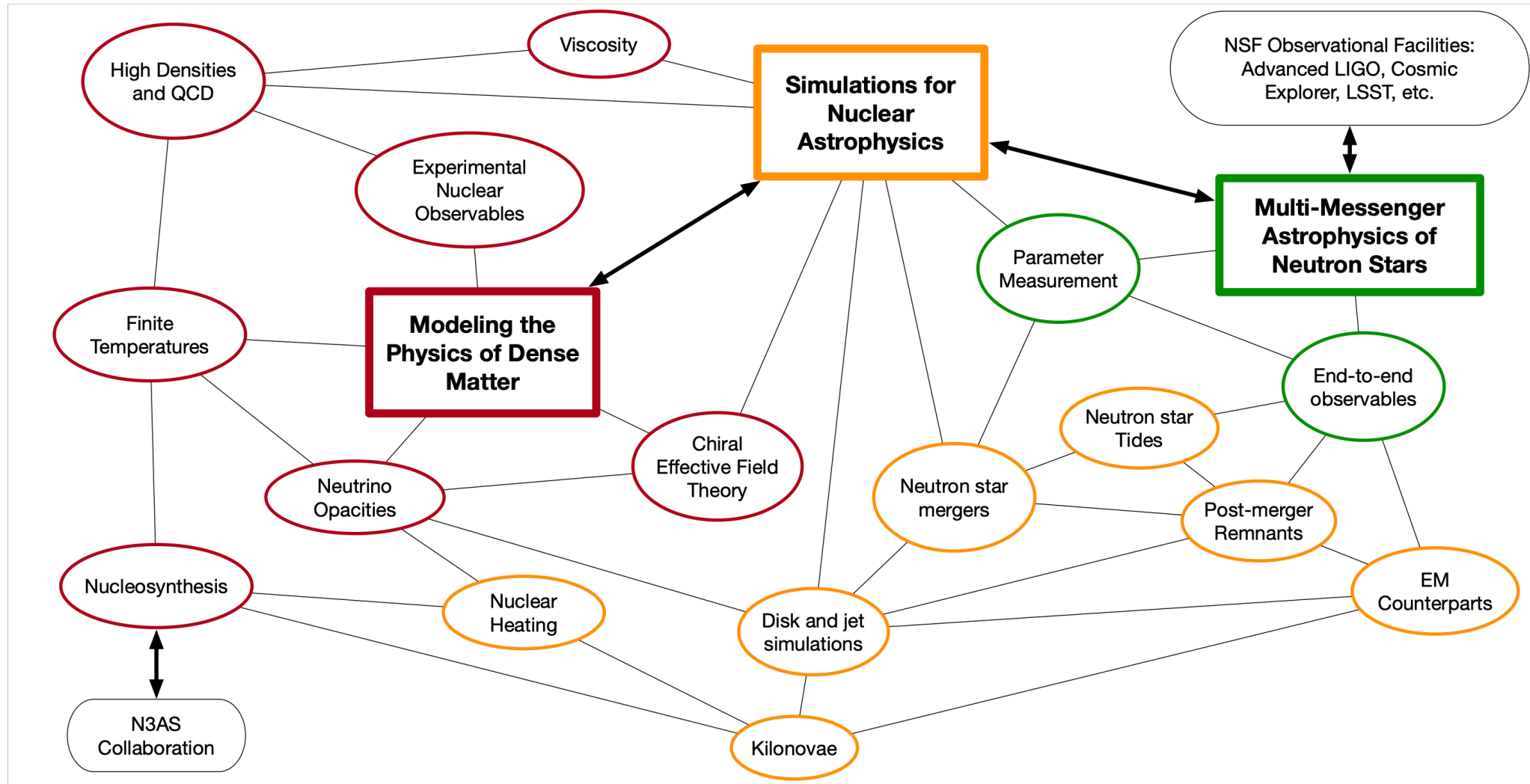


Talk by D. Blaschke on Tuesday

E. Most et al., PRL (2019)

The Problem is Too Big For One Group

Progress needs a **close, coordinated, and sustained** collaboration across different research groups



Conclusions

- State of the art results on QCD Equation of State and phase diagram from first principles
- Continued effort to increase density coverage
- Need to be complemented by phenomenological approaches
- Data from terrestrial and celestial experiments can help to validate/rule out models or fix their parameters

Backup slides

QCD matter under extreme conditions

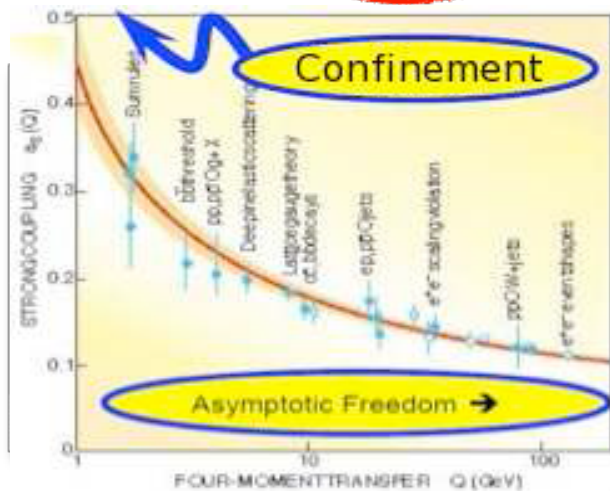
To address these questions, we need fundamental theory and experiment

Theory: Quantum Chromodynamics

- ▶ QCD is the fundamental theory of strong interactions
- ▶ It describes interactions among quarks and gluons

$$L_{QCD} = \sum_{i=1}^{n_f} \bar{\psi}_i \gamma_\mu \left(i\partial^\mu - g A_a^\mu \frac{\lambda_a}{2} \right) \psi_i - m_i \bar{\psi}_i \psi_i - \frac{1}{4} \sum_a F_a^{\mu\nu} F_a^{\mu\nu}$$

$$F_a^{\mu\nu} = \partial^\mu A_a^\nu - \partial^\nu A_a^\mu + i f_{abc} A_b^\mu A_c^\nu$$



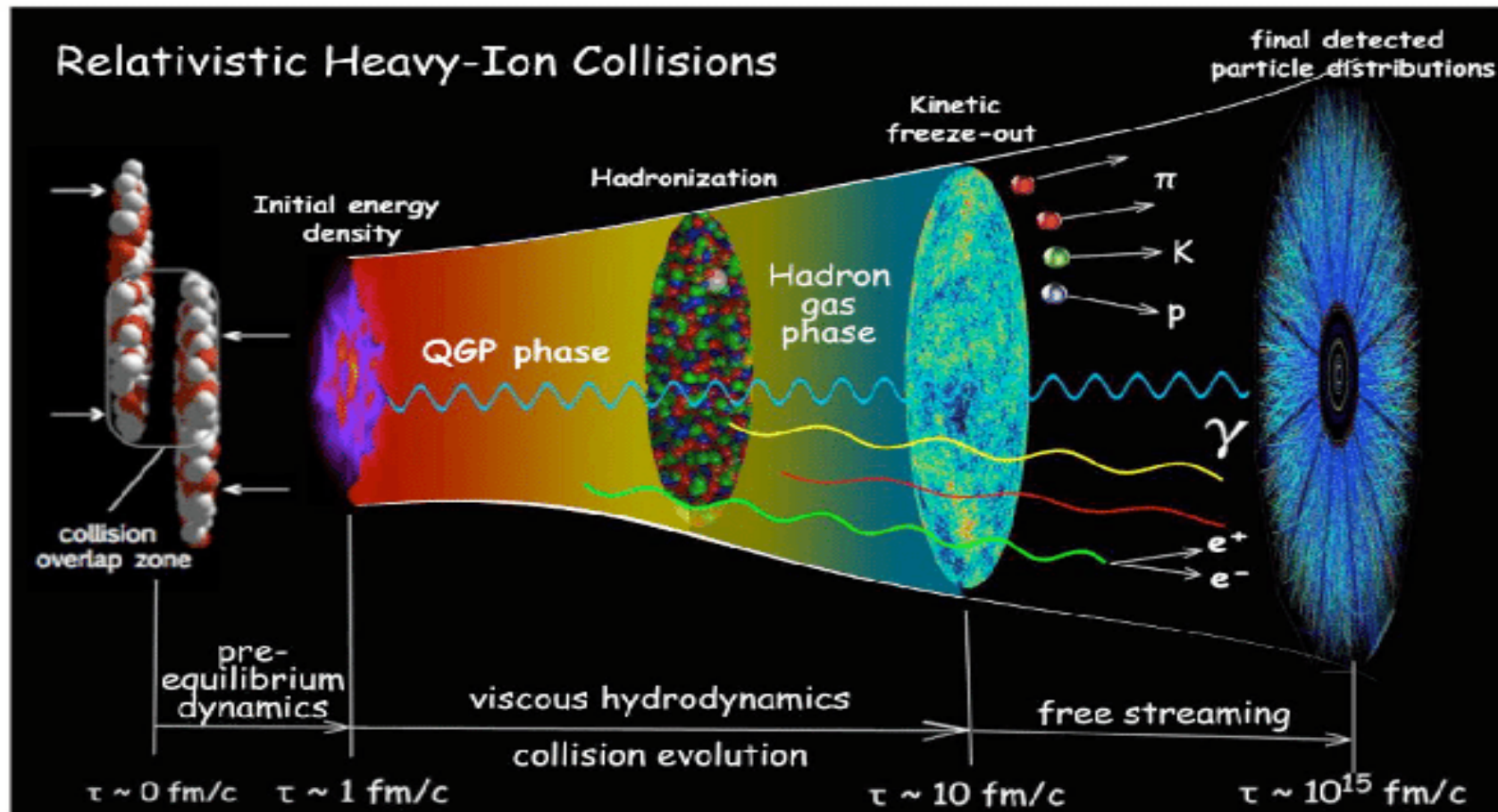
Experiment: heavy-ion collisions



- ▶ Quark-Gluon Plasma (QGP) discovery at RHIC and LHC:
- ▶ SURPRISE!!! QGP is a **PERFECT FLUID**
- ▶ Changes our idea of QGP (no weak coupling)
- ▶ Microscopic origin still unknown



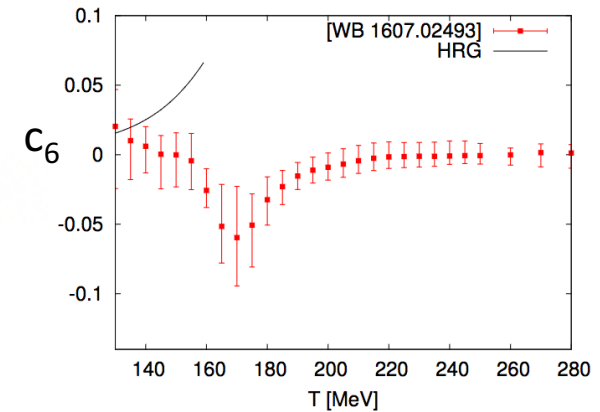
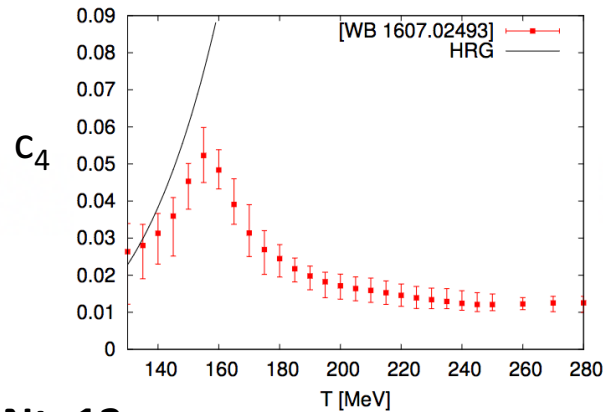
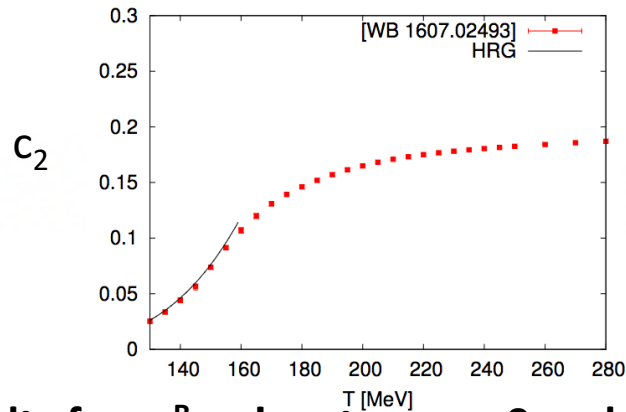
Anatomy of a heavy-ion collision



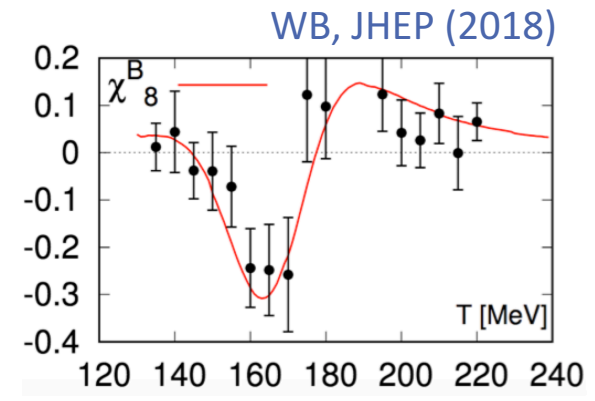
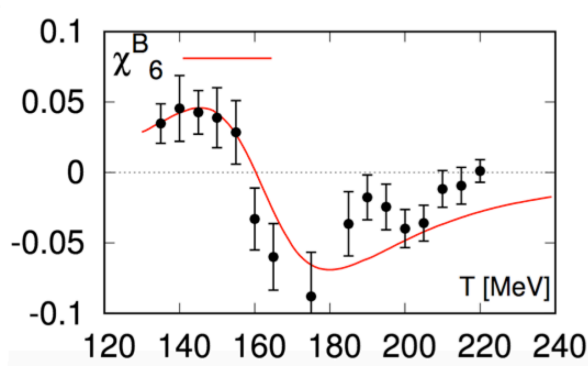
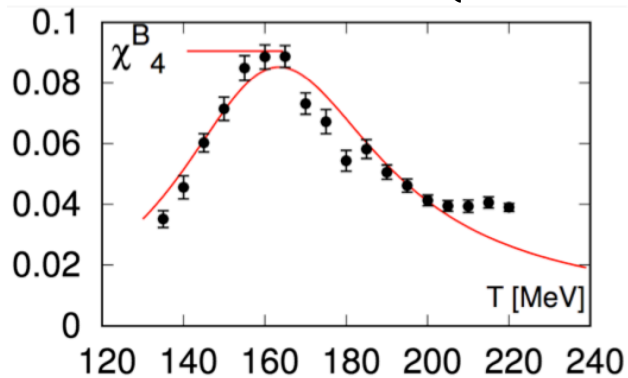
Pressure coefficients

Simulations at imaginary μ_B :

Continuum, $O(10^4)$ configurations, errors include systematics (WB: NPA (2017)) **Strangeness neutrality**



Results for $\chi_n^B = n!c_n$ at $\mu_S = \mu_Q = 0$ and $Nt=12$



Formulation

S. Borsanyi, C. R. et al., PRL (2021)

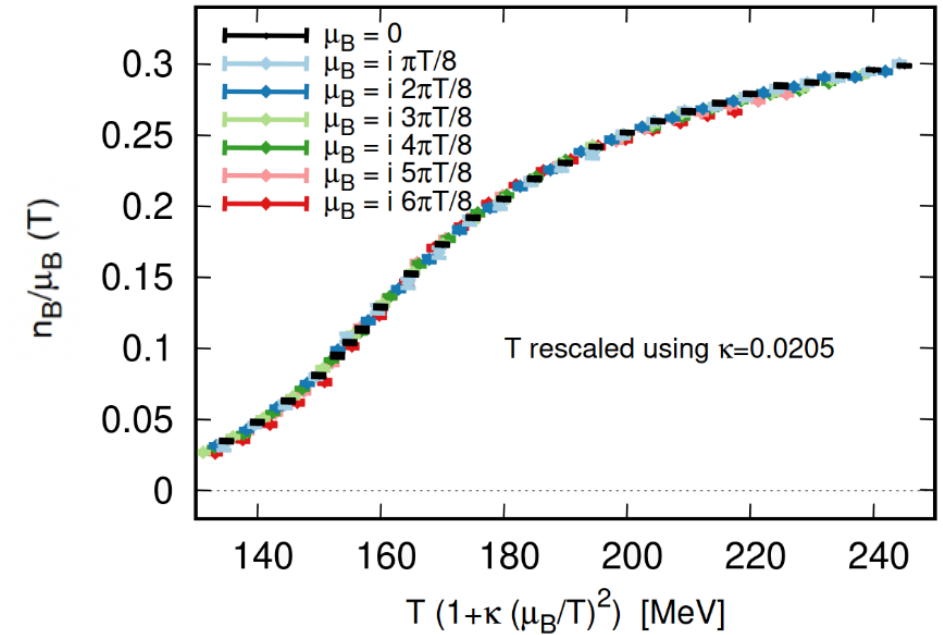
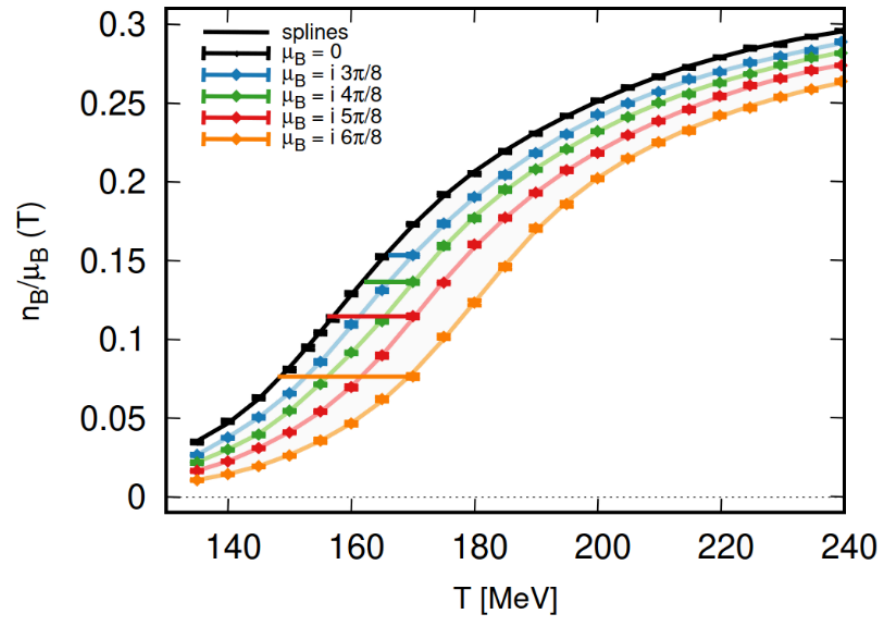
- We have observed the $\hat{\mu}_B$ -dependence seems to amount to a simple T - rescaling
- A simplistic scenario with a single T - independent parameter κ does not provide a systematic treatment which can serve as an alternative expansion scheme
- We allow for more than $\mathcal{O}(\hat{\mu}^2)$ expansion of T' and let the coefficients be T -dependent:

$$\frac{\chi_1^B(T, \hat{\mu}_B)}{\hat{\mu}_B} = \chi_2^B(T', 0) , \quad T' = T (1 + \kappa_2(T) \hat{\mu}_B^2 + \kappa_4(T) \hat{\mu}_B^4 + \mathcal{O}(\hat{\mu}_B^6))$$

- **Important:** we are simply re-organizing the Taylor expansion via an expansion in the shift

$$\Delta T = T - T' = (\kappa_2(T) \hat{\mu}_B^2 + \kappa_4(T) \hat{\mu}_B^4 + \mathcal{O}(\hat{\mu}_B^6))$$

- Comparing the (Taylor) expansion in $\hat{\mu}_B$ and our expansion in ΔT order by order, we can relate $\chi_n^B(T)$ and $\kappa_n(T)$



Simulations at $\text{Im}(\hat{\mu}_B)$: T -dependence of normalised baryon density ($\chi_1^B = n_B/T^3$) at finite $\hat{\mu}_B$ appears to be shifted from the value at $\hat{\mu}_B = 0$.

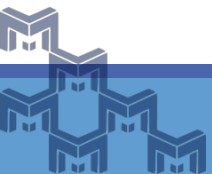
For the 0/0 limit, we have: $\frac{\chi_1^B(T, \hat{\mu}_B) \rightarrow 0}{\hat{\mu}_B \rightarrow 0} \rightarrow \frac{\partial \chi_1^B}{\partial \hat{\mu}_B} = \chi_2^B$

S. Borsanyi, C. R. et al., PRL (2021)

Main identity:
$$\frac{\chi_1^B(T, \hat{\mu}_B)}{\hat{\mu}_B} = \chi_2^B(T', 0)$$

with $T'(T, \hat{\mu}_B) = T \left(1 + \kappa_2 \cdot \hat{\mu}_B^2 + \kappa_4 \cdot \hat{\mu}_B^4 + \dots \right)$

captures the finite $\hat{\mu}_B$ dependence of the expansion



New **TExS EoS** based on coefficients $\kappa_{2/4}^{BB}(T)$ evaluated directly from lattice QCD simulations at $\mu_B = 0$

$$T'(T, \mu_B) = T \left(1 + \kappa_2^{BB}(T) \hat{\mu}_B^2 + \kappa_4^{BB}(T) \hat{\mu}_B^4 \dots \right)$$

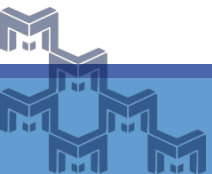
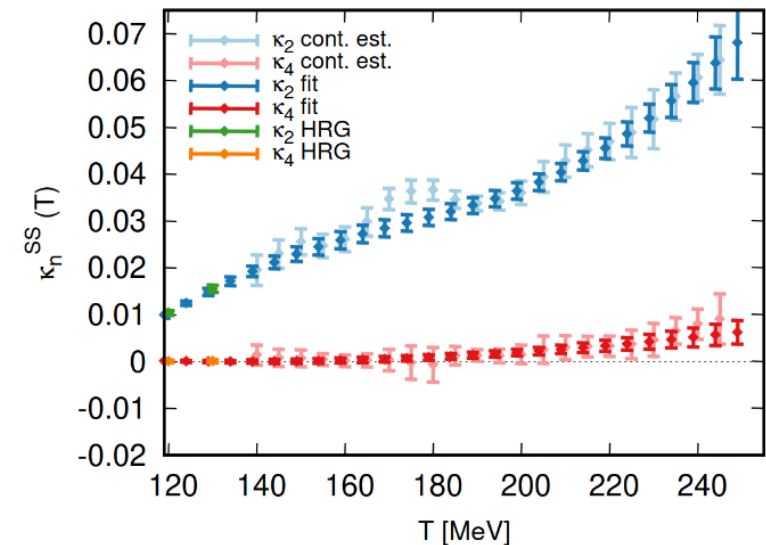
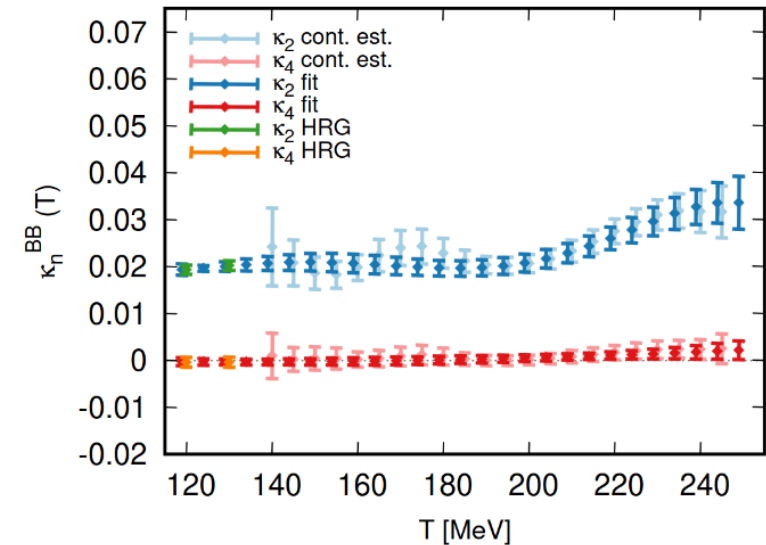
with coefficients $\kappa_i^{BB}(T)$ connected to Taylor coefficients $\chi_i^B(T)$:

- $\kappa_2^{BB}(T, 0) = \frac{1}{6T} \frac{\chi_4^B(T)}{\chi_2'^B(T)}$ with $\chi'(T) = \frac{\partial \chi(T)}{\partial T}$
- $\kappa_4^{BB}(T, 0) = \frac{1}{360T \times \chi_2'^B(T)^3} \left(3\chi_2'^B(T) \times \chi_6^B(T) - 5\chi_2''^B(T) \times \chi_4^B(T)^2 \right)$

⇒ Clear **separation of scales** between $\kappa_2(T)$ and $\kappa_4(T)$

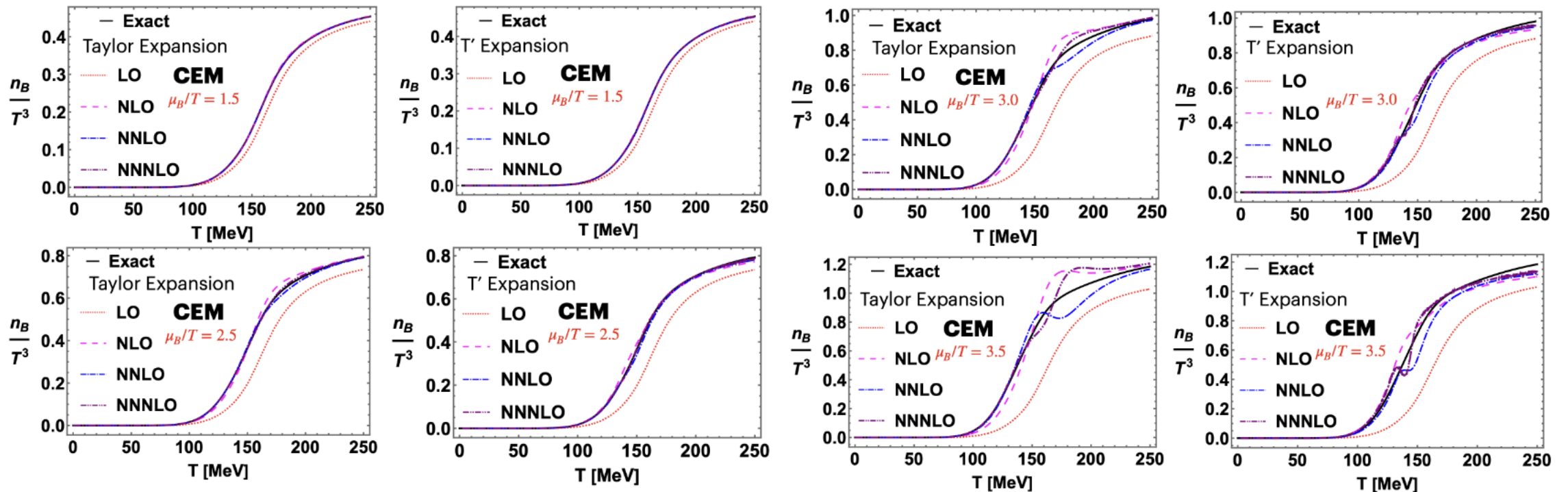
⇒ $\kappa_4(T)$ is almost 0 → **faster convergence**

S. Borsanyi, C. R. et al., PRL (2021)



Comparison between Taylor and new expansion scheme

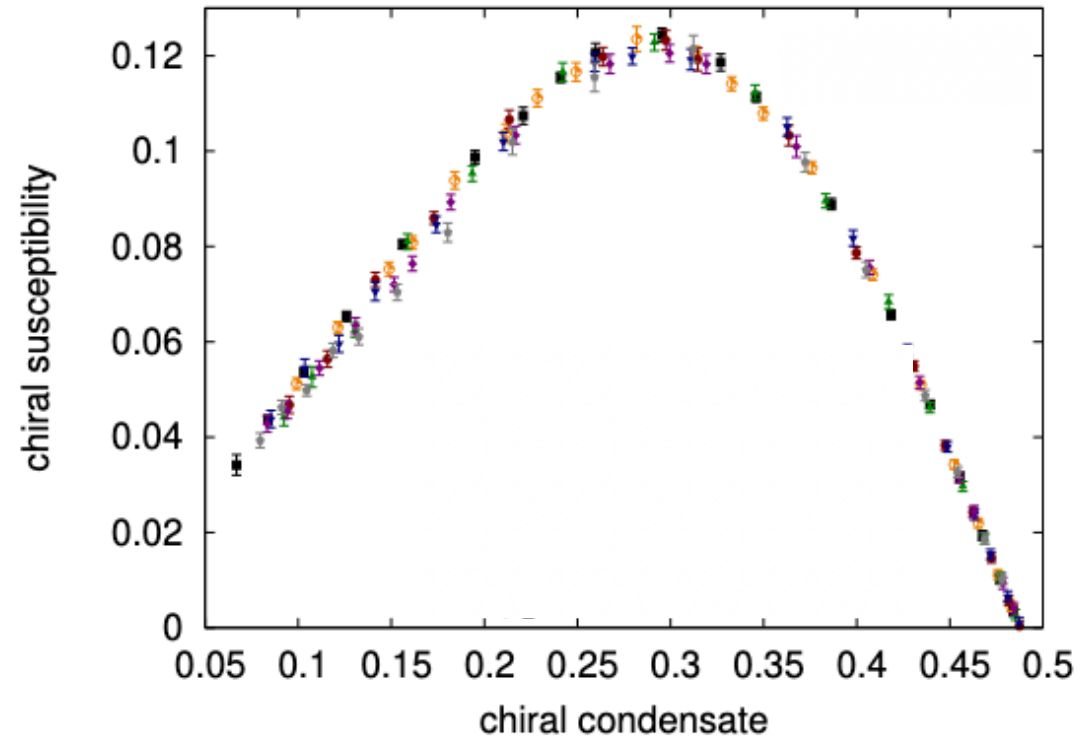
M. Kahangirwe et al., 2408.04588



Phase Diagram from Lattice QCD

The transition at $\mu_B=0$ is a smooth crossover

Aoki et al., Nature (2006)
Borsanyi et al., JHEP (2010)
Bazavov et al., PRD (2012)



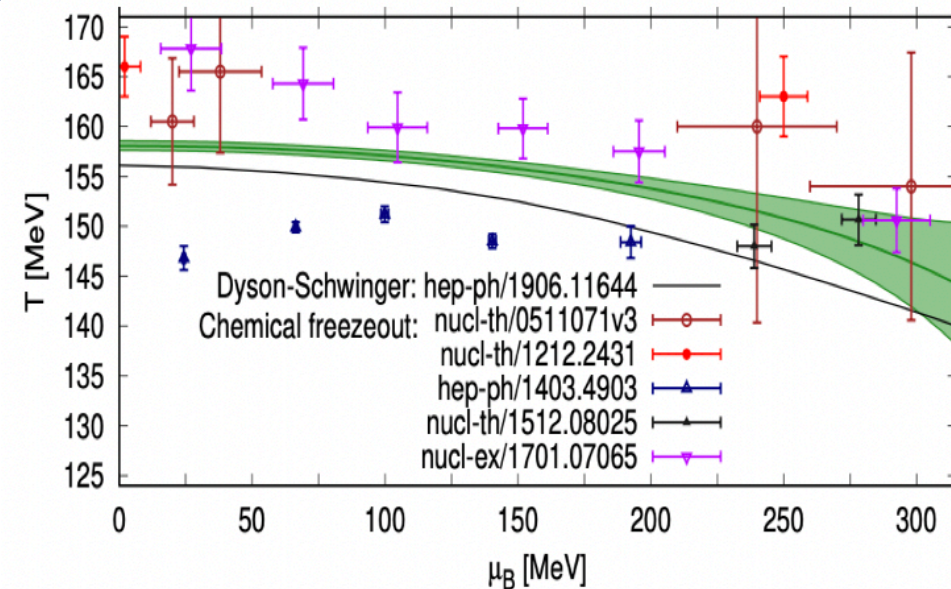
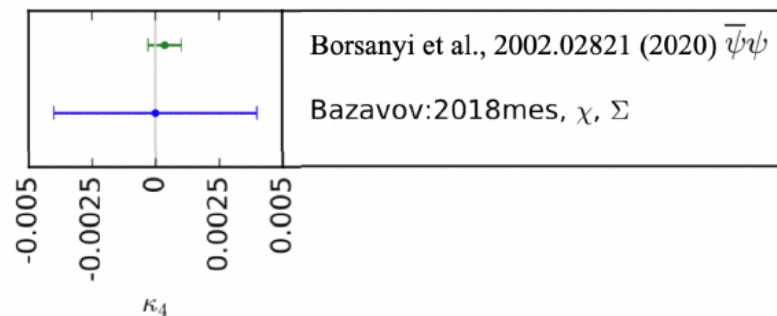
QCD transition temperature and curvature

$$\frac{T_c(\mu_B)}{T_0} = 1 - \kappa_2 \left(\frac{\mu_B}{T_0}\right)^2 - \kappa_4 \left(\frac{\mu_B}{T_0}\right)^4 + O(\mu_B^6)$$

Borsanyi, C. R. et al. PRL (2020)

- Latest results on T_0 from WB collaboration based on subtracted chiral condensate and chiral susceptibility

$T_0 = 158.0 \pm 0.6$ MeV

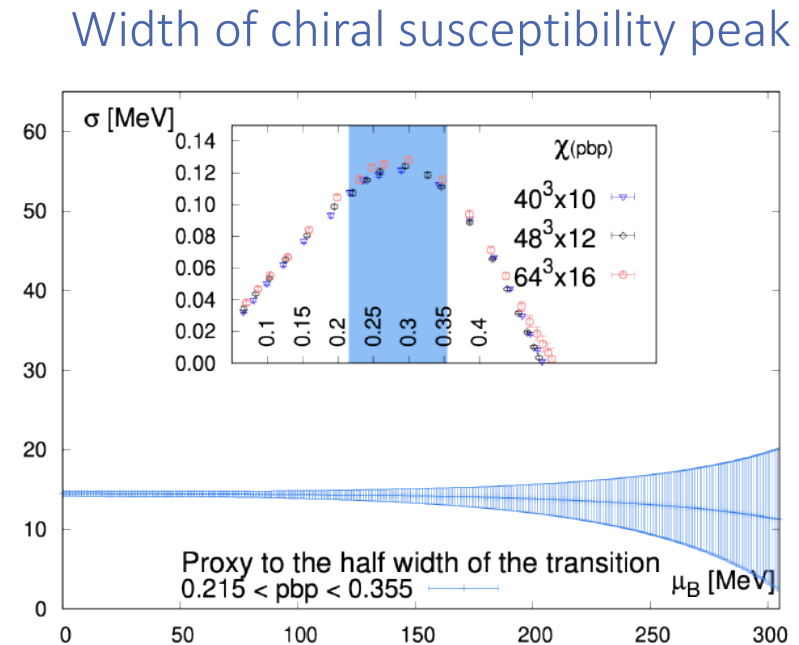
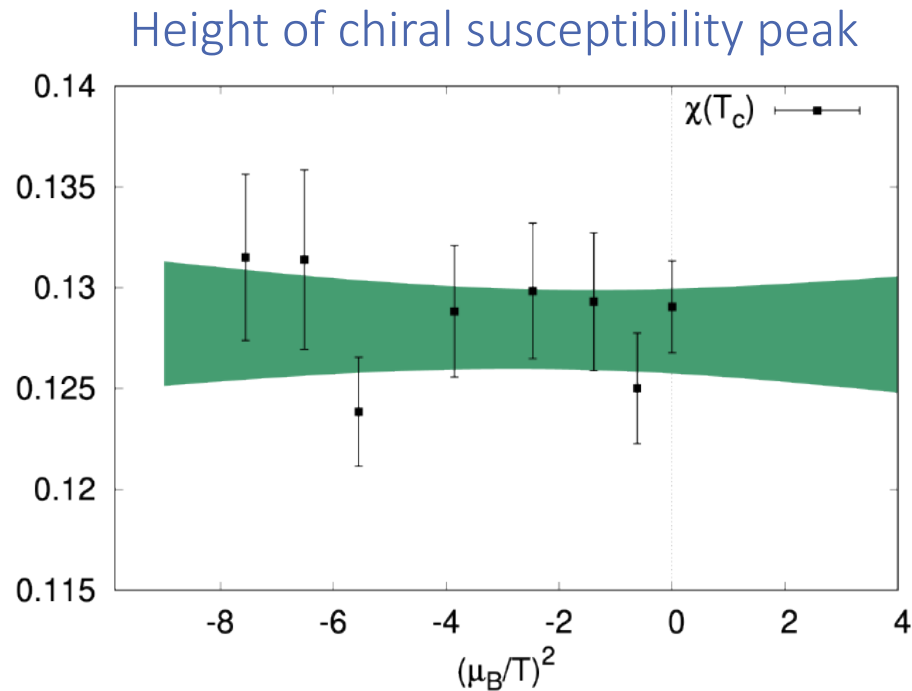


$$\kappa_2 = 0.0153 \pm 0.0018$$

$$\kappa_4 = 0.00032 \pm 0.00067$$

Limit on the location of the critical point

For a genuine phase transition, the height of the peak of the chiral susceptibility diverges and the width shrinks to zero

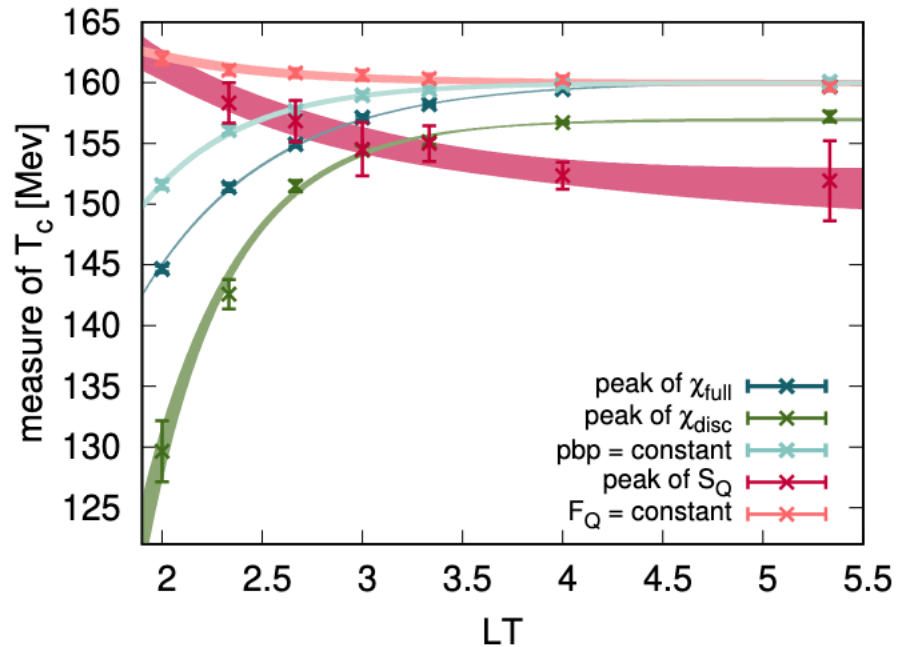


No sign of criticality for $\mu_B < 300$ MeV

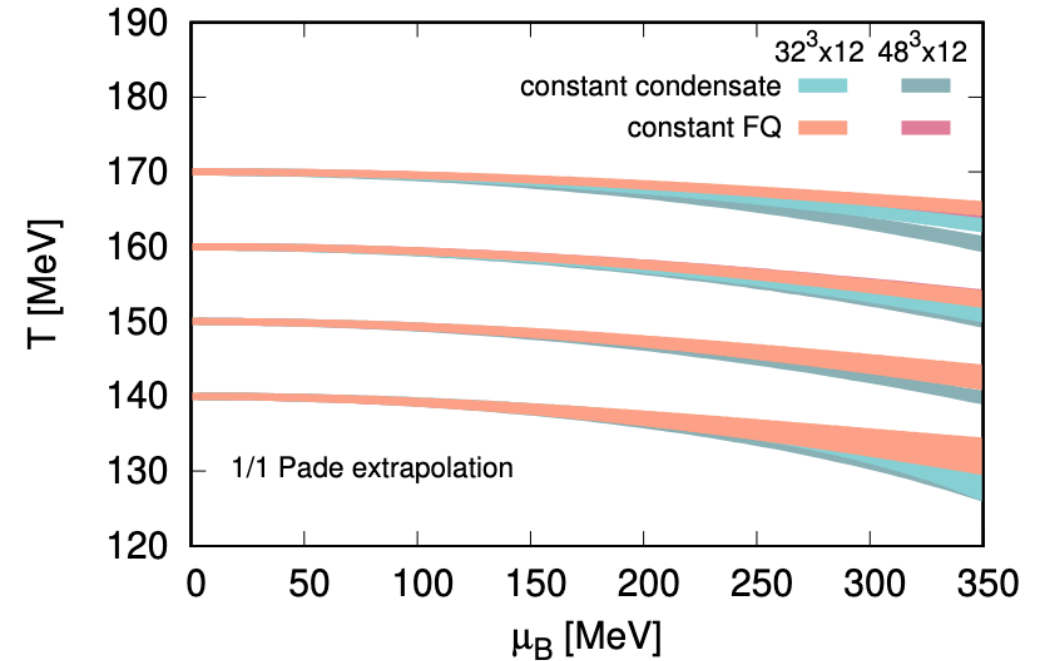
Borsanyi, C. R. et al. PRL (2020)

Chiral vs deconfinement observables

Volume dependence:



μ_B dependence:



S. Borsanyi et al., 2405.12320

Fluctuations of conserved charges

Definition:

$$\chi_{lmn}^{BSQ} = \frac{\partial^{l+m+n} p / T^4}{\partial(\mu_B/T)^l \partial(\mu_S/T)^m \partial(\mu_Q/T)^n}.$$

Relationship between chemical potentials:

$$\mu_u = \frac{1}{3}\mu_B + \frac{2}{3}\mu_Q;$$

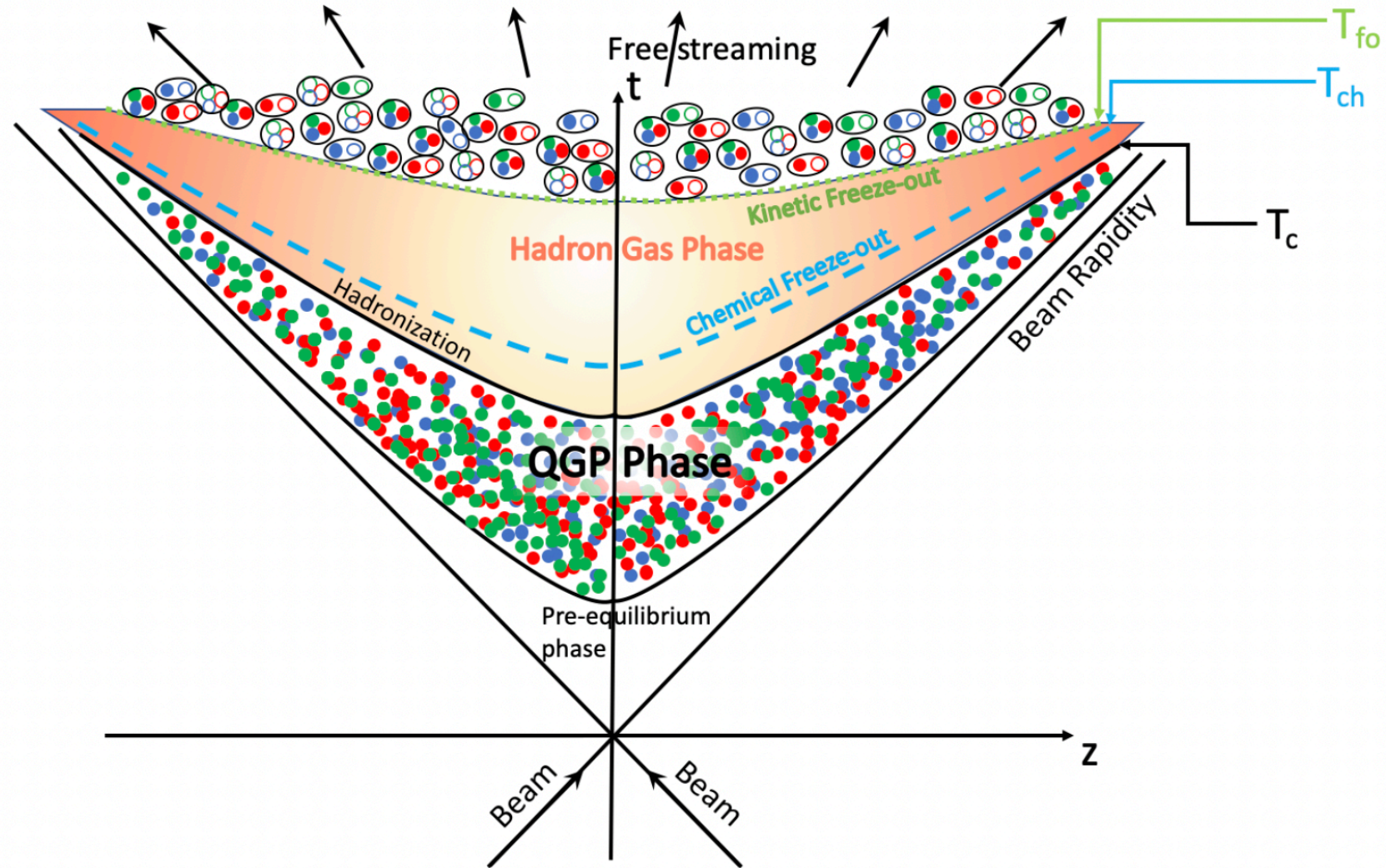
$$\mu_d = \frac{1}{3}\mu_B - \frac{1}{3}\mu_Q;$$

$$\mu_s = \frac{1}{3}\mu_B - \frac{1}{3}\mu_Q - \mu_S.$$

They can be calculated on the lattice and compared to experiment

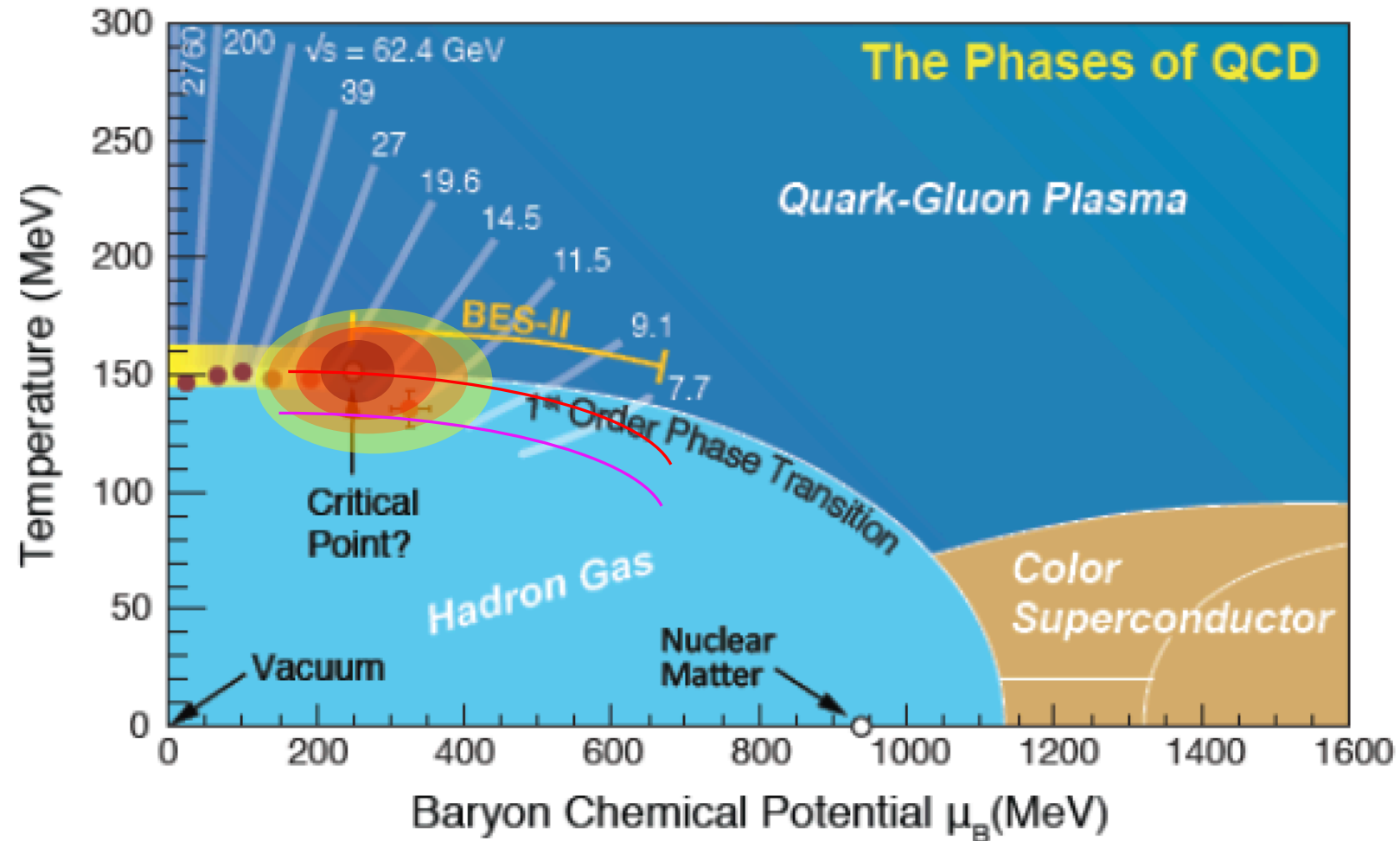
Evolution of a heavy-ion collision

- **Chemical freeze-out:** inelastic reactions cease: the chemical composition of the system is fixed (particle yields and fluctuations)
- **Kinetic freeze-out:** elastic reactions cease: spectra and correlations are frozen (free streaming of hadrons)
- Hadrons reach the detector



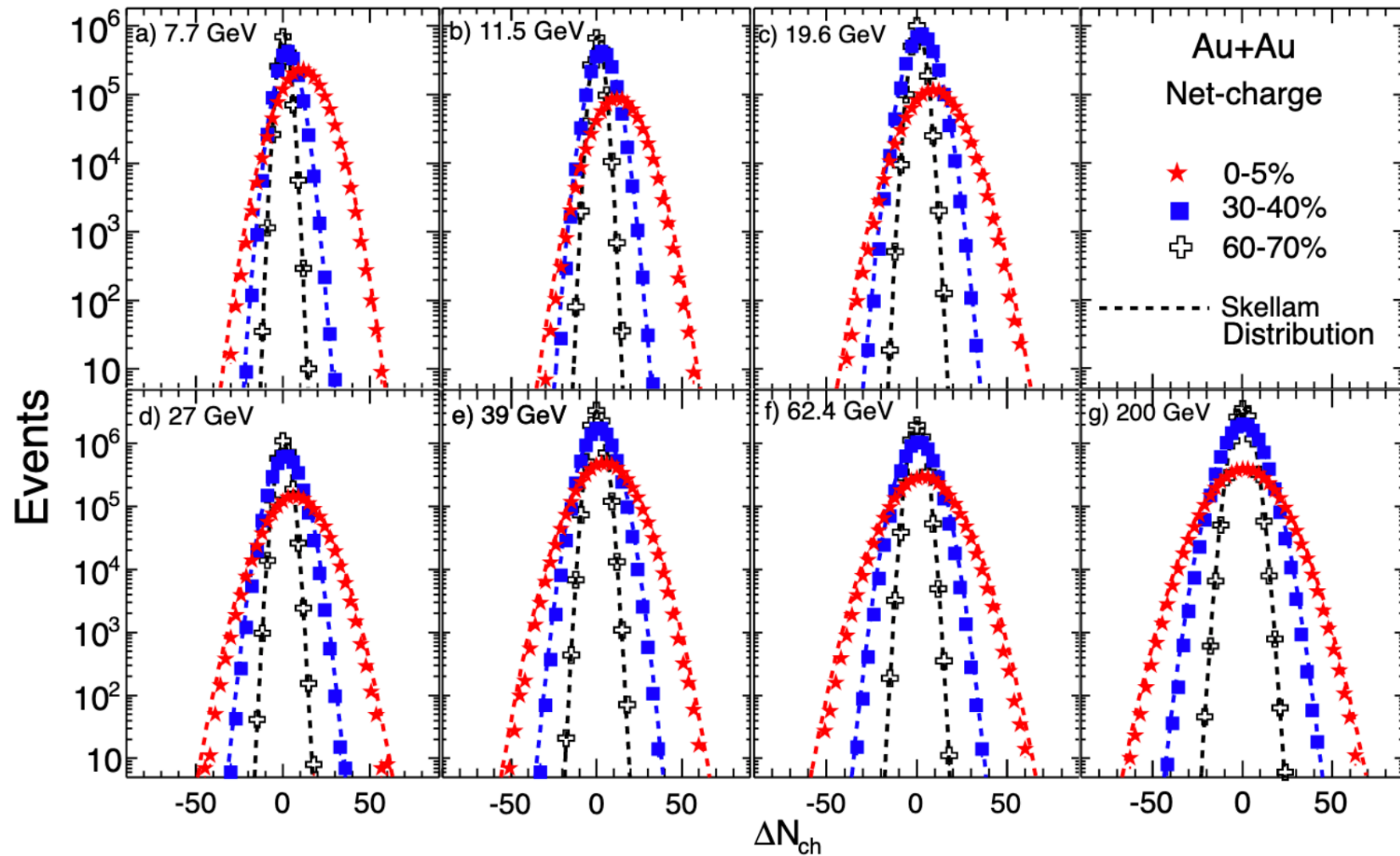
Evolution of a heavy-ion collision

- **Chemical freeze-out:** inelastic reactions cease: the chemical composition of the system is fixed (particle yields and fluctuations)
- **Kinetic freeze-out:** elastic reactions cease: spectra and correlations are frozen (free streaming of hadrons)
- Hadrons reach the detector



Connection to experiment

- Consider the number of electrically charged particles N_Q
- Its average value over the whole ensemble of events is $\langle N_Q \rangle$
- In experiments it is possible to measure its **event-by-event distribution**



STAR Collab., PRL (2014)

Connection to experiment

Fluctuations of conserved charges are the **cumulants** of their event-by-event distribution

$$\text{mean : } M = \chi_1$$

$$\text{variance : } \sigma^2 = \chi_2$$

$$\text{skewness : } S = \chi_3/\chi_2^{3/2}$$

$$\text{kurtosis : } \kappa = \chi_4/\chi_2^2$$

$$S\sigma = \chi_3/\chi_2$$

$$\kappa\sigma^2 = \chi_4/\chi_2$$

$$M/\sigma^2 = \chi_1/\chi_2$$

$$S\sigma^3/M = \chi_3/\chi_1$$

F. Karsch: Centr. Eur. J. Phys. (2012)

The chemical potentials are not independent: fixed to match the experimental conditions:

$$\langle n_S \rangle = 0$$

$$\langle n_Q \rangle = 0.4 \langle n_B \rangle$$

“Baryometer and Thermometer”

Let us look at the Taylor expansion of $R^{B_{31}}$

$$R_{31}^B(T, \mu_B) = \frac{\chi_3^B(T, \mu_B)}{\chi_1^B(T, \mu_B)} = \frac{\chi_4^B(T, 0) + \chi_{31}^{BQ}(T, 0)q_1(T) + \chi_{31}^{BS}(T, 0)s_1(T)}{\chi_2^B(T, 0) + \chi_{11}^{BQ}(T, 0)q_1(T) + \chi_{11}^{BS}(T, 0)s_1(T)} + \mathcal{O}(\mu_B^2)$$

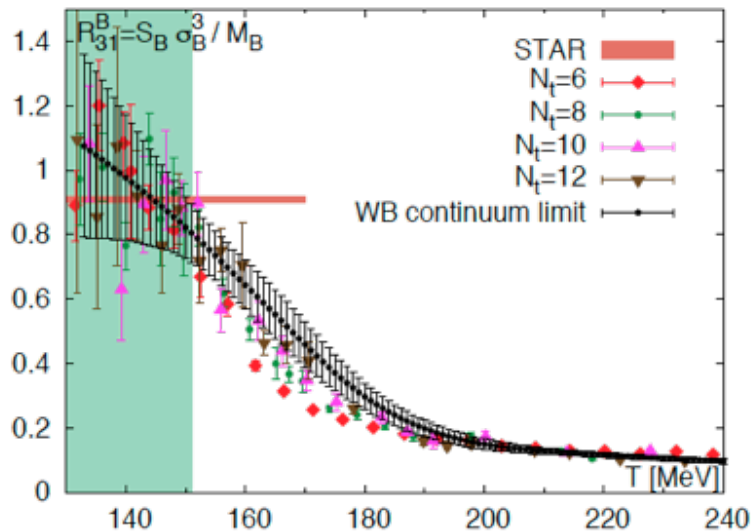
- To order μ_B^2 it is independent of μ_B : it can be used as a **thermometer**
- Let us look at the Taylor expansion of $R^{B_{12}}$

$$R_{12}^B(T, \mu_B) = \frac{\chi_1^B(T, \mu_B)}{\chi_2^B(T, \mu_B)} = \frac{\chi_2^B(T, 0) + \chi_{11}^{BQ}(T, 0)q_1(T) + \chi_{11}^{BS}(T, 0)s_1(T)}{\chi_2^B(T, 0)} \frac{\mu_B}{T} + \mathcal{O}(\mu_B^3)$$

- Once we extract T from $R^{B_{31}}$, we can use $R^{B_{12}}$ to extract μ_B

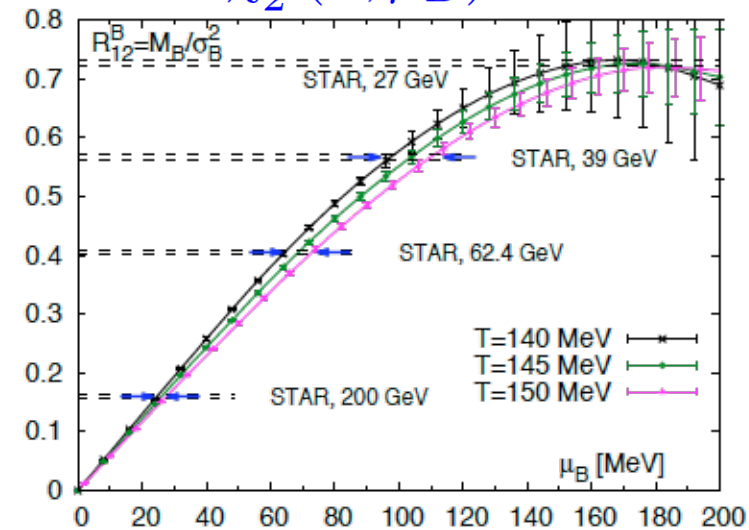
Freeze-out parameters from B fluctuations

➤ Thermometer: $\frac{\chi_3^B(T, \mu_B)}{\chi_1^B(T, \mu_B)} = S_B \sigma_B^3 / M_B$



Upper limit: $T_f \leq 151 \pm 4$ MeV

Baryometer: $\frac{\chi_1^B(T, \mu_B)}{\chi_2^B(T, \mu_B)} = \sigma_B^2 / M_B$



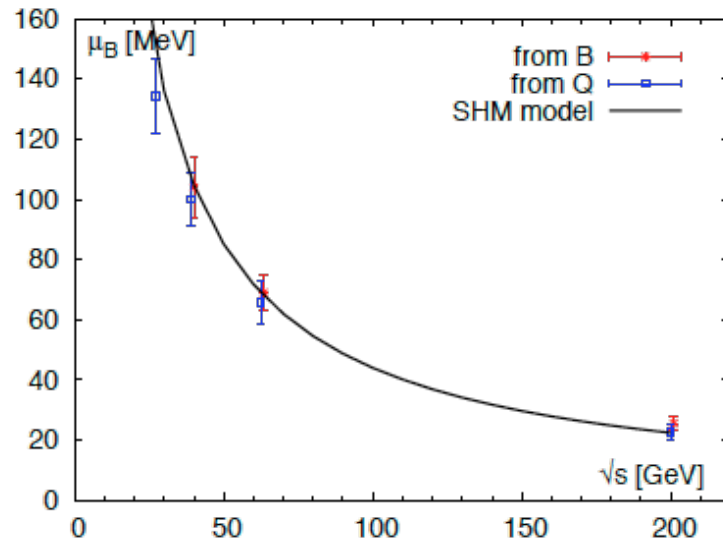
WB: S. Borsanyi et al., PRL (2014)
STAR collaboration, PRL (2014)

Consistency between freeze-out chemical potential from electric charge and baryon number is found.

Freeze-out parameters from B fluctuations

➤ Thermometer: $\frac{\chi_3^B(T, \mu_B)}{\chi_1^B(T, \mu_B)} = S_B \sigma_B^3 / M_B$

Baryometer: $\frac{\chi_1^B(T, \mu_B)}{\chi_2^B(T, \mu_B)} = \sigma_B^2 / M_B$



\sqrt{s} [GeV]	μ_B^f [MeV] (from B)	μ_B^f [MeV] (from Q)
200	25.8 ± 2.7	22.8 ± 2.6
62.4	69.7 ± 6.4	66.6 ± 7.9
39	105 ± 11	101 ± 10
27	-	136 ± 13.8

WB: S. Borsanyi et al., PRL (2014)
STAR collaboration, PRL (2014)

Upper limit: $T_f \leq 151 \pm 4$ MeV

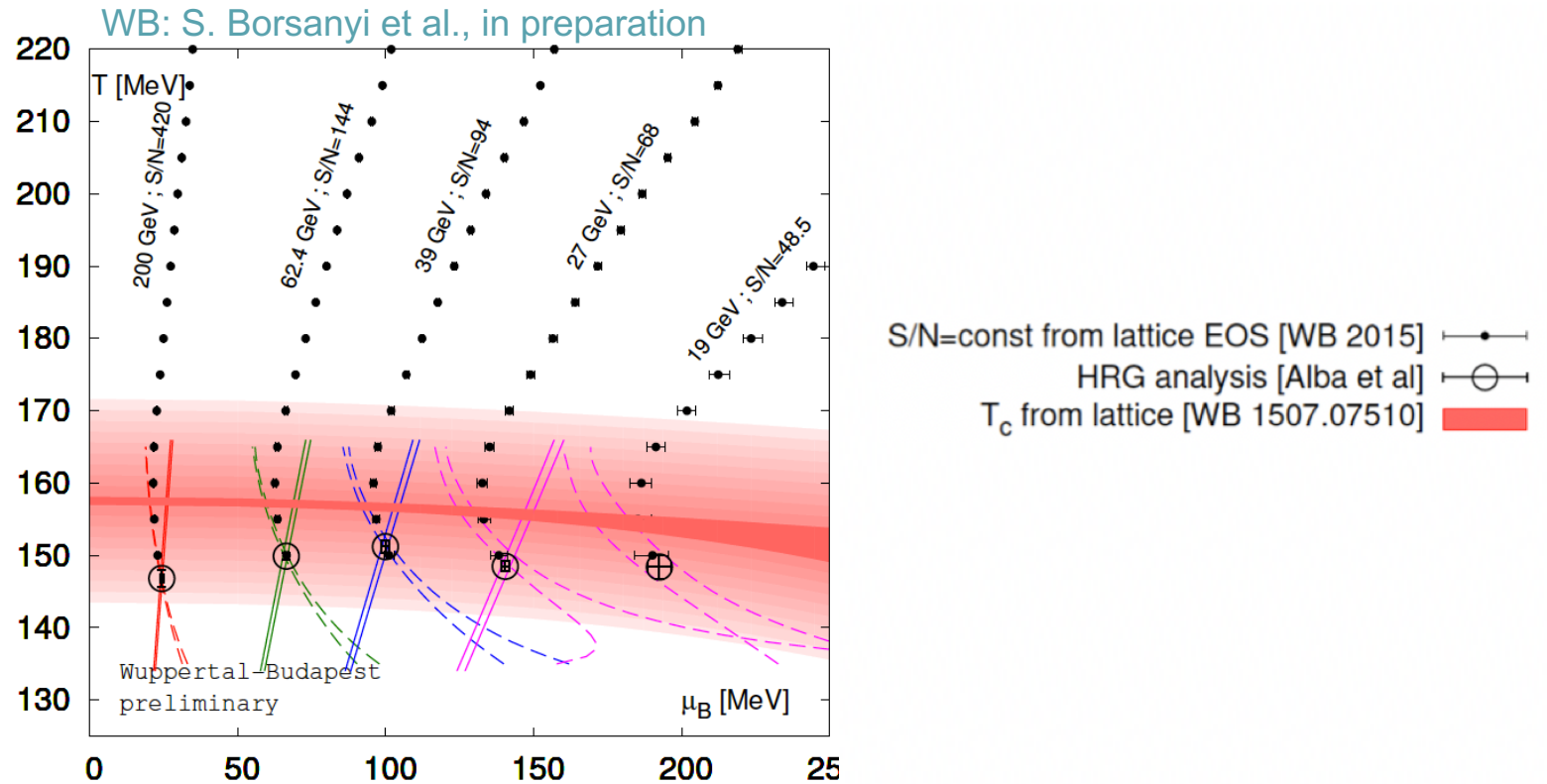
Consistency between freeze-out chemical potential from electric charge and baryon number is found.

Freeze-out line from first principles

Use T - and μ_B -dependence
of R_{12}^Q and R_{12}^B for a
combined fit:

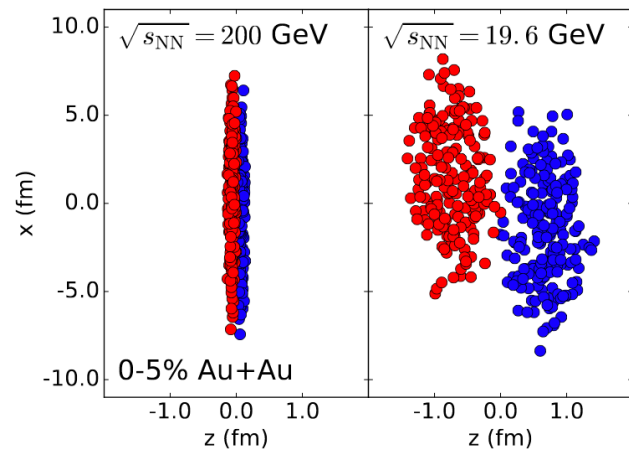
$$R_{12}^Q(T, \mu_B) = \frac{\chi_1^Q(T, \mu_B)}{\chi_2^Q(T, \mu_B)} = \frac{\chi_{11}^{QB}(T, 0) + \chi_2^Q(T, 0)q_1(T) + \chi_{11}^{QS}(T, 0)s_1(T)}{\chi_2^Q(T, 0)} \frac{\mu_B}{T} + \mathcal{O}(\mu_B^3).$$

$$R_{12}^B(T, \mu_B) = \frac{\chi_1^B(T, \mu_B)}{\chi_2^B(T, \mu_B)} = \frac{\chi_2^B(T, 0) + \chi_{11}^{BQ}(T, 0)q_1(T) + \chi_{11}^{BS}(T, 0)s_1(T)}{\chi_2^B(T, 0)} \frac{\mu_B}{T} + \mathcal{O}(\mu_B^3)$$



Scientific goals

- Model the fluctuating initial conditions for the baryon-asymmetric matter for baryon, electric charge, and strangeness



C. Shen, B. Schenke, PRC (2018)
C. Shen, B. Schenke, NPA (2019)

- Develop **(3+1)D** viscous hydrodynamic code which includes all conserved currents and connect it to model for initial conditions
- Extract transport properties of nuclear matter at finite baryon density

G. Denicol et al., PRC (2018)
L. Du et al., NPA (2019)

M. Li, C. Shen, PRC (2018)
C. Gale et al., NPA (2019)

Hydrodynamics evolution

- The sequential collisions between nucleons contribute as energy-momentum and net-baryon density sources to the hydrodynamic fields

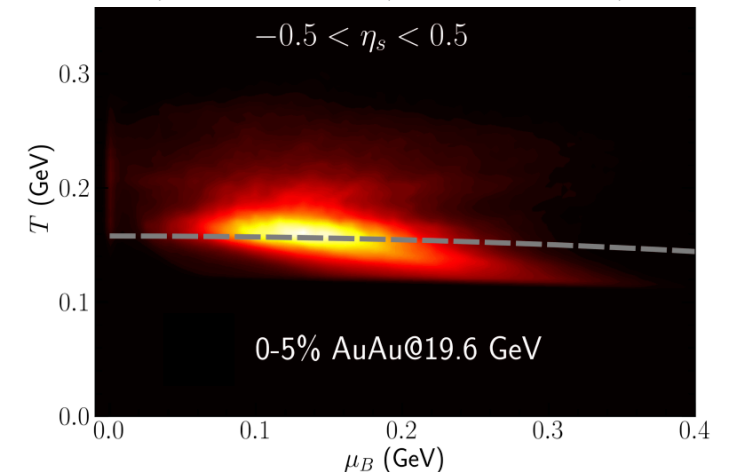
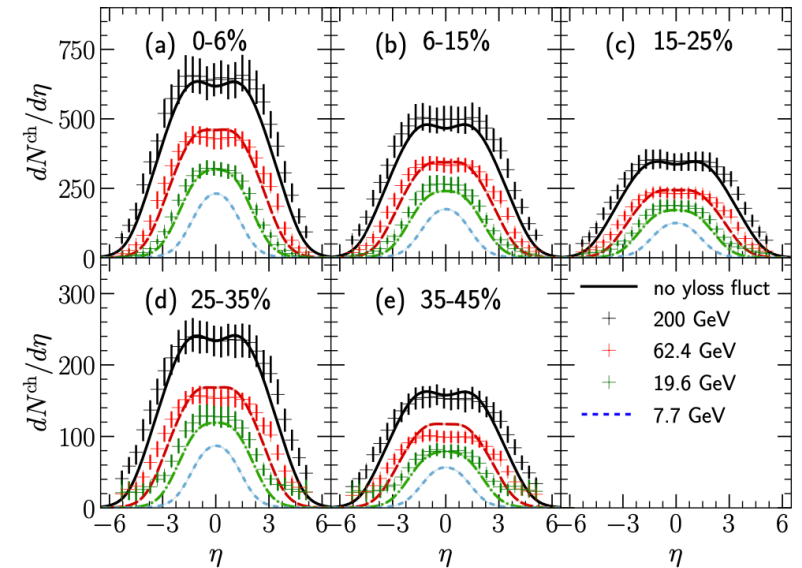
C. Shen, B. Schenke, PRC (2018)

L. Du et al., NPA (2019)

- For recent developments and an alternative method based on a minimal extension of the Glauber model see C. Shen, S. Alzhrani, PRC (2020)

- Relativistic viscous hydrodynamic simulations extended to include the propagation of net baryon current including its dissipative diffusion

C. Shen, B. Schenke, NPA (2018)



Hydrodynamics evolution

- The sequential collisions between nucleons contribute as energy-momentum and net-baryon density sources to the hydrodynamic fields

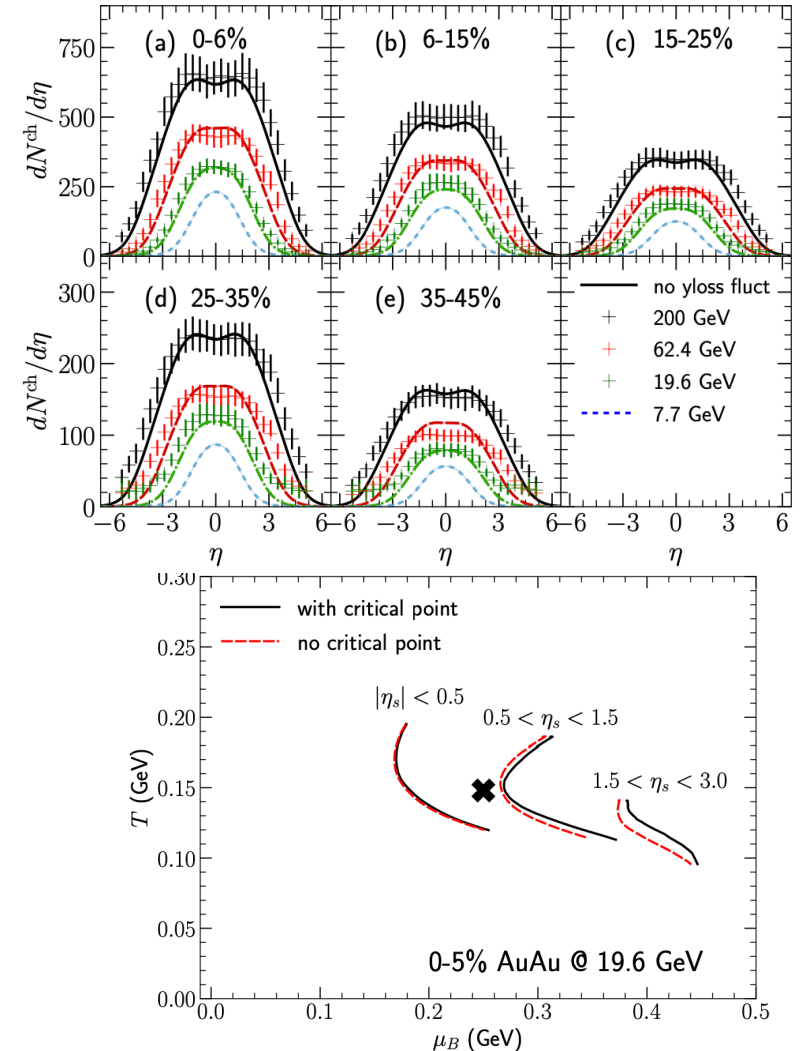
C. Shen, B. Schenke, PRC (2018);

L. Du et al., NPA (2019)

- For recent developments and an alternative method based on a minimal extension of the Glauber model see C. Shen, S. Alzhvani, PRC (2020);

- Relativistic viscous hydrodynamic simulations extended to include the propagation of net baryon current including its dissipative diffusion

C. Shen, B. Schenke, NPA (2018)



Dynamical modeling of fluctuations

One of the central goals of the BEST collaboration is to develop quantitative understanding of fluctuations near the CP

- Stochastic approach with noise

M. Nahrgang et al., PRD (2019)

- Deterministic approach in which correlation functions are treated as additional variables with the hydrodynamics ones (Hydro+)

M. Stephanov and Yi Ying, PRD (2018)

- So far only applicable to crossover side of phase boundary
- So far limited to two-point functions

See also Y. Akamatsu et al, PRC (2017 and 2018); M. Martinez and T. Schaefer, PRC (2019); X. An et al., PRC (2020)
S. Pratt and C. Plumberg, PRC (2019 and 2020)

Implementation

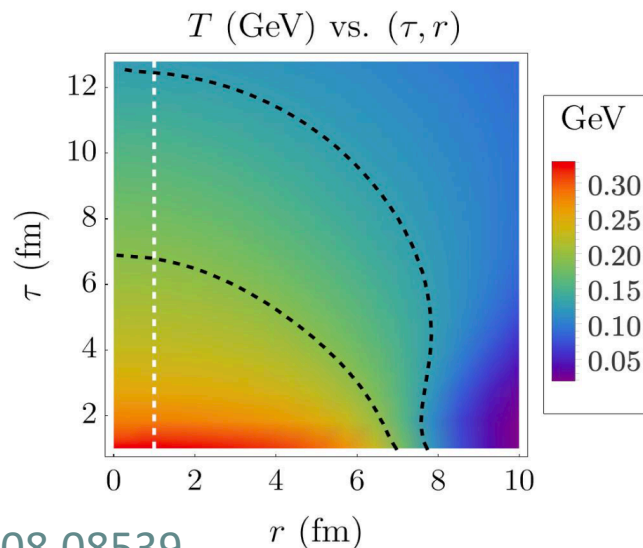
- Solution of stochastic hydro equations using a momentum filter by which fluctuating modes above a cutoff given by a microscopic scale are removed

M. Singh et al., QM2018 proceedings

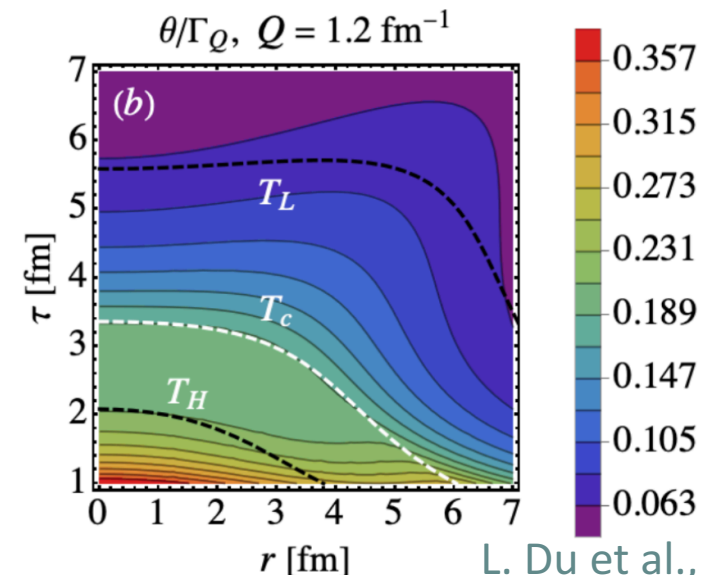
- Solution of full stochastic diffusive equation in a finite-size system with Gaussian white noise: critical slowing down is observed

M. Nahrgang et al., 1804.05728

- Hydro+ implemented in two main simulations



K. Rajagopal et al., 1908.08539



L. Du et al., 2004.02719

Things to keep in mind

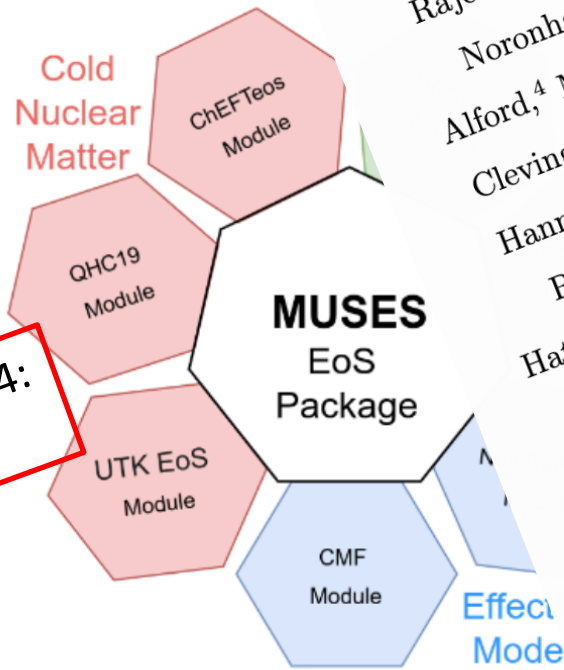
- Effects due to volume variation because of finite centrality bin width
 - Experimentally corrected by centrality-bin-width correction method
V. Skokov et al., PRC (2013), P. Braun-Munzinger et al., NPA (2017),
V. Begun and M. Mackowiak-Pawlowska (2017)
- Finite reconstruction efficiency
 - Experimentally corrected based on binomial distribution
A.Bzdak,V.Koch, PRC (2012)
- Spallation protons
 - Experimentally removed with proper cuts in p_T
- Canonical vs Gran Canonical ensemble
 - Experimental cuts in the kinematics and acceptance
V. Koch, S. Jeon, PRL (2000)
P. Braun-Munzinger et al., NPA (2017)
- Baryon number conservation
 - Experimental data need to be corrected for this effect
- Proton multiplicity distributions vs baryon number fluctuations
 - Recipes for treating proton fluctuations
M. Asakawa and M. Kitazawa, PRC(2012), M. Nahrgang et al., 1402.1238
- Final-state interactions in the hadronic phase
 - Consistency between different charges = fundamental test
J.Steinheimer et al., PRL (2013)

MUSES goals and milestones



- CyberInfrastructure of interoperating tools and services with
 - Upgrade of existing calculation tools to modern
 - **Equation of State (EoS) package** that can
 - **Web-based tools and services** +L
 - **Job management system** tha
 - Scalable, high-availability **depl**

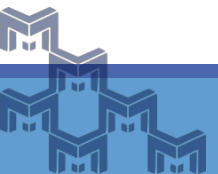
Theoretical and Experimental Constraints for the Equation of State of Dense and Hot Matter



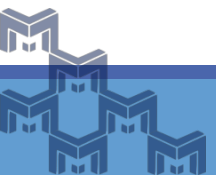
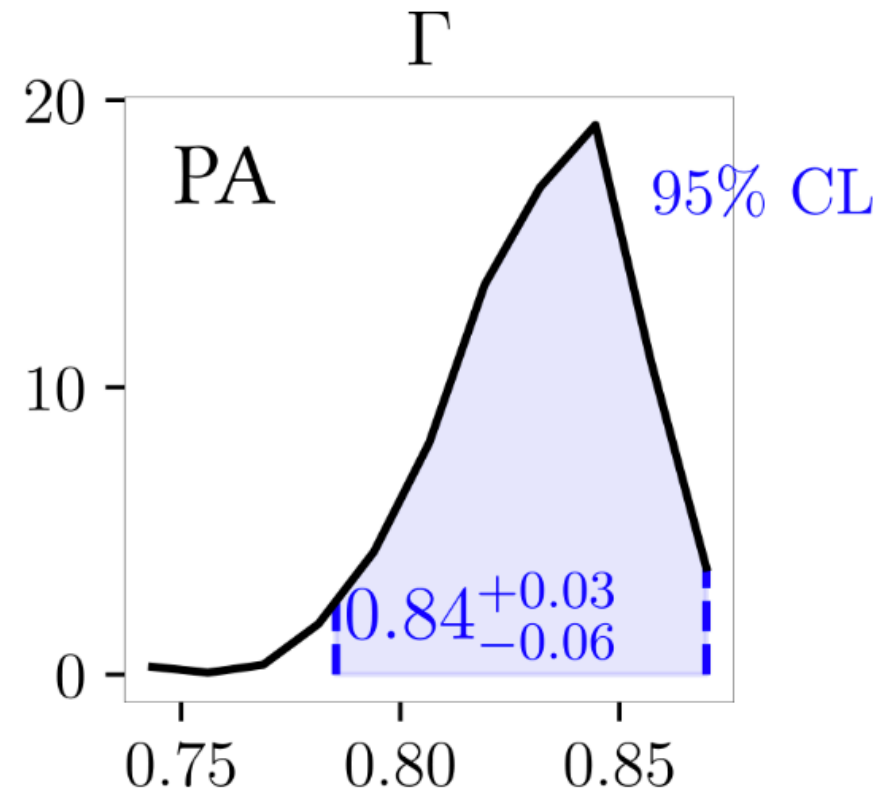
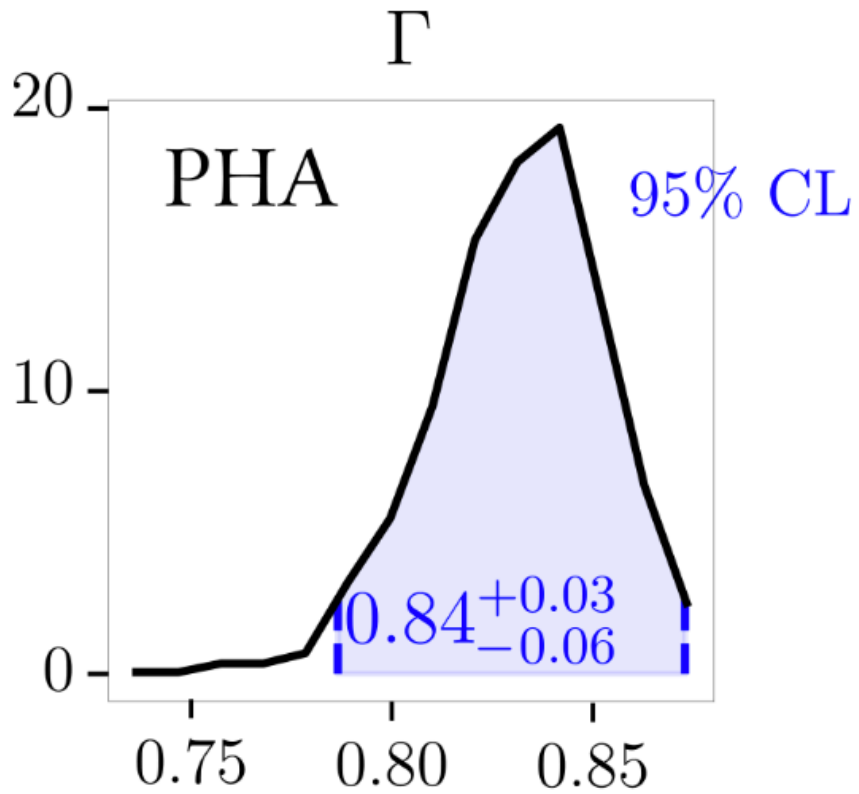
Rajesh Kumar,^{1,*} Veronica Dexheimer,^{1,†} Johannes Jahan,² Jorge Noronha,³ Jacquelyn Noronha-Hostler,³ Claudia Ratti,² Nico Yunes,³ Angel Rodrigo Nava Acuna,² Mark Alford,⁴ Mahmudul Hasan Anik,⁵ Katerina Chatzioannou,^{6,7} Hsin-Yu Chen,^{8,9} Alexander Clevinger,¹ Carlos Conde,³ Nikolas Cruz Camacho,³ Travis Dore,¹⁰ Christian Drischler,¹¹ Hannah Elfner,¹² Reed Essick,¹³ David Friedenberg,¹⁴ Suprovo Ghosh,¹⁵ Joaquin Grefa,² Roland Haas,³ Jan Hammelmann,¹⁶ Steven Harris,¹⁷ Carl-Johan Haster,^{18,19} Tetsuo Hatsuda,²⁰ Mauricio Hippert,³ Renan Hirayama,¹⁶ Jeremy W. Holt,¹⁴ Micheal Kahangirwe,² Jamie Karthein,²¹ Toru Kojo,²² Philippe Landry,²³ Zidu Lin,⁵ Matthew Luzum,²⁴ T. Andrew Manning,³ Jordi Salinas San Martin,³ Cole Miller,²⁵ Elias Roland Most,^{26,27,28} Debora Mroczek,³ Azwinndini Muronga,²⁹ Nicolas Patino,³ Jeffrey Peterson,¹ Christopher Plumberg,³⁰ Damien Price,² Constanca Providencia,³¹ Romulo Rougemont,³² Satyajit Roy,⁵ Hitansh Shah,² Stuart Shapiro,³ Andrew W. Steiner,^{5,33} Michael Strickland,¹ Hung Tan,³ Hajime Togashi,²² Israel Portillo Vazquez,² Pengsheng Wen,¹⁴ and Ziyuan Zhang⁴

(MUSES Collaboration)
Living Reviews in Relativity

- Development within the MUSES Framework: Multi-institutional collaboration for a unified solver for the equation of state, bridging models and applications
- Support and advising by cyberinfrastructure and computer-science experts T. Andrew Manning and Roland Haas
- Improved method to extract asymptotic UV scaling and thermodynamics
- Large boost in performance and numerical stability



- The parameter Γ is an indicator for the correlation among lattice data between neighboring points



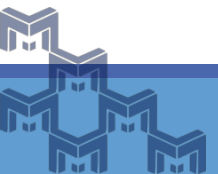
$$\phi''(r) + \left[\frac{h'(r)}{h(r)} + 4A'(r) - B'(r) \right] \phi'(r) - \frac{e^{2B(r)}}{h(r)} \left[\frac{\partial V(\phi)}{\partial \phi} + \frac{e^{-2[A(r)+B(r)]} \Phi'(r)^2}{2} \frac{\partial f(\phi)}{\partial \phi} \right] = 0,$$

$$\Phi''(r) + \left[2A'(r) - B'(r) + \frac{d[\ln f(\phi)]}{d\phi} \phi'(r) \right] \Phi'(r) = 0,$$

$$A''(r) - A'(r)B'(r) + \frac{\phi'(r)^2}{6} = 0,$$

$$h''(r) + [4A'(r) - B'(r)]h'(r) - e^{-2A(r)} f(\phi) \Phi'(r)^2 = 0,$$

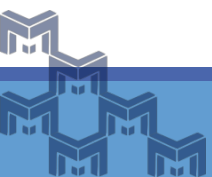
$$h(r)[24A'(r)^2 - \phi'(r)^2] + 6A'(r)h'(r) + 2e^{2B(r)}V(\phi) + e^{-2A(r)} f(\phi) \Phi'(r)^2 = 0,$$



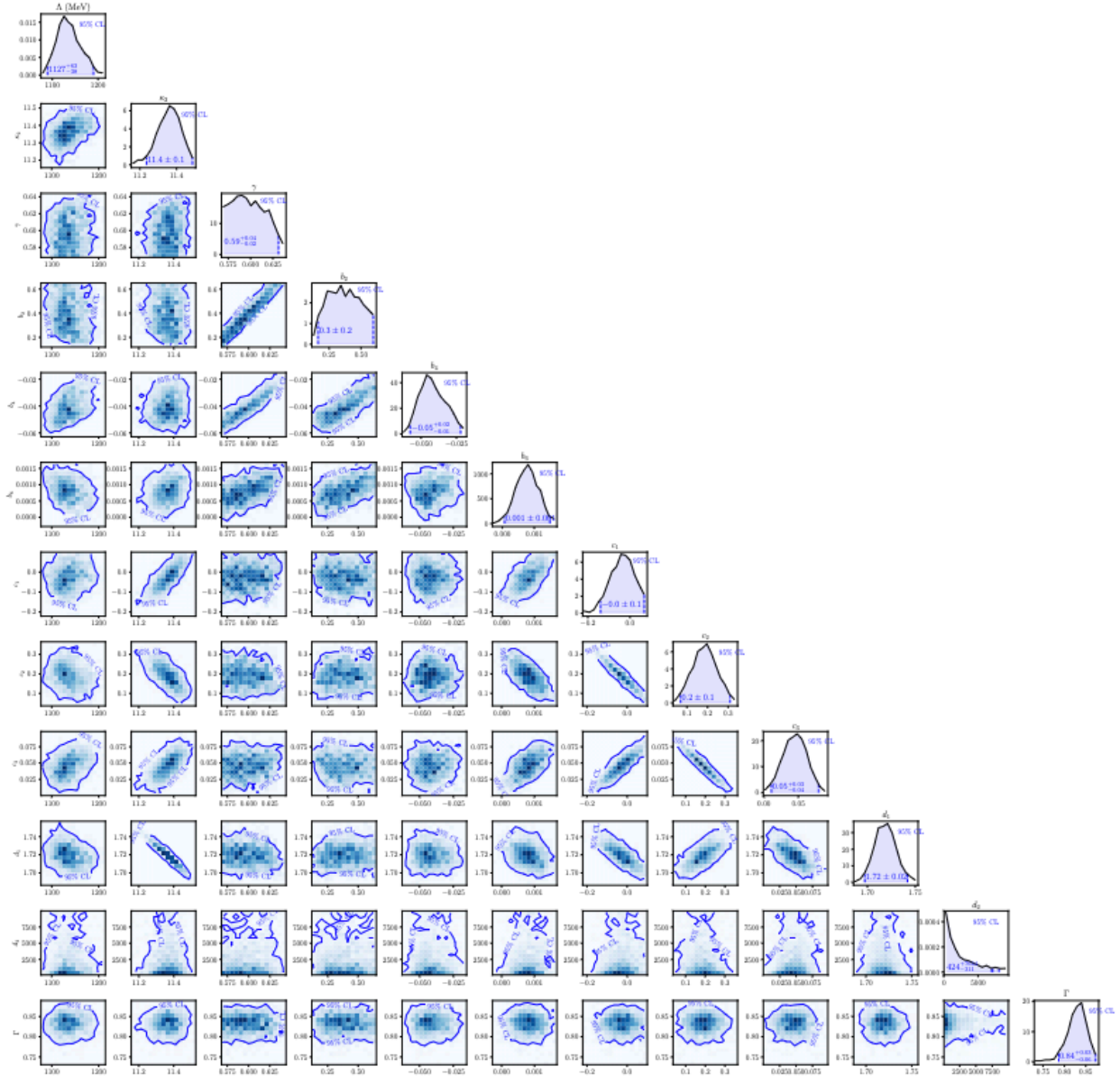
- Thermodynamics extracted from scalings after conversion to physical units.
- Requires near-boundary scalings,

$$\phi \sim \phi_A e^{-\nu A(r)}, \quad \Phi \sim \Phi_0^{\text{far}} + \Phi_2^{\text{far}} e^{-2A(r)}, \quad A \sim A_{-1}^{\text{far}} r + A_0^{\text{far}}$$

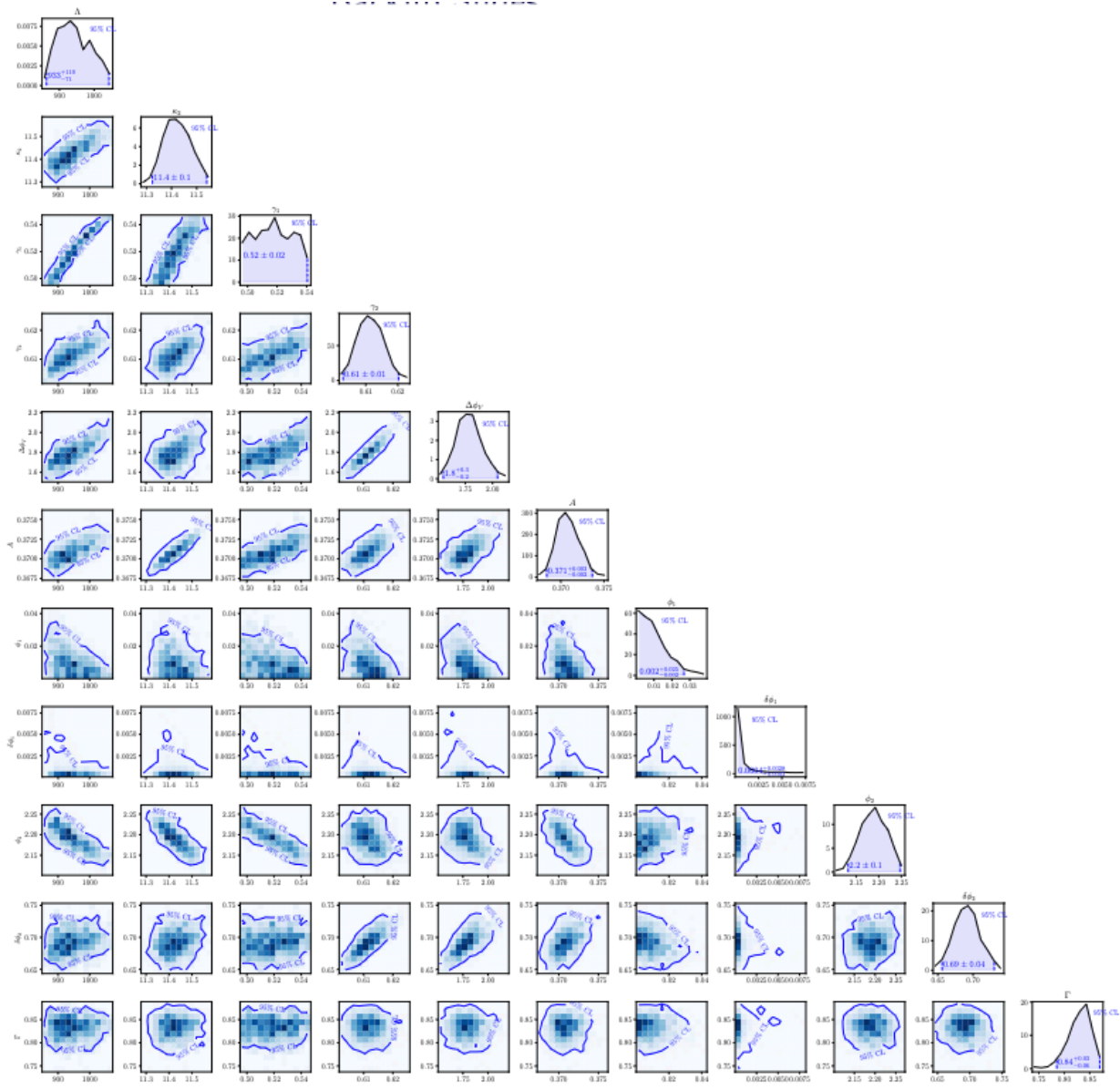
- Inversion to find ϕ_A and Φ_2^{far} :
large coefficient \times tiny number = pure noise.



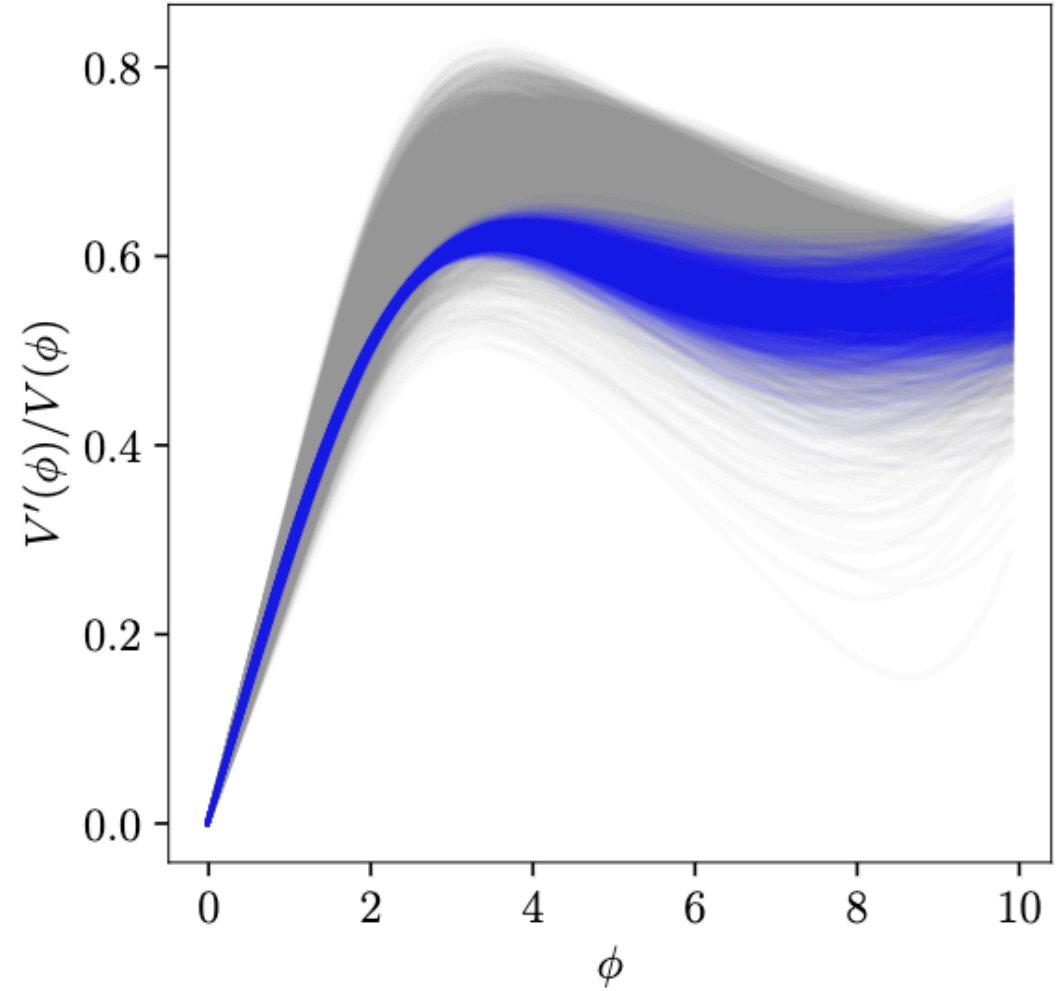
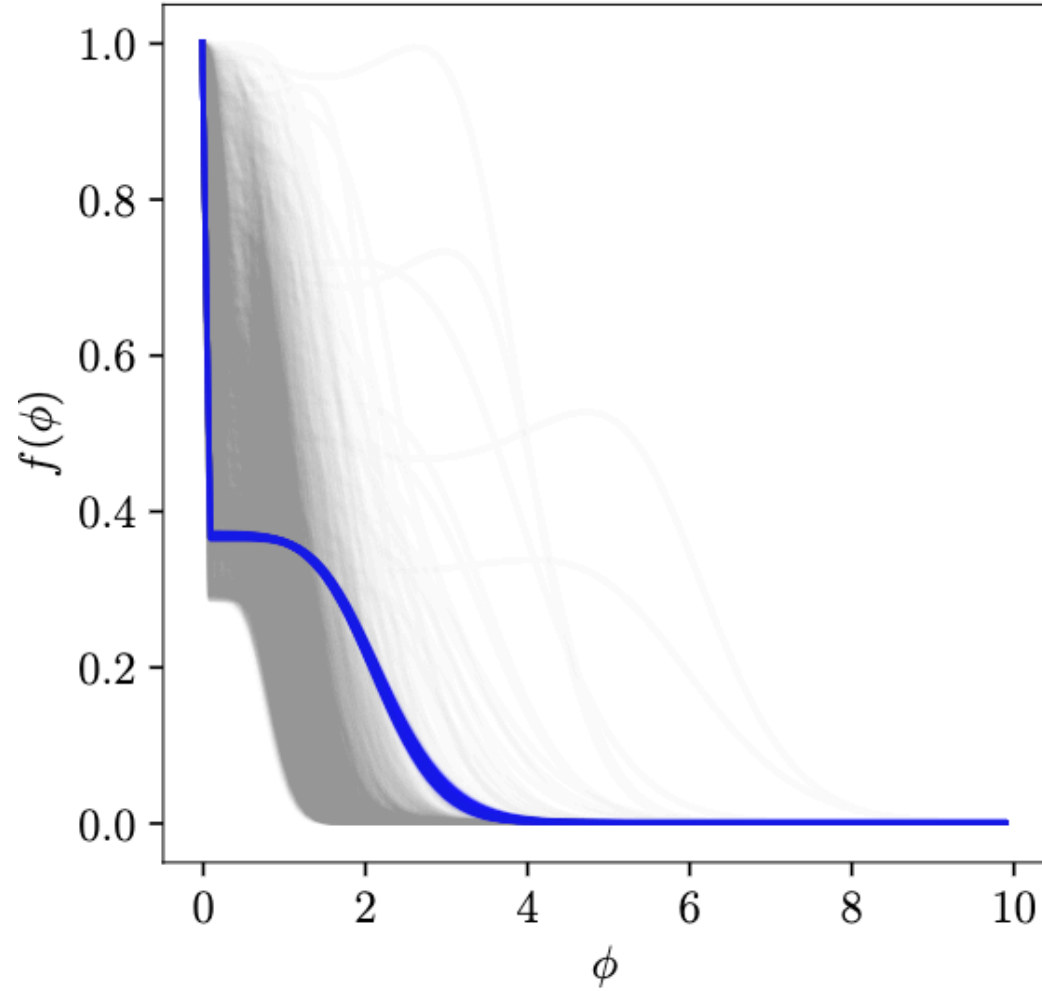
PHA model



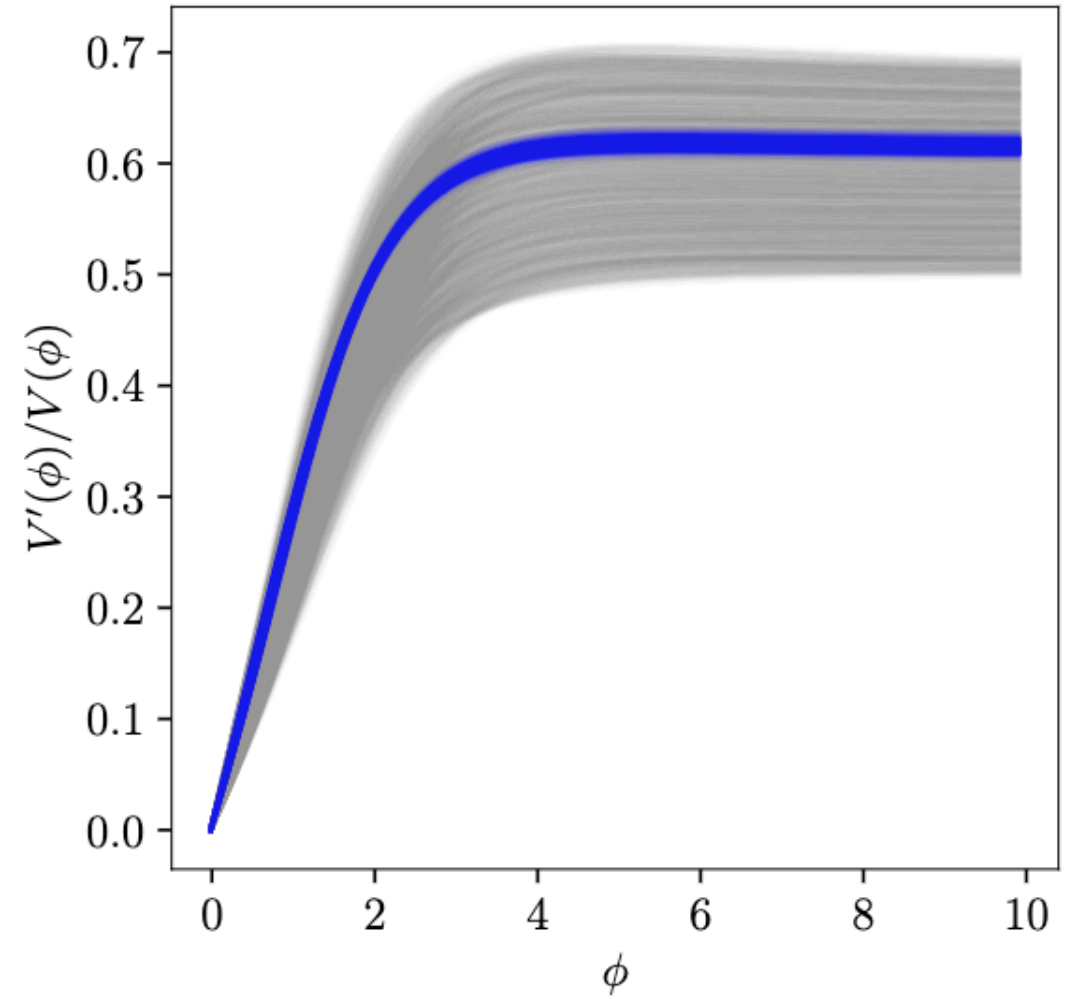
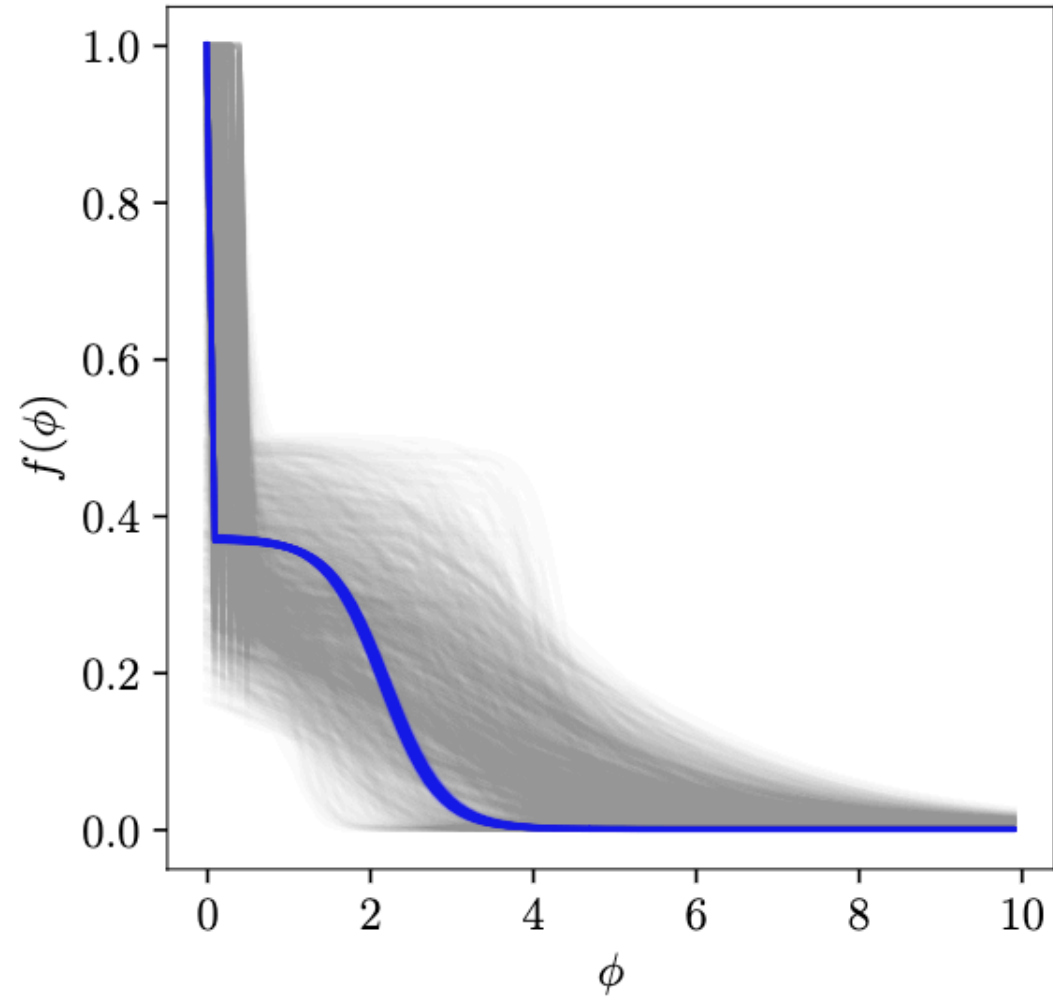
PA model



PHA Potentials



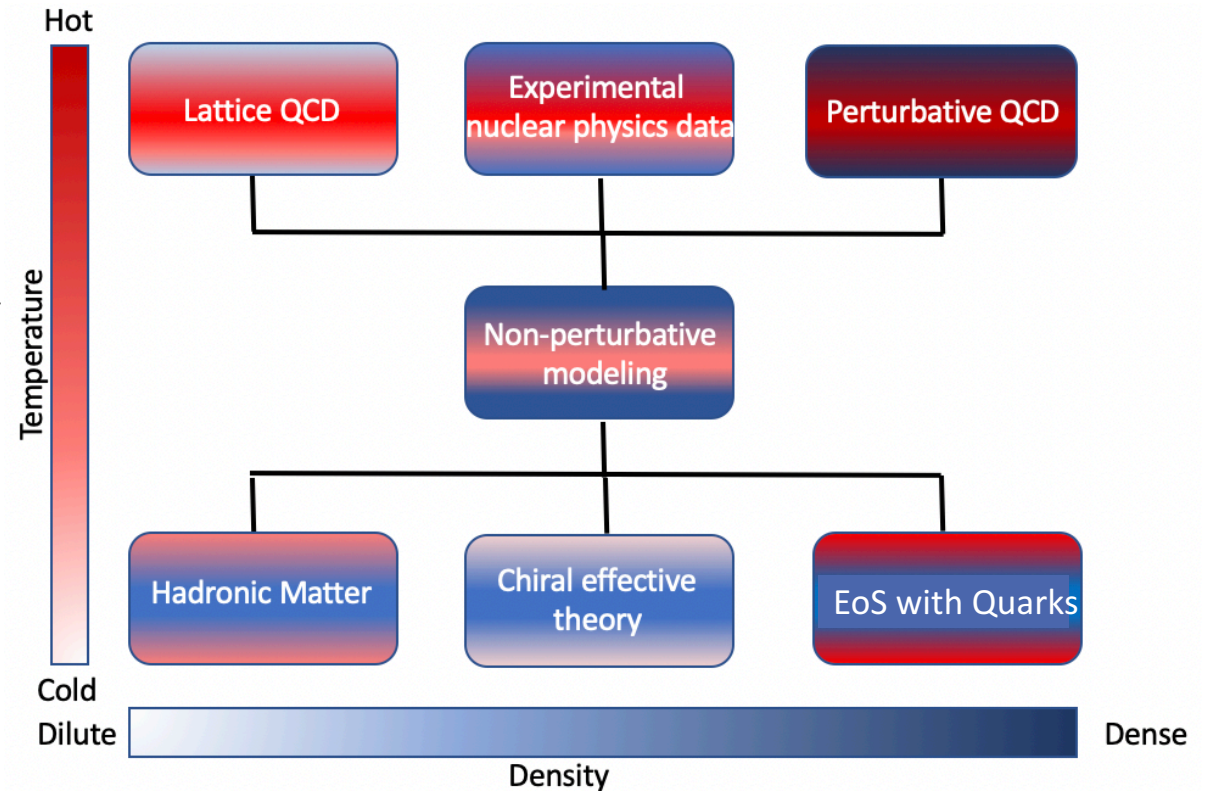
PA Potentials



Connecting High and Low Temperature QCD

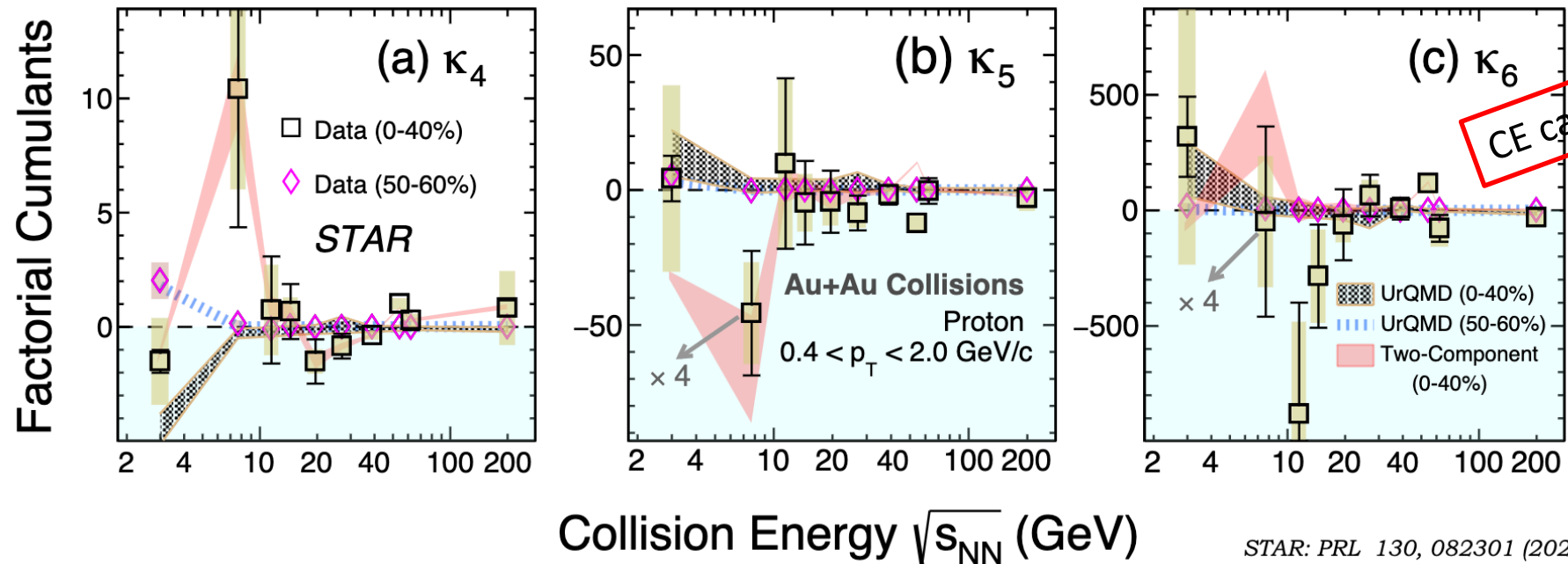
Using lessons learned from heavy-ion collisions

- Calculate lattice QCD equation of state, diagonal and off-diagonal fluctuations at small density
- Use them to constrain quantum many-body theory, accounting for quantum effects
- Apply these non-perturbative techniques in models with quark and gluon degrees of freedom, further constraining them with heavy-ion data



Lessons from heavy-ion collisions II

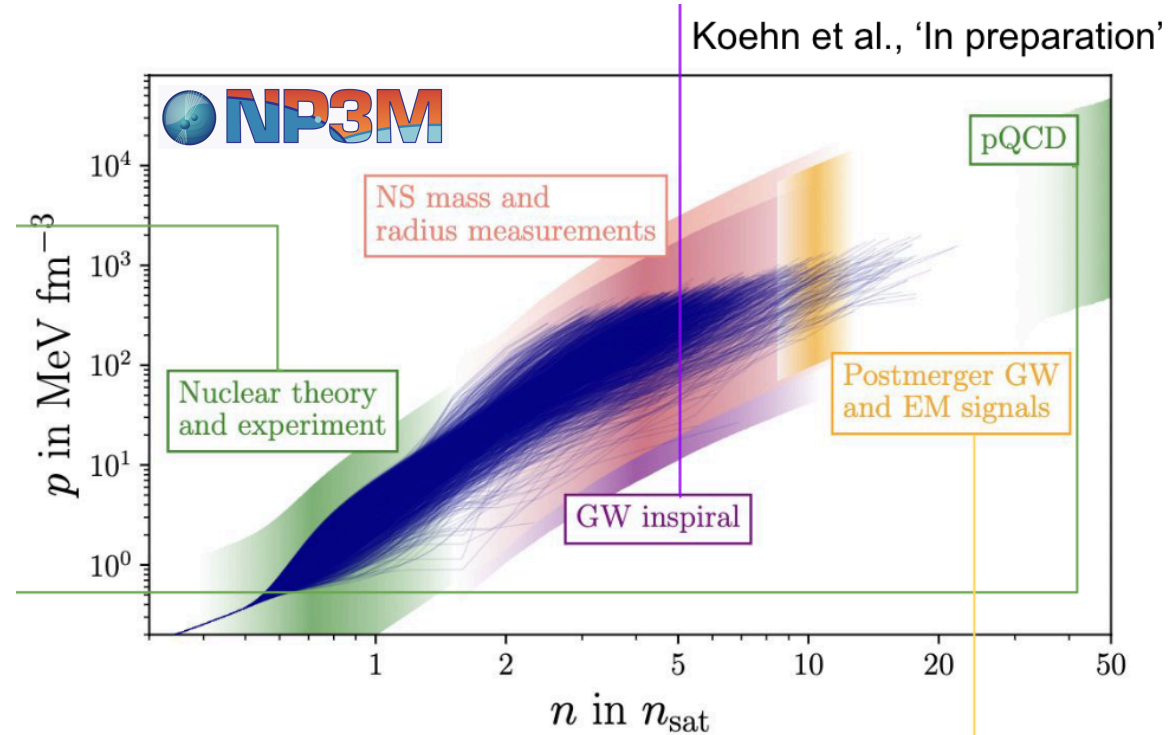
- Lowest collision energy at RHIC: 3 GeV in fixed target mode ($\mu_B \sim 750$ MeV)
- Results show that the system is purely hadronic



- If the critical point sits at $\mu_B > 750$ MeV, it cannot be seen in terrestrial experiments

EoS constraints

- Neutron Star observations can constrain the EoS



Somasundaram, Suleiman and Tews, in preparation

High-Temperature EoS Working group

Goals

Clevinger, Kumar, Grefa, Maslov, Dexheimer, Rapp, Ratti

- New level of understanding of the equation of state and spectral properties of strongly interacting matter
- Consider electric charge, strangeness, baryonic density, and temperature suitable for astrophysical applications

T-matrix approach

See talks by Maslov and Rapp

- Dynamical generation of resonances
- Parton interaction with resonances
- Provides a good description of the intermediate region of the QCD phase diagram

Hadronic EoS with hyperons

- Suitable to describe matter in the hadronic phase
- Contains the liquid-gas phase transition
- Parameters will be varied taking into account new constraints from Heavy-ion experiments

Self-consistent PNJL model

See talk by Maslov

- Describe the hadron-quark transition region in terms of bound state dissociation

Chiral Mean Field model

See talks by Dexheimer and Grefa

- Nonlinear realization of the SU(3) sigma model
- Beyond mean field approach

High-Temperature EoS Working group

Clevinger, Kumar, Greife, Maslov, Dexheimer, Rapp, Ratti

Goals

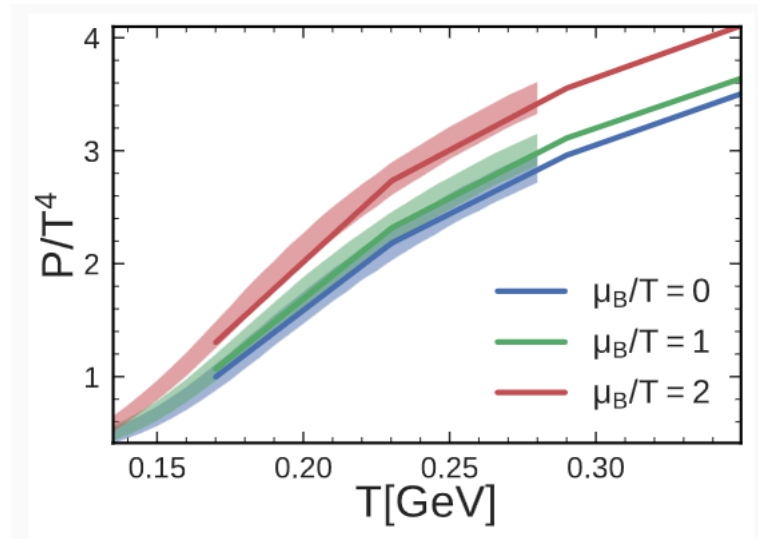
- New level of understanding
- Consider electric charge

strongly interacting matter
relevant for astrophysical applications

T-matrix approach

See talks by Maslov and Ratti

- Dynamical generation of resonances
- Parton interaction with resonances
- Provides a good description of the intermediate region of the QCD phase diagram



- T-matrix: Use lattice QCD results to fix the model parameters (see talk by Maslov)

- Parameters will be varied taking into account new constraints from Heavy-ion experiments

Self-consistent PNJL model

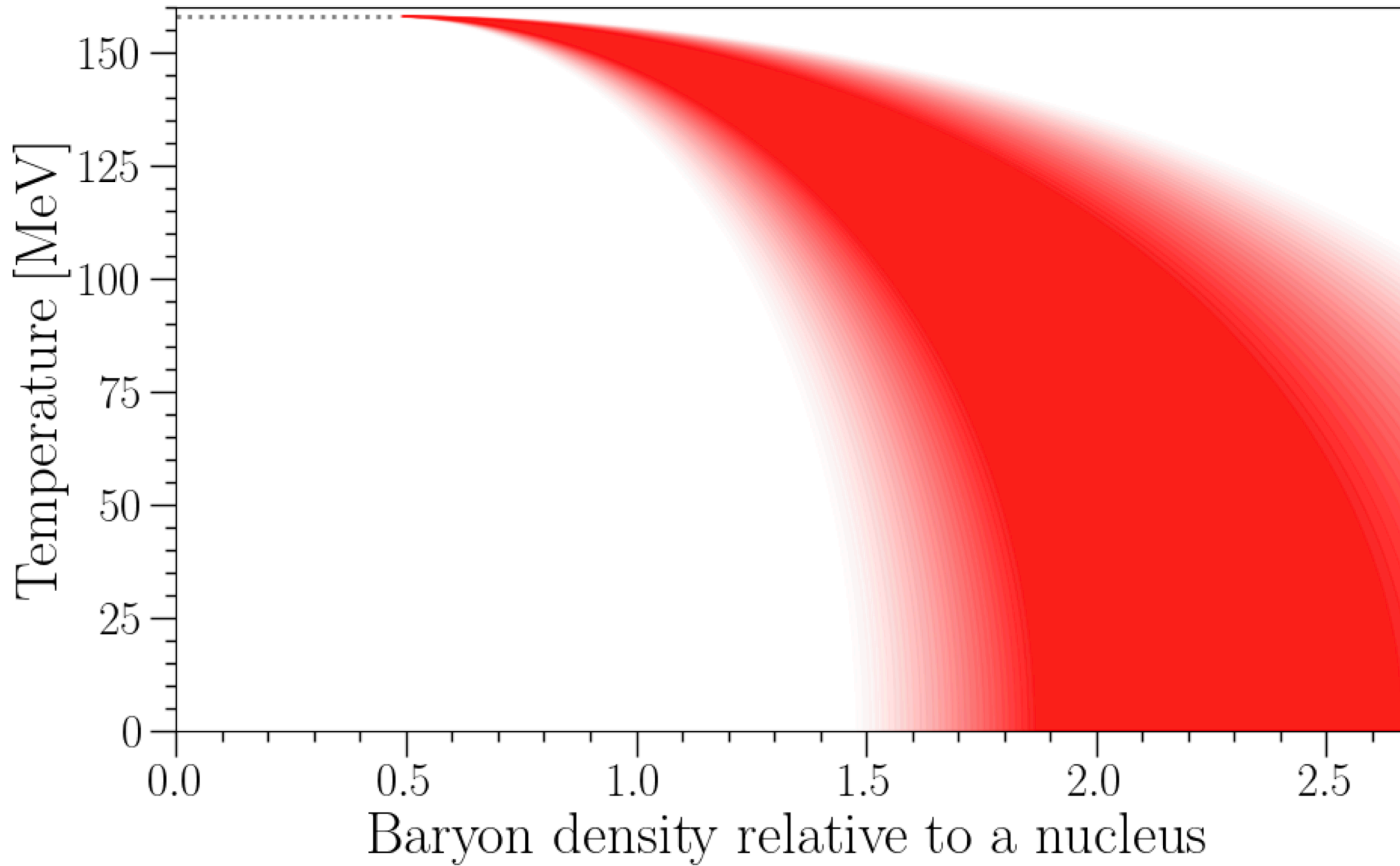
See talk by Maslov

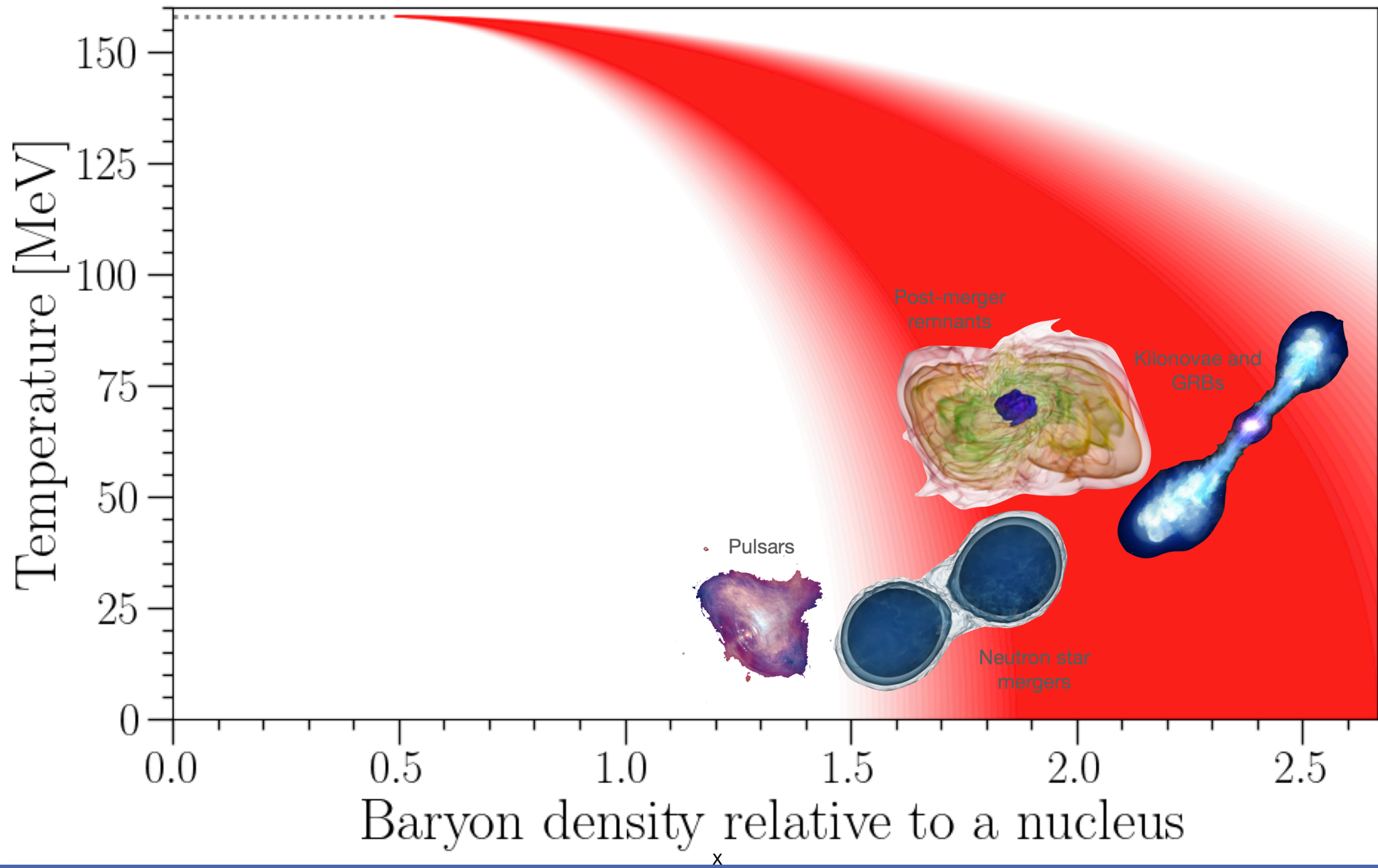
Describe the hadron-quark transition region in terms of bound state dissociation

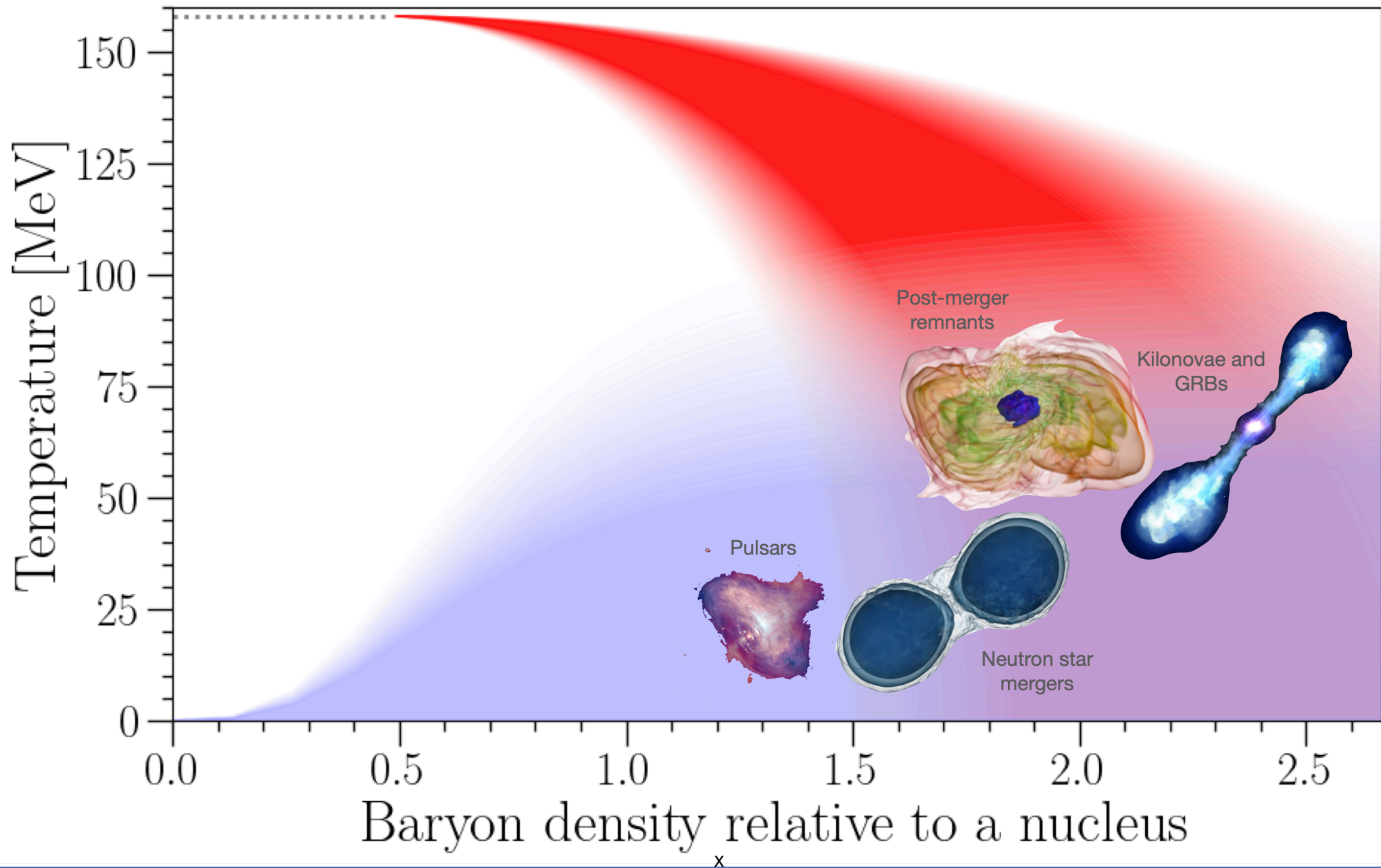
Relativistic Mean Field model

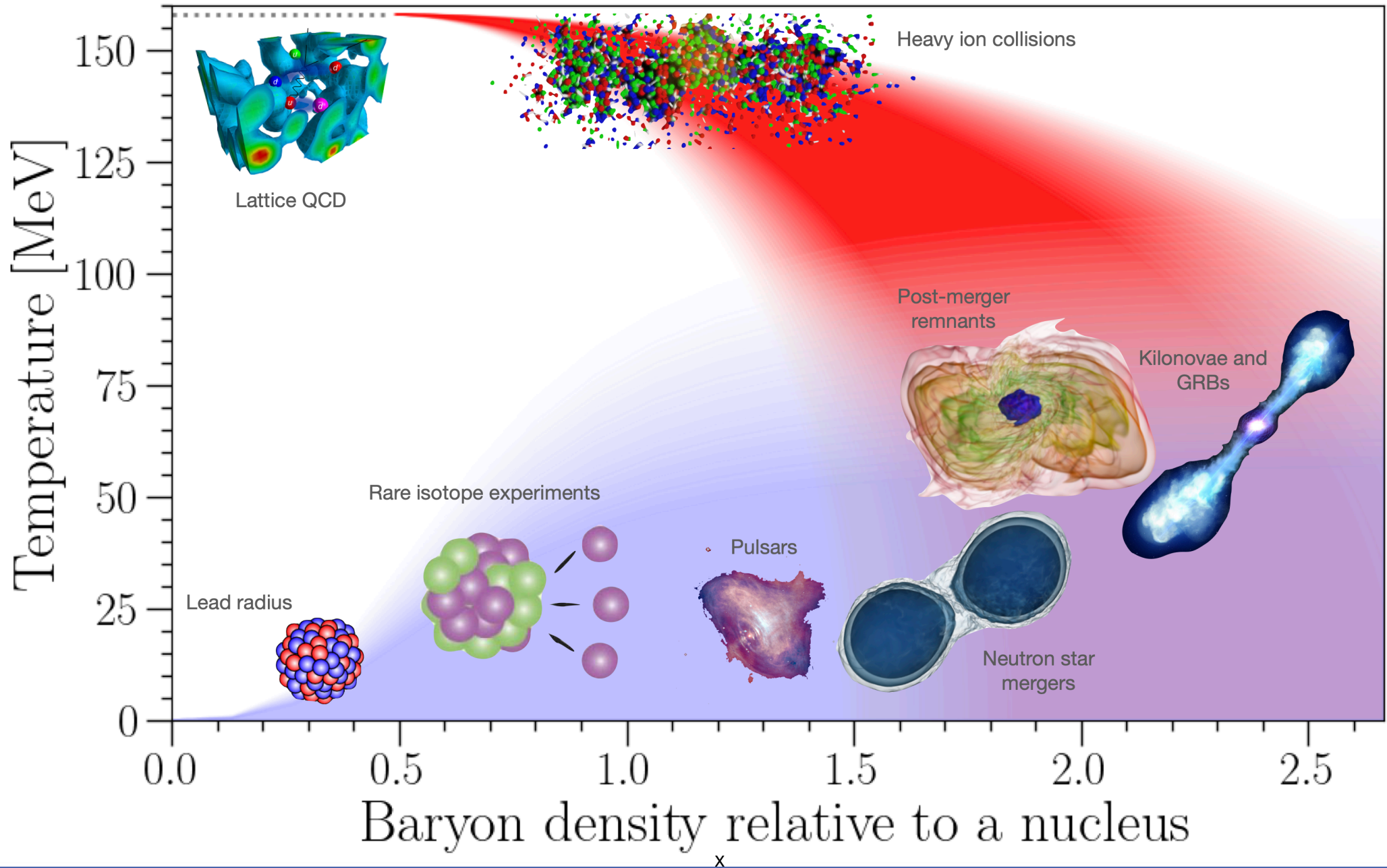
See talks by Dexheimer and Greife

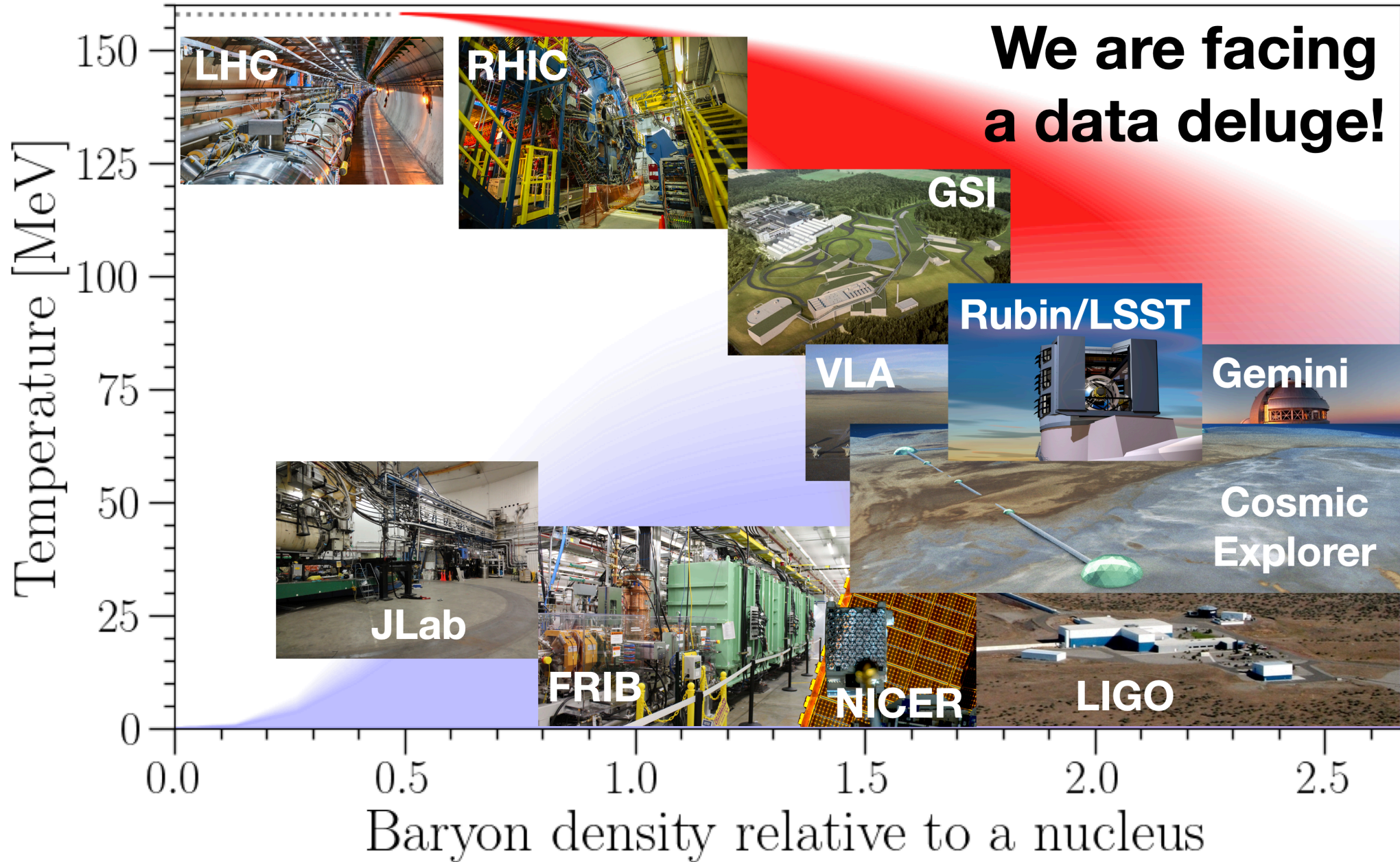
- Nonlinear realization of the SU(3) sigma model
- Beyond mean field approach



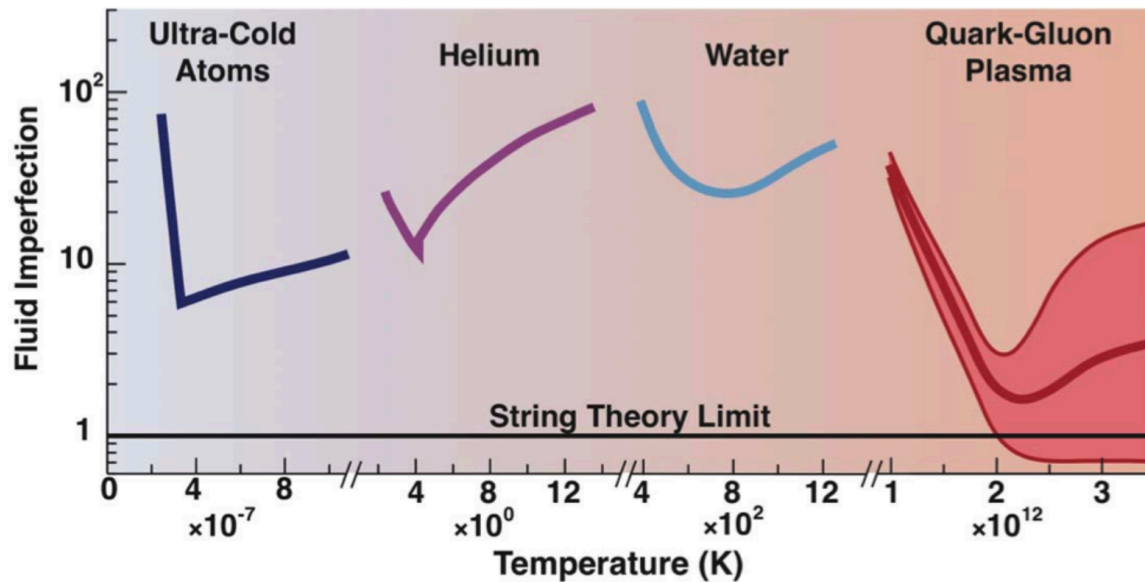






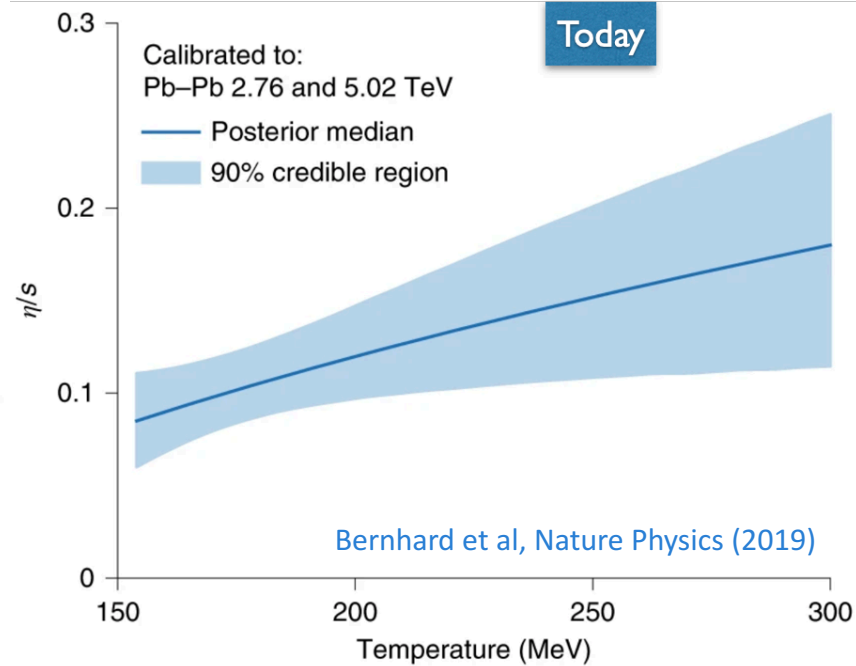


Nearly perfect fluidity



Kovtun, Son, Starinets,
PRL (2005)

$$\eta/s = 1/4\pi$$



- Hydrodynamic description of the system created in heavy-ion collisions works extremely well
- It needs an equation of state as input

A few Lessons learned

- Heavy ion collisions:
 - Phase transition at small μ_B is a smooth crossover
 - If a critical point exists, it is in the 3D-Ising model universality class
 - Equation of state and phase diagram are known from 1st principles at $\mu_B/T < 3.5$
 - Quark-Gluon Plasma is a strongly coupled fluid with very small viscosity/entropy
- Neutron star mergers:
 - GWs travel essentially at the speed of light
 - binary neutron star mergers are progenitors of short gamma ray bursts
 - they are prolific sites for the formation of heavy elements
 - constrained neutron-star radii to be between 9.5 and 13 km

Fermionic sign problem

- The QCD path integral is computed by Monte Carlo algorithms which sample field configurations with a weight proportional to the exponential of the action

$$Z(\mu_B, T) = \text{Tr} \left(e^{-\frac{H_{\text{QCD}} - \mu_B N_B}{T}} \right) = \int \mathcal{D}U e^{-S_G[U]} \det M[U, \mu_B]$$

- $\det M[\mu_B]$ complex \rightarrow Monte Carlo simulations are not feasible
- We can rely on a few approximate methods, viable for small μ_B/T :
 - Taylor expansion of physical quantities around $\mu_B=0$
Bielefeld-Swansea collaboration 2002; R. Gai, S. Gupta 2003
 - Simulations at imaginary chemical potentials
Alford, Kapustin, Wilczek, 1999; de Forcrand, Philipsen, 2002; D'Elia, Lombardo 2003

